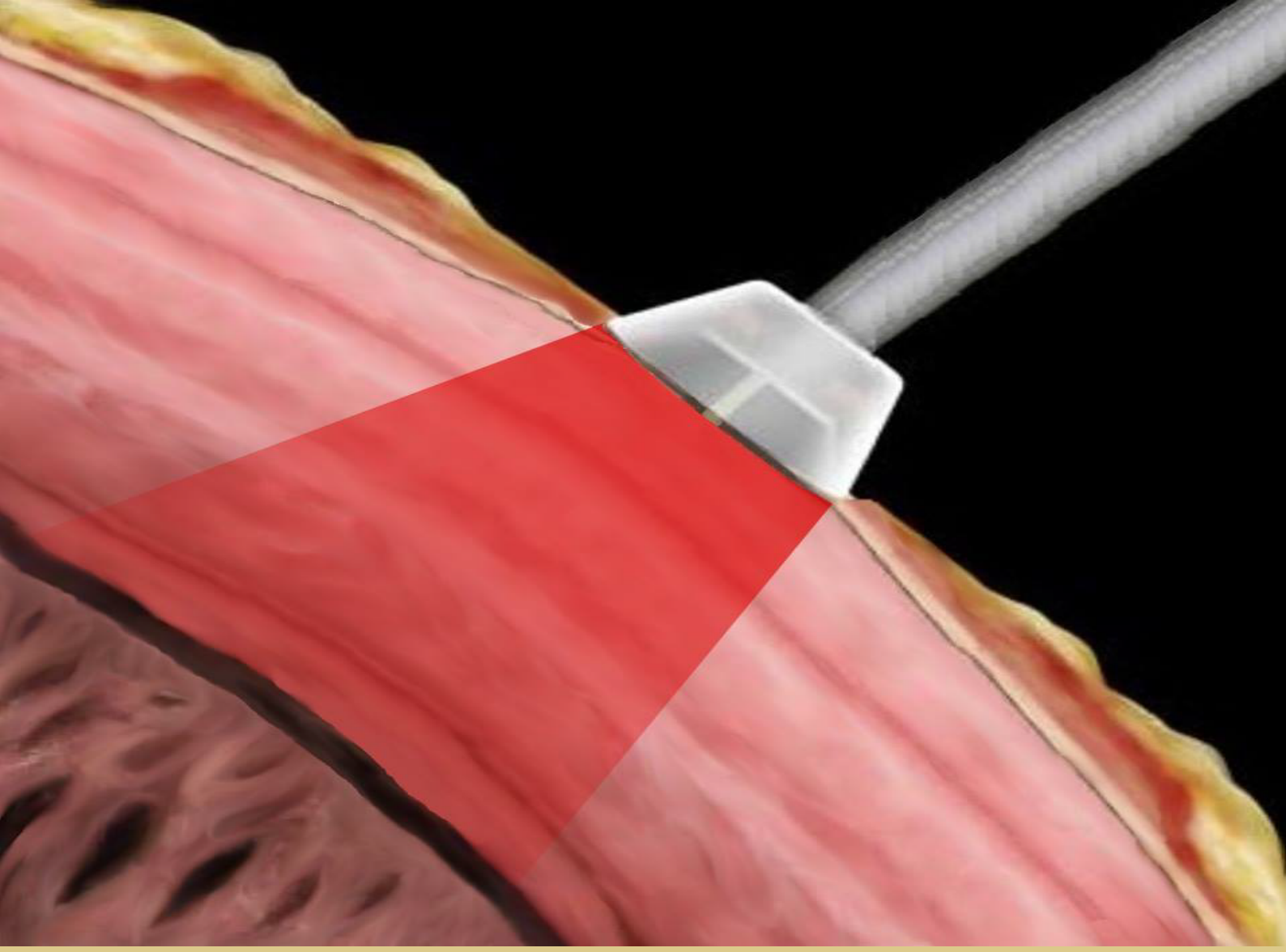

Matías Eduardo Antonio Mantineo

LASER Therapy in Inflammation: mechanisms, techniques and instrumentation

Doctoral thesis in Biomedical Engineering,
supervised by Prof. Dr. António Miguel Lino Santos Morgado
and Prof Dr. João José Carreiro Páscoa Pinheiro,
submitted to Faculty of Sciences and Technology, University of Coimbra

September 2014

· U C ·

Universidade de Coimbra

FACULTY OF SCIENCES AND TECHNOLOGY

DEPARTMENT OF PHYSICS

LASER THERAPY IN INFLAMMATION:

Mechanisms, techniques and instrumentation

Scientific Supervisor:

Prof. Doutor António Miguel Lino Santos Morgado

Co-Supervisor:

Prof. Doutor João José Carreiro Páscoa Pinheiro

Thesis submitted in accordance with the requirements of the University of Coimbra for the degree of Doctor in Biomedical Engineering

MATÍAS EDUARDO ANTONIO MANTINEO

SEPTEMBER 2014

This work was funded by Erasmus Mundus “EADIC, Europe Argentina for Development, Innovation and Change” Scholarships and by FEDER, through the Programa Operacional Factores de Competitividade- COMPETE and by National funds through FCT- Fundação para a Ciência e Tecnologia in the frame of “Centro de Instrumentação- Unidade 217/94”.

EADIC - ERASMUS MUNDUS
EXTERNAL COOPERATION WINDOW LOT 16

COMPETE
PROGRAMA OPERACIONAL FACTORES DE COMPETITIVIDADE

FCT
Fundação para a Ciência e a Tecnologia
MINISTÉRIO DA CIÊNCIA, TECNOLOGIA E ENSINO SUPERIOR

QREN
QUADRO DE REFERÊNCIA ESTRATÉGICO NACIONAL
PORTUGAL 2007.2013

UNIÃO EUROPEIA
FEDER

To my family

To my friends

Acknowledgements

It would not have been possible to write this doctoral thesis without the help and support of the kind people around me, to only some of whom it is possible to give particular mention here. Above all, I would like to thank to Professor António Miguel Lino Santos Morgado for the supervision of the present work and for his support, suggestions and useful comments along the work; to Professor João José Carreiro Páscoa Pinheiro for having accepted the co-supervision of the present work and for all the encouragement provided; to Professor Flávio Nelson Fernandes Reis for all the support, suggestions and fruitful lessons in animal experimentation; to Professor António Francisco Rosa Gomes Ambrósio for all the laboratorial support and suggestions; to Ana Raquel Sarabando Santiago for the useful laboratorial tips and also to all my colleagues in the Lab, for their support, collaboration and the wonderful time we spent working together.

This thesis would not been possible without some special persons like my parents, who always give me all that they can ever since my mother's womb and for their unconditional love and also Ornella and Tomás for the love and happiness they bring into my life, my friends for the infinite tolerance, Portugal and the portuguese people for making me feel like this is my home in this beautiful period and finally God for enlighten my steps and always give me hope and peace.

Summary

The objective of this work was to evaluate the influence of irradiation parameters on the Low Level Laser Therapy (LLLT) treatment of the acute phase of skeletal muscle inflammation, through the measurement of cytokines expression in systemic serum and analysis of muscle tissue. Although our experiments were not designed to validate any of the LLLT action mechanisms, we intended to discuss their results in the framework of the currently most accepted LLLT cellular-level mechanism, which is based on the role of Cytochrome C Oxidase (CCO) as a primary photo-acceptor to red and near-infrared radiation

We used Wistar rats with a controlled inflammation induced in the gastrocnemius muscle. The animals were treated using continuous (830 and 980 nm) and pulsed laser illumination (830 nm) as well as continuous LED illumination (850 nm). Animals were divided into five groups per wavelength (10, 20, 30, 40 and 50 mW), plus a control group. LLLT was applied during five days, with constant irradiation time and area. TNF-α, IL-1β, IL-2 and IL-6 cytokines were quantified by ELISA. Inflammatory cells were counted using microscopy. Identical methodology was used with pulsed illumination. Average power (40 mW) and duty cycle were kept constant (80%) at five frequencies (5, 25, 50, 100 and 200 Hz). When irradiating with non-coherent (LED) light, we used only a radiant power of 40 mW.

For continuous irradiation, treatment effects occurred for all doses, with reduction of TNF-α, IL-1β and IL-6 cytokines and number of inflammatory cells, when compared to controls. Continuous irradiation at 830 nm was more effective, a result explained by the action spectrum of cytochrome c oxidase. Best results were obtained for 40 mW, with data suggesting a biphasic dose response. PW irradiation was only effective for higher frequencies, a result that might be related to the rate constants of CCO internal electron transfer process. LED irradiation did not produce a treatment effect when compared with controls.

Keywords

Low Level Laser Therapy (LLLT), cytokines, muscle inflammation, animal model.

Resumo

O objectivo deste projecto foi avaliar a influência dos parâmetros de irradiação no tratamento por terapia laser de baixa intensidade (LLLT – Low Level Laser Therapy) da fase aguda da inflamação do músculo esquelético, através da medição da expressão de citocinas na circulação sistémica e da análise histológica de amostras de tecido muscular. Embora as nossas experiências não tenham sido concebidas para validar qualquer um dos mecanismos de acção da LLLT, pretendemos discutir seus resultados no âmbito do mecanismo celular de actualmente mais aceite, que se baseia no papel da Citocromo C Oxidase (CCO), como foto-aceitador primário da radiação vermelha e infravermelha próxima.

Utilizámos ratos Wistar com uma inflamação controlada induzida no músculo gastrocnémio. Os animais foram tratados com irradiação laser contínua (980 e 830 nm) e pulsada (830 nm) bem como com irradiação LED contínua (850 nm). Os animais foram divididos em cinco grupos por comprimento de onda (10, 20, 30, 40 e 50 mW), além de um grupo de controlo. A LLLT foi aplicada durante cinco dias, com tempo de irradiação e área irradiada constante. As citocinas TNF-α, IL-1β, Il-2 e IL-6 foram quantificadas por ELISA. As células inflamatórias foram contadas através de microscopia. Metodologia idêntica foi usada com iluminação pulsada. A potência média (40 mW) e o ciclo de trabalho - "*duty cycle*" - (80%) foram mantidos constante para cinco frequências de impulsos (5, 25, 50, 100 e 200 Hz). Na irradiação com luz não-coerente (LED), usámos apenas um valor de potência radiante (40 mW).

Para irradiação contínua, ocorreram efeitos de tratamento para todas as doses, com redução da concentração das citocinas TNF-α, IL-1β e IL-6 e do número de células inflamatórias, relativamente ao observado nos animais de controlo. A irradiação contínua para o comprimento de onda 830 nm foi mais eficaz, um resultado explicado pelo espectro de acção da Citocromo C Oxidase. Os melhores resultados foram obtidos para a potência de 40 mW, com os dados a sugerir uma resposta de dose bifásica. A irradiação pulsada só foi eficaz para as frequências mais altas, um resultado que pode estar relacionado com as constantes de taxa do processo de transferência interno de electrões na CCO. A irradiação com luz não coerente (LED) não produziu um efeito de tratamento quando comparada com os controlos.

Palavras-Chave

Terapia laser de baixa potência (LLLT), citocinas, inflamação muscular, modelo animal.

Contents

List of Abbreviations

ANOVA	Analysis of variance
ARRIVE	Animal Research: Reporting of In Vivo Experiments
ATP	Adenosine Triphosphate
cAMP	cyclic adenosine monophosphate
CCO	cytochrome c oxidase
COX2	cyclooxygenase 2
FDA	Food and Drug Administration
GaAs	Gallium arsenide
GaAlAs	Aluminium gallium arsenide
HeN	Helium Neon
IFN-γ	Interferon gamma
IL	Interleukin
LASER	Light Amplification by Stimulated Emission of Radiation
LED	Light Emitting Diode
LLLT	Low Level Laser Therapy
mRNA	messenger Ribonucleic acid
Nd:YAG	Neodymium-doped Yttrium Aluminum Garnet
NIR	Near Infrared
NO	nitric oxide
NSAIDs	Non-Steroidal Anti-Inflammatory Drugs
PGE2	prostaglandin E2
PGG2	prostaglandin endoperoxide
PGH2	prostaglandin H2
PGI2	prostacyclin
ROS	Reactive Oxygen Species
SOD	superoxide dismutase
SPIE	The International Society for Optical Engineering
TNF	Tumor Necrosis Factor
UV	Ultra Violet
VEGF	Vascular Endothelial Growth Factor
WALT	World Association of Laser Therapy

List of Tables

List of Figures

1. Objectives

There are evidence that suggests that the results obtained by Low Level Laser Therapy in the treatment of inflammatory processes are the result of direct influence of laser irradiation on the expression of anti- and pro-inflammatory cytokines on the circulatory serum.

The aim of this study is to determine the influence of laser irradiation parameters, including wavelength, dose, power and interaction time, the expression of anti-inflammatory cytokines and pro-inflammatory cytokines (IL-1β, IL-2, IL-6 and TNF-α) in the circulatory serum, and to evaluate the clinical consequences of this effect at cellular level.

2. Introduction

2.1 What is Low Level Laser Therapy?

According to The National Library of Medicine (USA) - Medical Subject Headings, Low Level Laser Therapy (LLLT) is a: “Treatment using irradiation with light at low power intensities and with wavelengths in the range 540 nm - 830 nm. The effects are thought to be mediated by a photochemical reaction that alters cell membrane permeability, leading to increased mRNA synthesis and cell proliferation. The effects are not due to heat, as in laser surgery. Low-level laser therapy has been used in general medicine, veterinary medicine, and dentistry for a wide variety of conditions, but most frequently for wound healing and pain control” [1]. It is a good definition but has some inaccuracies. Setting a LLLT wavelength limit at 830 nm is not correct, since the effects of LLLT also occur for greater wavelengths. The mention to the cell membrane permeability mechanism is another problem in the definition, since it is incompatible with the role of cytochrome c oxidase as the primary photoacceptor for red-NIR radiation, which is the basis of the currently most widely accepted LLLT mechanism (see section 2.5).

Another term to refer Low Level Laser Therapy is Photobiomodulation Therapy. This is probably the term preferred by the scientific community of this research field. That is “a light therapy using lasers or LEDs to improve tissue repair, reduce pain and inflammation wherever the beam is applied” and it “has been used for many years on sports injuries, arthritic joints, neuropathic pain syndromes, back and neck pain” [2].

In the last years several systematic reviews have documented the positive effects of LLLT. The British Journal of Sports Medicine (the sport medicine journal of BMJ – British Medical Journal) published a systematic review concerning surgical and conservative interventions for frozen shoulder [3], where it found “strong evidence for the effectiveness of steroid injections and laser therapy in short-term and moderate evidence for steroid injections in mid-term follow-up”. In another systematic review on the treatment of tennis elbow, information was presented regarding the effectiveness and safety of several interventions, including LLLT [4]. The authors concluded that, when compared to sham treatment and other non-laser interventions, LLLT is more effective at reducing pain, improving pain-free grip strength and increasing global improvement after treatment at up to 2 months.

The International Association for the Study of Pain, a well-known organization in musculoskeletal pain studies, reviewed the published evidence on the diagnosis and treatment of myofascial pain syndrome, publishing a guideline on this subject where it states that “laser therapy shows strong evidence of effectiveness for pain relief” [5]. Neck pain treatment is a LLLT indication too. Two systematic reviews from World Health Organization (Bone and Joint Task Force) [6] and Lancet [7] recommend the use and provide strong evidence on the efficacy of LLLT in the management of neck pain. The lancet review states “that LLLT reduces pain immediately after treatment in acute

neck pain and up to 22 weeks after completion of treatment in patients with chronic neck pain".

A systematic review and meta-analysis meant to assess the clinical effectiveness of LLLT in the treatment of tendinopathy found that "LLLT can potentially be effective in treating tendinopathy when recommended dosages are used" [8]. At the same time, the Orthopaedic Section of American Physical Therapy Association clinical guidelines recommend LLLT in the treatment of Achilles Tendinitis [9], stating that "clinicians should consider the use of low level laser therapy to decrease pain and stiffness in patients with Achilles tendinopathy". Other systematic reviews and meta-analysis listed on the Database of Abstracts of Reviews of Effects (DARE), which groups only quality-assessed reviews, found positive effects of LLLT on the treatment of cancer therapy-induced oral mucositis [10] and of chronic joint disorders [11].

The published literature contains several studies showing that LLLT is effective in a wide range of conditions. Positive results are found in the reduction of some types of pain, in cases of musculoskeletal disorder like arthritis, osteoarthritis, tendinopathy, chronic joint disorders and neck pain, on the treatment of chronic periodontitis, on the healing of infections around dental implants, in the treatment of skeletal muscle inflammation and on wound healing. There are also positive results when dealing with ocular conditions, like optic nerve trauma, optic neuropathy, retinal injury, retinitis pigmentosa, phototoxicity, and age-related macular degeneration. In what concerns central nervous system conditions, there are reports of LLLT having positive effects in anoxic brain injury, stroke, acute and chronic traumatic brain injury, neurodegeneration, age-related memory loss and cognitive and mood disorders [12]. However more evidence is still necessary to prove the therapy effectiveness since in many cases LLLT results were not positive. In many cases, this is due to wrong usage of the therapy, mainly because of dosimetry errors, like too low or too much energy or irradiance delivered [13,14]. This situation is further hampered by the fact that errors and omissions on LLLT papers are frequent. Usually there is no verification of beam parameters and in many situations the number of reported parameters is inadequate to reproduce the experiments [15]. Inappropriate anatomical treatment location and concurrent patient medication are also reported as causes for some published LLLT failures. The Food and Drug Administration (FDA) considers LLLT devices as experimental but allows their use in research studies [16]. LLLT devices were cleared for marketing by FDA through the Premarket Notification/510(k) process (that is device manufacturers have to notify FDA of their intent to market the device at least 90 days in advance) as adjunctive devices for temporary relief of pain, based on the presentation of clinical data to support such claims. A search in the 510(k) Premarket Notification database found more than 30 devices. In Asia, South America and Europe, the use of LLLT is much more common.

Low-level Laser Therapy is an active research topic. In addition to the need for more evidence on the therapy results and on the best techniques of administration (local irradiation, wavelength, power density and energy, pulsed or continuous emission, interaction time and pulse repetition rate), it is necessary to clarify the cellular mechanisms mediated by LLLT. The scientific production indexed in PubMed with the term "Low-Level Laser Therapy", has been increasing (see Figure 2.1).

At the end of September 2014, over of 4100 references were indexed, with an emphasis in animal studies. The most frequent applications are wound healing, pain management and the new topic of bone regeneration. In terms of medical specialties, the most cited are dentistry, dermatology and physical and rehabilitation medicine [17].

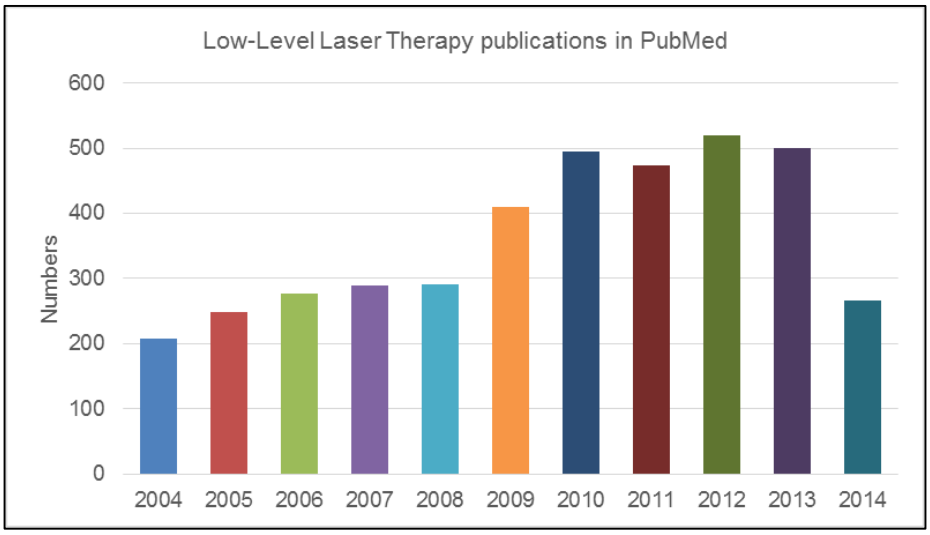

Figure 2.1– Evolution of LLLT publications referenced in PubMed, from 2004 until the end of September 2014.

For the progress of clinical LLLT as a science and as clinical tool, it is essential that its principles of action are fully studied and understood. That implies to know the processes of light propagation on biological tissue and the interaction mechanisms between radiation and tissue, as well as to identify the primary molecular photo-acceptors that mediate LLLT action and the cascade of molecular and cell processes that area triggered by light absorption.

2.1.1 Laser – Tissue Interaction

Here we will review the current knowledge on light propagation on biological tissue and on the interaction mechanisms between radiation and tissue. The review will be directed to the application discussed on this thesis: the treatment of skeletal muscle injuries using LLLT. This option implies to focus the light propagation discussion on specific tissues, the skin and the skeletal muscle. It also implies to discuss more thoroughly the photochemical and thermal interaction mechanisms: the photochemical mechanism is the one involved in LLLT and thermal interactions should not occur during LLLT administration, a condition that it is important to verify.

2.1.1.1 Light propagation in biological tissue: Skin and muscle

In order to assure that a valid dose of light reaches the target tissue, it is necessary to know how light propagates in biological tissue. This is particularly true when the target tissue is not located at the skin surface as is the case when treating skeletal muscle inflammation. Moreover, when studying the action of LLLT in a given tissue for different irradiation wavelengths, as is the case of

our work, it is necessary to know what is the actual irradiance at the tissue or, at least, to warrant that the irradiance at the tissue is the same for all used wavelengths. For fulfilling this requirement when studying non-exposed tissues it is not enough to have the same irradiance at the air-skin interface, since light propagation through the skin can affect differently the various wavelengths. It is necessary to know how the tissues lying before the treatment target affect light propagation. This can be done through experiments in tissue samples or in adequate phantoms, or by computational modeling, using analytical or Monte-Carlo techniques, based on the optical properties of those tissues, namely their absorption and scattering coefficients well as their scattering anisotropy.

When laser radiation propagates in a biological tissue, it undergoes two types of first-order interactions: absorption and scattering. In the first, all the energy of the photons is transferred to the tissue, part of which can be converted back into photons (through fluorescence and phosphorescence processes). In the second, there is no energy loss (elastic scattering), but there is a change in the direction of propagation. The combination of these processes of interaction determines the depth of penetration of laser light in biological tissue [18,19].

The energy state change of a molecular or atomic species from a lower to a higher energy level implies the absorption of one photon with energy equal to the energy difference, $E_{ph} = \Delta E$, between the two levels [20]:

$$\frac{hc}{\lambda} = E_{final} - E_{initial} \quad (2.1)$$

Similarly, the decay from a higher energy level to a lower level occurs with an emission of energy equal to the energy difference between the two levels.

In the quantum model, photon absorption by molecules or atoms leads to an increase of their internal energy. The spectral regions where these transitions take place are called absorption bands and are different for each molecular or atomic species.

The most frequent absorption process is between electronic levels. At room temperature, the energies of a group of molecules correspond to the vibrational and rotational bands on the electronic ground state, S_0. When these molecules absorb energy, they will change their state to an energy level located within one of the electronic singlet states S_n. The number of excited molecules (intensity of absorption) depends on the irradiance of the excitation light beam and on the transition probability for photons of a specific energy. The oscillator strength, f, is used to characterize the intensity of absorption and depends on the integral of the absorption spectrum according to:

$$f = 4.315 \times 10^{-9} \int \varepsilon_\nu d\nu, \quad (2.2)$$

where ε_ν is the molar extinction coefficient at the frequency ν. When oscillator strength is close to one, we have allowed transitions. Small values of oscillator strength indicate forbidden transitions [20].

The second frequent absorption process involves vibrational levels within a given electronic level.

The vibrational levels represent the molecule vibration states. The molecular vibrations are quantized and result in a series of energy levels for each vibrational mode of molecule. Generally, infra-red photons are involved in these vibrational transitions.

The less prevalent absorption process involves rotational levels within a single electronic level. These rotational levels result from the quantization of the molecular rotational motions. The transitions involve photons from far infra-red to submillimeter spectrum regions.

The absorption cross section σ_a can be defined for a localized absorber like,

$$\sigma_a = \frac{P_{abs}}{I_0}, \quad (2.3)$$

where P_{abs} is the amount of power absorbed out a plane wave of intensity I_0.

The absorption coefficient can characterizes a medium with a uniform distribution of identical absorbing particles, with the absorbers density ρ, according to

$$\mu_a = \rho\sigma_a, \quad (2.4)$$

And its reciprocal is defined as the absorption mean free path or absorption length, and represents the distance in which the incident light is reduced to 37% of its initial intensity,

$$I_a = \frac{1}{\mu_a} \quad (2.5)$$

For a medium, the absorption coefficient is defined as:

$$dI = -\mu_a I dz, \quad (2.6)$$

where dI is the differential intensity of a collimated light traversing an path dz with absorption coefficient μ_a. Integrating, we arrive to the Beer-Lambert Law,

$$I = I_0 e^{-\mu_a z}, \quad (2.7)$$

which can be expressed as

$$I = I_0 e^{-\varepsilon_\lambda a z}, \quad (2.8)$$

where,

ε_λ is the molar extension coefficient [cm^2/mol] at wavelength λ

a [mol/cm^3] is the molar concentration of the absorption species

z is the thickness [cm]

The radio of transmitted intensity I to incident intensity I_0 is defined as transmission:

$$T = \frac{I}{I_0} \quad (2.9)$$

And the attenuation, absorbance (A) or optical density (OD) of a medium is given by:

$$A = OD = \log_{10}\left(\frac{I_0}{I}\right) T = -\log_{10}(T) \quad (2.10)$$

Scattering occurs when a photon encounters a localized region with a refractive index which differs from the refractive index of the neighboring regions. That localized region can be either a particle or a refractive index non-uniformity caused by a local change in a physical property like fluid density. The scattering properties can be quantified by the scattering cross section. When a monochromatic plane wave, with an irradiance I_0, meets a scattering object, a fraction of its radiant power will scattered. The scattering cross section is defined as the ratio of the scattered power, P_{scatt}, to the incident irradiance,

$$\sigma_s(\hat{s}) = \frac{P_{scatt}}{I_0}, \quad (2.11)$$

where $\hat{s}$ identifies the plane wave propagation direction.

The differential cross section gives the angular distribution of scattered radiation (see Figure 2.2),

$$\frac{d\sigma_s}{d\Omega}(\hat{s}, \hat{s}'), \quad (2.12)$$

where the unit vector $\hat{s}'$ defines the axis of a cone of solid angle $d\Omega$ originating from the scatterer. Assuming that the object is spherically symmetric, it is possible to write the scattering cross section as a constant for a given wavelength,

$$\sigma_s(\hat{s}) = \sigma_s, \quad (2.13)$$

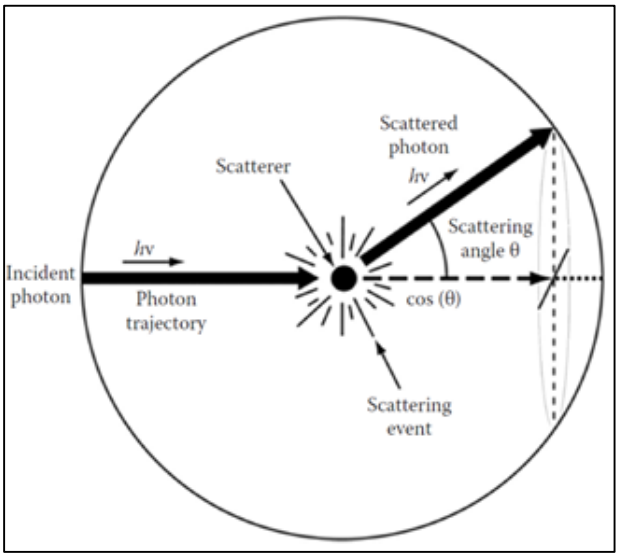

Figure 2.2– Angular distribution of scattering (Retrieved from [20]).

For a spherical case, the differential cross section depends only on the angle (θ) between the incident and scattered light directions and on the polarization states of the incoming and outgoing waves,

$$\frac{d\sigma_s}{d\Omega}(\hat{s}, \hat{s}') = \frac{d\sigma_s}{d\Omega}(\hat{s} \cdot \hat{s}'), \quad (2.14)$$

where $(\hat{s} \cdot \hat{s}') = \cos\theta$

The scattering coefficient is defined for a medium with a uniform distribution of identical scatterers, with a density ρ, according to

$$\mu_s = \rho\sigma_s, \tag{2.15}$$

The reciprocal of the scattering coefficient is the scattering mean free path. This is the average distance travelled by a photon between two successive scattering events.

The anisotropy of scattering can be measured by the coefficient of anisotropy *g*, which is the average value of the cosine of the scattering angle given by:

$$g = \int_{-1}^{1} \cos\theta \, p(\cos\theta) \, d(\cos\theta) \tag{2.16}$$

with $p(\hat{s} \cdot \hat{s}') = p(\cos\theta)$ the scattering phase function, which corresponds to the angular probability function of a photon being scattered by an angle θ. Zero anisotropy corresponds to isotropic scattering, while *g* = 1 identifies extremely forward scattering. Backscattering corresponds to *g* = -1.

The main absorbers of biological tissues, like skin or muscle, are water, hemoglobin and melanin. Figure 2.3 shows the absorption spectra of these molecules for visible and near-infrared (NIR) radiation. From the analysis of these spectra, we conclude that the window for maximum light penetration into the skin is located between 800 and 1000 nm, in the NIR spectral region.

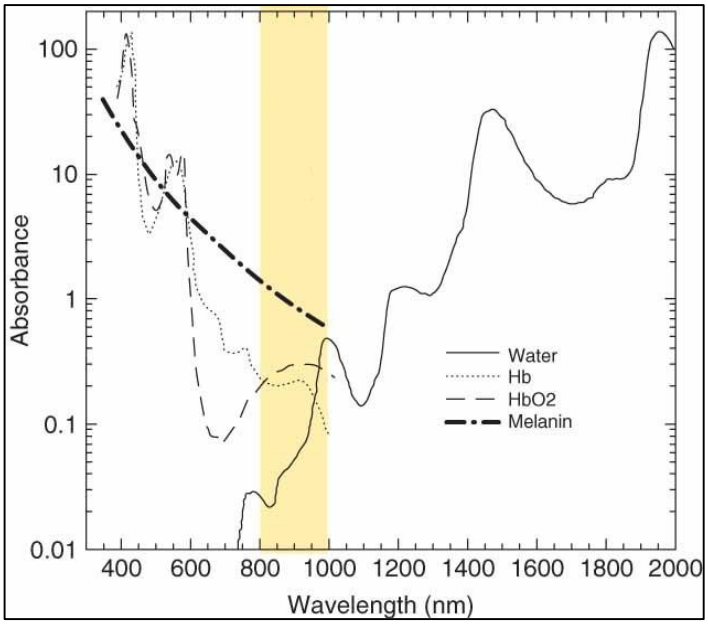

Figure 2.3– Absorption spectra of the main absorbing species of human skin (Retrieved from [21]).

Normally, the epidermis light absorption prevails is mainly due to melanin [22], especially in the shorter wavelengths. Melanin is a polymer found in the melanosome, which is a membranous particle containing several melanin granules. The absorption coefficient (μ_{a_mel}) of single

melanosome depends on wavelength according to [23]:

$$\mu_{a\_mel}(\lambda) = (6.6 \times 10^{11})(\lambda^{-3.33})[cm^{-1}] \quad (2.17)$$

where λ is the wavelength in nanometers. Along with the dominant contribution from melanin, it is also necessary to take into account a small baseline skin absorption. An approximated calculation [24] of the absorption coefficient for this baseline absorption was derived from measurements with samples of neo-natal skin, which corresponded to epidermis without melanin and bloodless dermis. This coefficient, $\mu_{a\_skinbaseline}$, is also a function of wavelength (λ):

$$\mu_{a\_skinbaseline}(\lambda) = (7.84 \times 10^{8})(\lambda^{-3.25})[cm^{-1}] \quad (2.18)$$

Another set of measurements made with bloodless rat skin samples, which are optically similar to neo-natal skin, yielded a slightly different behavior for the dependence of the absorption coefficient with the wavelength [25]:

$$\mu_{a\_skinbaseline}(\lambda) = 0.244 + 85.3\, e^{-\frac{\lambda-154}{66.2}}\,[cm^{-1}] \quad (2.19)$$

Usually, this last expression is the one used to model skin baseline absorption since it reproduces better the experimental data for bloodless tissues.

The combination of baseline skin absorption and the melanin absorption defines the so called net epidermal absorption coefficient:

$$\mu_{a\_epi} = (f_{mel})\left(\mu_{a\_mel}\right) + (1 - f_{mel})\left(\mu_{a\_skinbaseline}\right) \quad (2.20)$$

where f_{mel} is the volume of the epidermis occupied by melanosomes (volume fraction). A light skinned adult has a volume fraction of melanosomes ranging from 1.3% to 6.3%, while the values for moderately pigmented individuals go from 11% to 16%. Dark pigmented Africans have volume fractions between 18% and 43% [26]. Figure 2.4 shows the absorption coefficient of the epidermis for volume fractions of 5%, 13% and 40%. It also shows the absorption coefficient for a single melanosome and the baseline skin absorption according to the measurements reported by Steven Jacques [25].

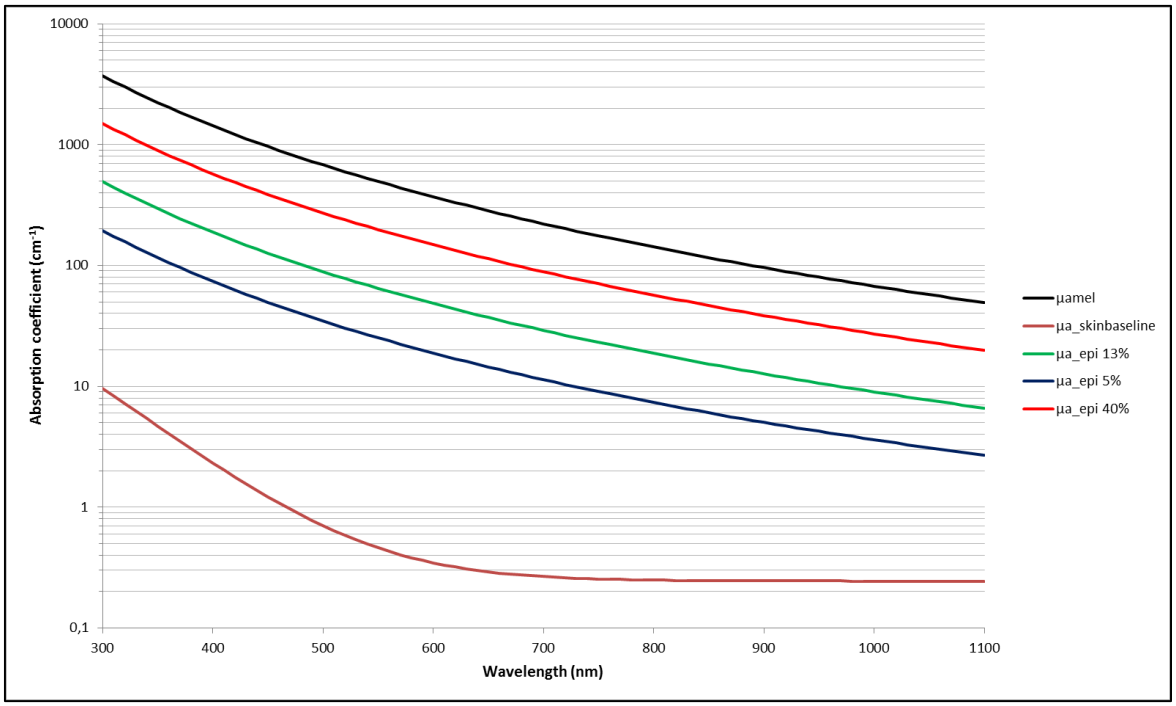

Figure 2.4– Absorption coefficient of the epidermis for volume fractions of 5%, 13% and 40%.

Regarding the dermis light absorption, it depends strongly on the cutaneous blood perfusion, since the dominant absorber is hemoglobin.

In order to get the absorption coefficient of dermis perfused with blood it is necessary to take into account the average volume fraction of blood, f_{blood}.This approach assumes a uniform distribution of blood in the dermis. This results on the following expression for the absorption coefficient of the dermis:

$$\mu_{a\_derm} = (f_{blood})(\mu_{a\_blood}) + (1 - f_{blood})(\mu_{a\_skinbaseline}) \quad (2.21)$$

where f_{blood} is typically 0,2%; μ_{a_blood} is the absorption coefficient of whole blood, defined for a 45% hematocrit; $\mu_{a\_skinbaseline}$ is the baseline absorption coefficient of bloodless dermis, which is similar to the baseline absorption coefficient of melaninless epidermis.

In what concerns scattering, there are no significant differences between the scattering coefficients for the epidermis and the dermis. The scattering anisotropy also does not differ between epidermis and dermis, presenting values in the range of 0.7-0.95, varying with wavelength.

When light propagation in a medium can be adequately described by photon diffusion it is usual to use the reduced scattering coefficient to describe the scattering properties of the medium. This coefficient lumps the scattering coefficient and the anisotropy according to:

$$\mu_s' = \frac{\mu_s}{1 - g} \quad (2.22)$$

The reduced scattering coefficient of the dermis includes contributions from Mie scattering and from Rayleigh limit. The Mie scattering is used when the scatterer dimensions are similar to the light wavelength. The Rayleigh limit of Mie scattering occurs from scatterers much smaller than the photon wavelength. In the dermis, the scattering by large cylindrical collagen fibers is handled using the Mie formalism, while scattering from small collagen fibers and other cellular structures can be treated using the much simpler Rayleigh formalism.

The reduced scattering coefficient of the dermis large collagen fibers was calculated using a cylindrical Mie theory [27]. The dependence on wavelength is given by [26]:

$$\mu'_{s\,Mie} = 2 \times 10^{5} \lambda^{-1.5} \left[cm^{-1}\right] \quad (2.23)$$

The Rayleigh scattering has a λ^{-4} behavior due to scattering by smaller structures like collagen fibers striations. The Rayleigh scattering of the dermis is well reproduced by [26]:

$$\mu'_{s\,Rayleigh} = 2 \times 10^{12} \lambda^{-4} \left[cm^{-1}\right] \quad (2.24)$$

Bashkatov et al. [28] measured transmittance and reflectance from skin samples in the wavelength range 400–2000 nm, using a commercial spectrophotometer with an integrating sphere and the inverse adding–doubling method to determine the reduced scattering coefficients. These authors also individualized contributions from Mie and Rayleigh scattering, obtaining different results, particularly for the Mie scattering:

$$\mu'_{s\,Mie2} = 73.7 \lambda^{-0.22} \left[cm^{-1}\right] \quad (2.25)$$

$$\mu'_{s\,Rayleigh2} = 1.1 \times 10^{12} \lambda^{-4} \left[cm^{-1}\right] \quad (2.26)$$

According to the authors, the discrepancies result from the natural dissipation of tissue properties and the effects of tissue preparation and storage methods. The results obtained by

The scattering behavior of dermis is obtained by summing the Mie and Rayleigh scattering contributions from collagen fibers. The scattering behavior is dominated by Rayleigh scattering at wavelengths below 650 nm and by Mie scattering from fibers for the longer wavelengths. The visible to near-infrared spectral region, which is the region of interest for our work, is affected by both types of scattering. Figure 2.5 shows the wavelength behavior for the reduced scattering coefficient of dermis and for its components, as reported by Steven Jacques [26].

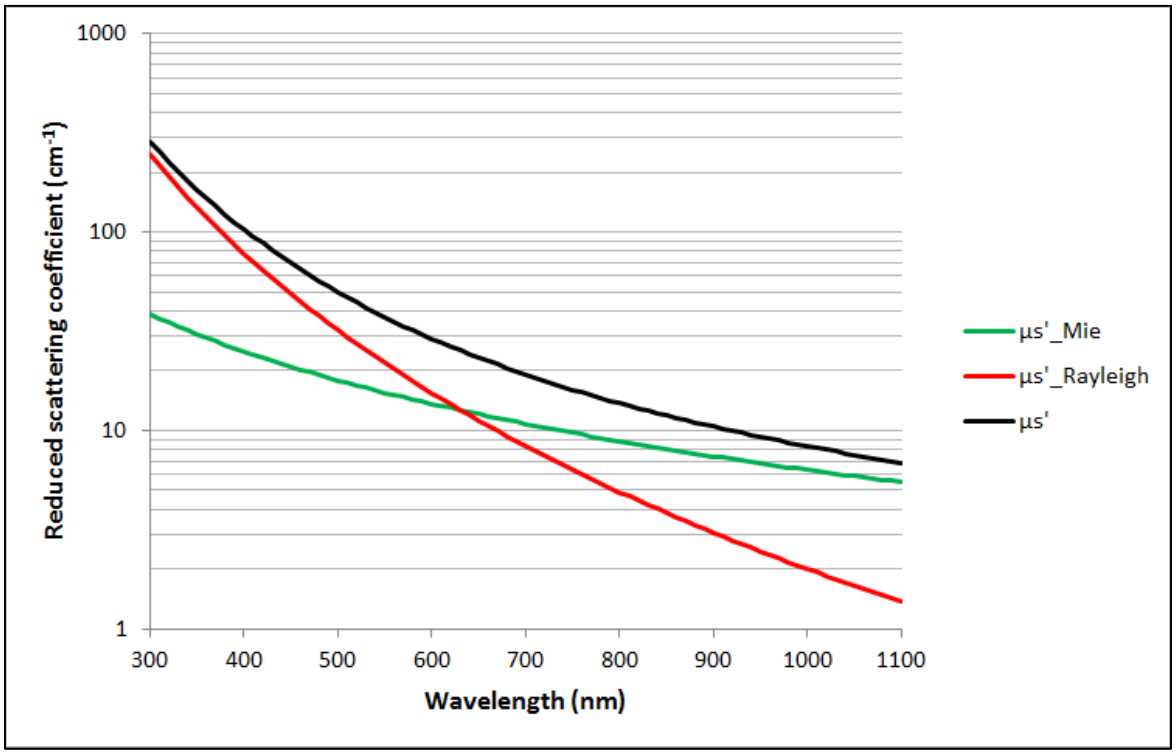

Figure 2.5– Wavelength behavior for the reduced scattering coefficient of dermis and for its components.

There are few published reports concerning measurements of absorption and scattering parameters and their wavelength behavior for muscle tissue and most of them do not cover the wavelengths we used on our work or present results just for a few individual photon wavelengths. One exception is the work from Oliveira et al. [29] that presents measurements on rat abdominal wall muscle in the 400 – 100 nm range. Simpson et al. [30] also presented measurements of absorption and reduced scattering coefficients over a wide wavelength range (618 – 1039 nm). Their dataset is available at the webpage of the Biomedical Optics Research Laboratory from UCL Department of Medical Physics and Biomedical Engineering [31]. Figure 2.6 was obtained from this dataset.

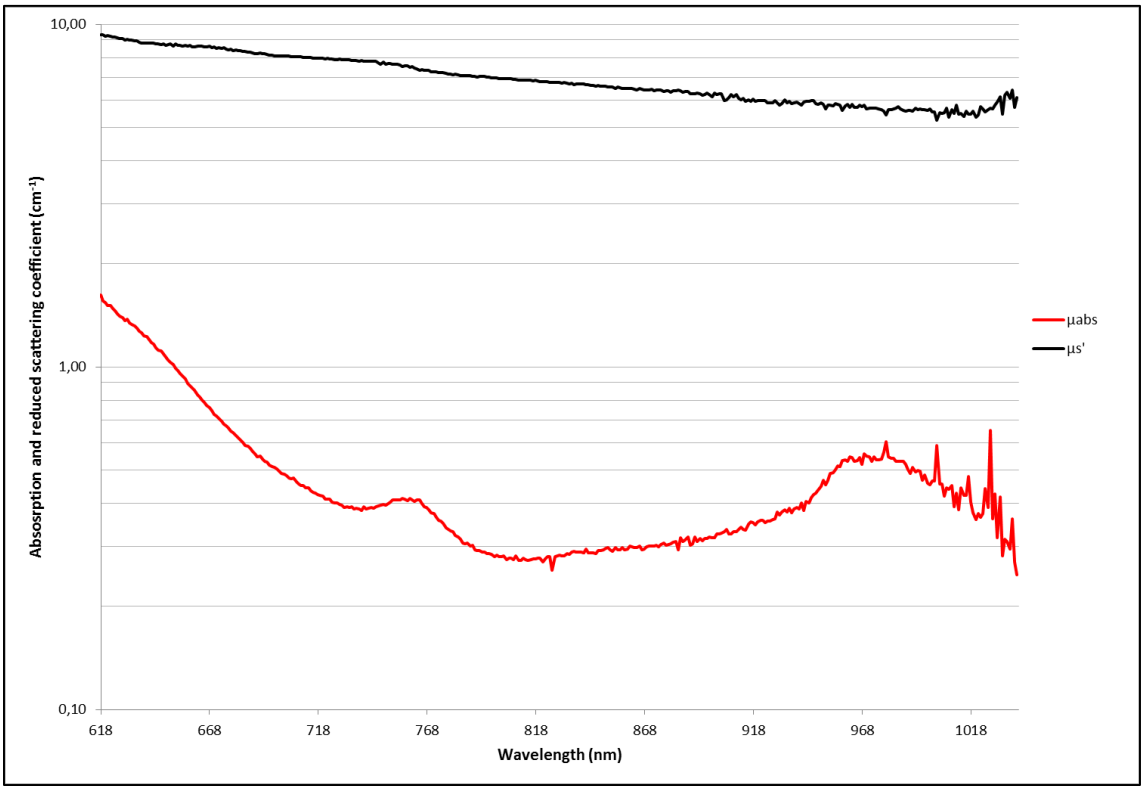

Figure 2.6– Wavelength behavior for the absorption coefficient and the reduced scattering coefficient.

Muscle is made up of muscle fibers which, in turn, are made from myofibrils, which are long cylinders of about 1-2 µm diameter. This size implies Mie scattering. The space between myofibrils is full of sarcoplasma, which contains cellular organelles that will result in scattering in the Rayleigh limit. Light absorption in the muscle is mainly by hemoglobin and water [32].

For laser radiation to produce an effect in biological tissue, it is necessary to deposit energy in that tissue. Yet the type of effect produced does not depend only on the amount of energy deposited. The biological effects of laser radiation are the result from various biophysical mechanisms, always depending on how the energy is deposited in tissue, and particularly the interaction time.

We can group these biophysical mechanisms in the thermal, electrochemical, photochemical and photoablatives categories [33].

2.1.1.2 Thermal Mechanisms

As the name implies, the effects produced by laser radiation through these mechanisms result from the increase of temperature in the tissue. To analyze the effects of light absorption on the tissue temperature, we must consider three different phenomena: the conversion of light into heat, the heat transfer and the tissue reaction. The tissue reaction depends on the final temperature and on the heating time [33].

A thermal effect implies the existence of a heat source. The source is performed by conversion, after absorption, of light into heat. The energy structure of most molecules is composed by

electronic, vibrational and rotational energy levels. Within each electronic level there are several vibrational states; and within each vibrational state there are several rotational states. When a molecule absorbs a photon, it transitions from its ground state to a higher electronic, vibrational, or rotational state, depending on the absorbed photon energy. This is an instantaneous process, occurring in a time-scale of 10^{-15} s. An increase in the vibrational and rotational energy of a molecule manifests in higher temperature of the absorbing tissue by increasing the molecule's internal kinetic energy but mainly by transferring excess energy to other molecules through collisions, increasing their kinetic energy while de-exciting. The process of converting light into heat is very fast (10^{-13} – 10^{-12} s) which ensures that the primary heating volume corresponds, with the irradiated volume.

Heat transfer through tissue will increase the heated volume, defining a secondary volume. It is this volume that should be considered when studying the reaction of the tissue to the heating process. Heat transfer occurs mainly by conduction. The influence of blood flow in the heat transfer inside the tissues (convective transport) is negligible, particularly with short laser pulses, except in highly perfused tissues or in regions with considerable blood flow.

On the next paragraphs we will discuss with more detail the energy absorption process that leads to the increase of temperature in the tissue as well as the heat conduction process resulting in the definition of a secondary heat volume.

Considering a continuous laser beam incident on tissue surface, the light distribution is given by the irradiance (E) and by the position in the tissue $\mathrm{X} = (x, y, z)$ [34].

The absorbed power density corresponds to the absorbed optical energy per volume per unit of time and is expressed by:

$$H = \mu_a \mathrm{E} \tag{2.27}$$

where $\mu_a(\mathrm{X})$ is the absorption coefficient, expressed in m^{-1}.

This expression comes from a one-dimensional model with a pure absorber with light incident on it. The difference between the irradiance at depths of z and $z + dz$ is $\mathrm{E}(z) - \mathrm{E}(z + dz)$. When some power has been absorbed, this difference is non-zero. The absorbed power density corresponds to the irradiance variation per unit of depth:

$$H = \frac{E(z) - E(z+dz)}{dz} \rightarrow -\frac{\partial E}{\partial z} \text{ as } dz \rightarrow 0 \tag{2.28}$$

and the irradiance is: $\mathrm{E} = \mathrm{E}_0 \mathrm{e}^{-\mu_a \mathrm{z}}$. Them:

$$H = -\frac{\partial E}{\partial z} = \mu_a \mathrm{E}_0 \mathrm{e}^{-\mu_a \mathrm{z}} = \mu_a \mathrm{E} \tag{2.29}$$

$H(\mathrm{X})$ is the optical energy deposited in the tissue per unit of volume and per unit of time.

Let us now consider a pulsed laser beam striking the tissue surface. In this case the irradiance will be changing in time according to:

$$\mathrm{E}(\mathrm{X},t) = \mathrm{E}(\mathrm{X})f(t) \tag{2.30}$$

where $f(t)$ is the temporal shape of the pulse. The absorbed power density is:

$$H(\mathrm{X},t) = \mu_a(\mathrm{X})\mathrm{E}(\mathrm{X})f(t) \tag{2.31}$$

and the absorbed energy can be expressed as

$$Q = \int_0^\infty H(\mathrm{X},t)\,dt = \mu_a \mathrm{E}\int_0^\infty f(t)dt \tag{2.32}$$

To calculate the temperature rise due to the absorption of energy it is necessary to use the concept of specific heat capacity, C_p, which is the amount of heat to be supplied to one mass unit of a substance to increase its temperature by one degree, while keeping the pressure constant, and be calculated using:

$$C_p = \frac{1}{\rho}\left(\frac{\partial Q}{\partial T}\right)_p \tag{2.33}$$

The heat increase dQ and the resulting temperature increase dT are linked by:

$$dQ = \rho C_p dT \tag{2.34}$$

where ρ is the density. A good approximation for the specific heat capacity C_p of a biological tissue is:

$$C_p = 1550 + 2800\left(\frac{\rho_w}{\rho}\right)\ [Jkg^{-1}K^{-1}] \tag{2.35}$$

where $\rho_w$is the density of the water and ρ is the tissue density.

The deposited heat will spread by conduction to the surrounding tissue. We can describe the heat flow by the amount of energy that flows through a perpendicular surface, per unit of time, using the so called heat flux vector $\boldsymbol{q} = (q_x, q_y, q_z)$. This heat flux is proportional to the temperature gradient:

$$\nabla T = \left(\frac{\partial T}{\partial x}, \frac{\partial T}{\partial y}, \frac{\partial T}{\partial z}\right) \tag{2.36}$$

The relationship between heat flux and temperature gradient is:

$$\boldsymbol{q} = -\kappa \nabla T \tag{2.37}$$

where the constant k is the thermal conductivity which, for soft tissue can be approximated by

$$\kappa = 0.06 + 0.57\left(\frac{\rho_\omega}{\rho}\right) \tag{2.38}$$

The heat diffusion equation explains how the temperature is transmitted in space during a certain period of time. Let us consider an elementary volume of tissue $dxdydz$ centered in a tissue point with coordinates x, y, z. The principle of conservation of energy establishes that the amount of heat entering the volume $dxdydz$ per unit of time and volume results in an equal increase in heat energy within $dxdydz$, per unit volume and time. Therefore

$$\rho C_p \left(\frac{\partial T}{\partial t}\right) = -\nabla \cdot \mathbf{q} + H \quad (2.39)$$

or, using the definition of heat flux vector,

$$\rho C_p \frac{\partial T}{\partial t} - \nabla \cdot (\kappa \nabla T) = H \quad (2.40)$$

When the tissue thermal conductivity κ is uniform, the heat diffusion equation is:

$$\rho C_p \frac{\partial T}{\partial t} - \kappa \nabla^2 T = H \quad (2.41)$$

or

$$\frac{\partial T}{\partial t} - D\nabla^2 T = \frac{H}{\rho C_p} \quad (2.42)$$

where $D \equiv \frac{\kappa}{\rho C_p}$ is named thermal diffusivity.

As we said, heat can also be transferred by convection. Whenever this process is relevant, the heat carried away by the blood flow leads to the introduction of a loss term H_p in the previous equation:

$$H_p = P\rho_b C_b (T - T_b) \quad (2.43)$$

Here ρ_b is the blood density, $C_b$is the blood specific heat capacity, T_b is the blood temperature and P is the blood perfusion, defined as which is the volume of blood flowing through a unit volume of tissue per second. This change defines the so called bioheat equation:

$$\rho C_p \left(\frac{\partial T}{\partial t} - D\nabla^2 T\right) = H - H_p \quad (2.44)$$

The thermal effect obtained by laser irradiation depends on the final temperature of the irradiated tissue. This is a function of laser irradiance (power per unit area), irradiation time as well as on the thermal dissipation processes [35,36]. Depending on the final temperature, the following effects can occur:

Hyperthermia: it is a moderate temperature increase in tissue, which involves values in the range of 41 °C to 44 °C. This can result in cell death due to changes in the enzymatic processes.

Coagulation: corresponds to irreversible necrosis without immediate tissue destruction. This process involves tissue temperatures in the range of 50 °C to 100 °C, with an irradiation time of the order of few seconds. It produces desiccation and tissue shrinkage through proteins and collagen denaturation.

Volatilization: it involves loss of material. If the temperature exceeds 100 °C there is vaporization of the water contained in the tissue, which leads to the formation of steam. At the border of the volatilization region there will be a region of necrosis by coagulation.

2.1.1.3 Electromechanical Mechanisms

The electromechanical mechanisms arise from phenomena as plasma formation, explosive vaporization or cavitation, which result from optical breakdown of the absorbing medium [33]. These mechanisms have been applied successfully to microsurgery.

For high optical irradiances, in the range between 10^{10} and 10^{13} W/cm^2, the intrinsic absorption coefficient of a material medium changes. This process, which occurs even for transparent media like cell cytoplasm or water, is called non-linear absorption. The intense electrical fields in the focal volume of high irradiance laser beams cause the ionization of the absorbing medium and the generation of quasi-free electrons (electrons promoted to a conduction band). Plasma formation occurs when the density of quasi-free electrons is approximately 10^{21} cm^{-3} [33,37].

The process of plasma formation by absorption of a laser beam after optical breakdown can occur through one of these four mechanisms: multiphoton ionization, quantum tunneling, avalanche (impact) ionization and thermionic emission, although this last one is not relevant in laser microbeam interactions. The relationship between these processes is shown in Figure 2.7.

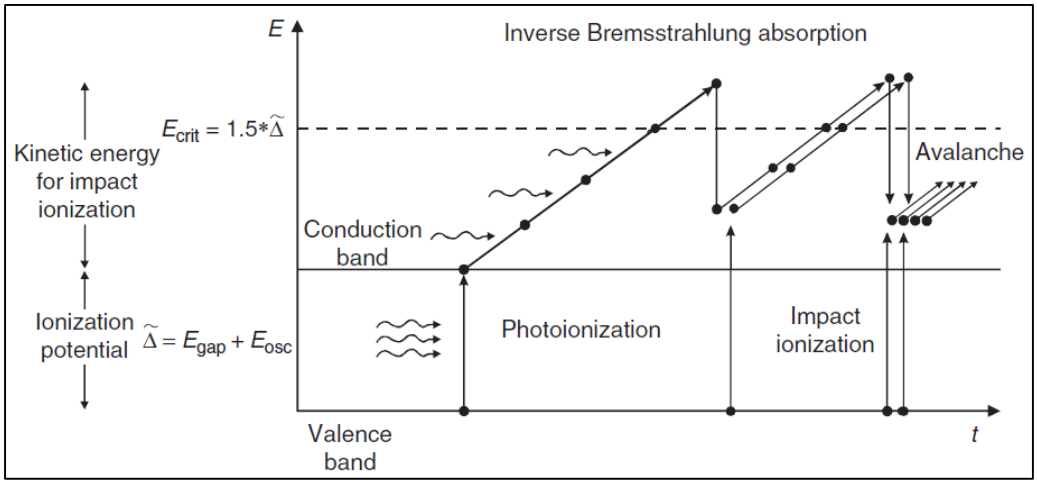

Figure 2.7– Schematic diagram between different generation processes of free electrons (Retrieved from [37,38]).

The production of free electrons can be explained by treating the absorption medium as a semiconductor. In order to raise an electron from the valence to the conduction band it is necessary to provide an energy at least equal to the ionization potential, Δ. In water this accounts to an energy of 6.5 eV. Moreover, as the electrons oscillate while interacting with the electric field of the laser beam, an additional energy is required to ionize the electrons. The total potential ionization potential can be calculated by [38]:

$$\tilde{\Delta} = \Delta + \frac{e^2 + E^2}{4m\omega^2} \quad (2.45)$$

Here *e* is the electron charge, *E* is the amplitude of the electric field, $\omega = 2\pi c/\lambda$ is its angular frequency and *m* is the reduced mass of the electron - hole pair, given by $m = m_c m_v/(m_c + m_v)$.

Multiphoton ionization corresponds to the near-simultaneous absorption of more than one photon. The cross-section of this process is proportional to the n-power of the beam irradiance, with n the number of photons required for ionization. Quantum tunneling is a quantum spontaneous process where an electron crosses the potential energy barrier between the valence and the conduction band and appears in the excited state. These two photoionization processes do not require the existence of free electrons in the focal volume of the laser beam. Therefore, they are adequate to obtain the primary (seed) electron which will start the plasma formation process. The irradiance and the frequency of the laser beam define which of these two photoionization processes dominates.

In the avalanche ionization process, also called cascade ionization process, it is necessary the presence of at least one electron in the conduction band, usually provided by the processes described in the previous paragraph. A free electron within the focal volume will absorbs laser beam photons through inverse Bremsstrahlung absorption. This process is based on a transition, where a free electron is present in the initial and final states. Compliance with conservation laws of energy and momentum implies that inverse Bremsstrahlung absorption must take place in the electric field of an ion A+ or a neutral atom. The process is schematically represented as

$$h\nu + e + A^+ \rightarrow e + A^+ + E_{kin} \quad (2.46)$$

and it increases the electron kinetic energy. If this electron absorbs several photons, its energy will be larger than a threshold value E_{th} and it will be capable of producing an additional free electron through collision with molecules. This is called impact ionization and its threshold energy E_{th} is given by [37]:

$$E_{th} = \left(\frac{1 + 2\mu}{1 + \mu}\right)\tilde{\Delta} \quad (2.47)$$

where $\mu = m_c/m_v$ is the ratio between the masses of the free electron and the hole in the valence band.

The two electrons resulting from impact ionization may in turn acquire enough kinetic energy to ionize another two electrons starting a process of avalanche ionization, where the number of free electrons increases geometrically.

The next equation is the rate equation for the density of free electrons, ρ [37]:

$$\frac{d\rho}{dt} = \eta_{mp} + \eta_{casc}\rho - g\rho - \eta_{rec}\rho^2 \quad (2.48)$$

where η_{mp} is the rate of multiphoton ionization, η_{casc} is the rate of avalanche ionization, g is the rate of electron loss through diffusion and η_{rec} is the electron-hole recombination rate, corresponding to processes where a quasi-free electron returns to the valence band. Computational simulation based on this rate equation make possible to do some generalizations on the dominant mechanisms in plasma formation process:

- Long pulses (nanosecond): avalanche ionization.
- Short pulses (picosecond): Avalanche and multiphoton ionization contribute equally to plasma formation
- Ultrashort pulses (femtosecond): multiphoton ionization and/or quantum tunneling depending on ratio between the frequency of the optical radiation and the tunneling frequency (usually called the Keldysh parameter [37]).

Regarding the dependence of the optical breakdown on pulse width, it was shown that, for pulse durations shorter than 10 ps, electron–ion recombination and electron diffusion are not relevant and it is produced only one set of free electrons during irradiation [38]. The threshold radiant exposure practically does not depend on pulse duration, but the irradiance will increase greatly for shorter pulse durations, since in this regime the generation of free electrons depends greatly on multiphoton absorption or quantum tunneling [39]. This is a consequence of the shorter exposure, with less time available for producing a cascade of ionization events.

For pulses larger than than 10 ps, free electrons are continually generated and recombining during the laser exposure. In this situation, the limiting process is multiphoton absorption that provides the seed electrons to avalanche ionization. As it is necessary to exceed a threshold irradiance to obtain seed electrons, the threshold radiant exposure for optical breakdown must increase for longer pulse durations [37].

The energy absorption provided by the plasma high free electron density leads to local high values of temperature and pressure. These local increases result in thermomechanical processes that are responsible for cell damage. For longer pulse durations (>10 ps), the temperature rise associated with optical breakdown and plasma formation leads to direct vaporization of tissue. The high temperatures and pressures in the laser beam focal volume cause plasma expansion, compressing the surrounding tissue and generating a shock wave. The expansion also cools the plasma,

promoting electron–ion recombination events and the formation of a cavitation bubble. This bubble will expand until the internal pressure of the bubble reaches the vapor pressure of the liquid. When this happens, the hydrostatic pressure of the surrounding tissue collapses the gas bubble.

For shorter pulse durations, the energy density of the plasma is lower and the temperature does not reach a value enough to vaporize the tissue by itself. In this case, the temperature rise acts in combination with the mechanical stresses generated by the thermoelastic response of the tissue, causing bubble formation and fracture. The size of the cavitation bubble and the duration of expansion and collapse increase with pulse duration and energy.

The mechanical stresses resulting from the expansion of cavitation bubbles can result in the permeabilization of cell membranes and the lysis of entire cells around the focal volume [40]. For nanosecond pulses, when the pulse energy is much higher than the optical breakdown threshold, the resulting plasma will have a high energy density and a temperature on the order of several thousand degrees Kelvin. This results in violent effects on the tissue, although with enough precision for laser microsurgery applications [41,42].

With picosecond pulses, multiphoton ionization starts to dominate the optical breakdown process, decreasing the contribution of the avalanche ionization process. Therefore the threshold irradiance for optical breakdown is significantly higher than for nanosecond pulses. The resulting plasma will have lower energy density and temperature, when compared to optical breakdown by nanosecond laser pulses, and will cause much less damage by direct vaporization and by cavitation bubble dynamics [43]. This behavior translates into better precision in microsurgery applications.

Finally, in the femtosecond regime all quasi-free electrons are generated by multiphoton ionization and quantum tunneling. Multiphoton ionization allows a fine adjustment of the free electrons density in the beam focal volume and the generation of plasma with low energy density. Using multiple pulses is then possible to create very controlled photochemical damage of tissue through the generation of cytotoxic reactive oxygen species as well as through photodissociation events. Moreover, the threshold radiant exposure for optical breakdown is minimized, decreasing the energy available for disruptive mechanical effects. This signifies improved precision for localized microsurgery. .

2.1.1.4 Photoablative Mechanisms

The absorption of ultraviolet light can break molecular bonds since the energy of UV photons exceeds the dissociation energy of many molecular bonds. These processes break chemical bonds without material heating, with a result similar to the one obtained with a scalpel. This is called ablative photodecomposition or photoablation.

The photoablation process requires that the rate at which bonds are broken is greater than the rate at which they reform. It also requires irradiance value in the range of 10^7–10^8 W/cm^2 at laser pulse durations in the nanosecond range. Above this irradiance threshold, we obtain a well-defined

ablation depth, which depends on the absorption coefficient of the tissue and on the laser irradiance.

The minimum condition to break a chemical bond is that the absorbed photon energy ($h\nu = hc/\lambda$) exceeds the dissociation or binding energy. In Table 2.1, we can see the binding energies for chemical bonds found commonly in biological tissues, and the maximum laser wavelength that can break such bonds.

Table 2.1– Binding energies and peak wavelengths to break these bonds. Adapted from [33] using data from [44].

Binding	Energy Binding (eV)	Wavelength (nm)
C-H	3.5	353
O-H	4.5	274
H-H	4.6	268
O-O	5.1	242
C-C	6.2	199
N-O	6.5	190
C-N	7.9	156

As shown in Table 2.1 almost all wavelengths correspond to UV radiation. Then, photoablative mechanisms occur mainly for ultraviolet lasers.

It is important to note that photoablation competes with thermal interactions. While in photoablation the energy of a single UV photon is enough to dissociate a molecule, in thermal interactions, the photon energy is not high enough for the molecule to reach a repulsive state leading to dissociation. The molecule is just promoted to a vibrational level within the ground state or to a vibrational level belonging to a low electronic excited state. Afterwards, the absorbed energy dissipates to heat through non-radiative relaxation and the molecule returns to its ground state. The parameter that distinguishes the two interaction mechanisms is the photon energy.

2.1.1.5 Photochemical Mechanisms

Photochemical mechanisms occur when light absorption initiates chemical effects or chemical reactions [45]. The most know example of a photochemical mechanism is photosynthesis. In what concerns the medical application of light, photochemical mechanisms are a major component of Photodynamic Therapy (PDT) and of Low Level Laser Therapy (LLLT), also called Photobiomodulation Therapy. Photochemical mechanisms occur at very low levels of irradiance (approx. 1 W/cm^2) and for large exposure times (duration greater than one second).

A chromophore[1] capable of causing light-induced reactions in other non-absorbing molecules is called a photosensitizer. After excitation, the photosensitizer experiences several simultaneous or sequential decays which result in intramolecular transfer reactions. If these decays leave the photosensitizer in a triplet excited state, there is a considerable probability of triggering photochemical reactions involving other molecular species, due to the long lifetime of the metastable triplet state. At the end of these reactions, highly cytotoxic reactants are produced causing irreversible oxidation of cell structures [45]. This is the rational of PDT where a chromophore receptor acts as a catalyst. The photosensitizer is excited through light absorption, stores the photo energy during a time that may range from milliseconds to seconds and its deactivation leads to toxic compounds, leaving the photosensitizer in its original state.

The potential reaction kinetics of the photosensitizer are listed in Table 2.2.

Table 2.2– Potential reaction kinetics of the photosensitizer.
Adapted from [33] using data from [45].

Excitation	
▪ Singlet state absorption	$^1S + h\nu \Rightarrow {}^1S^*$
Decays	
▪ Radiative singlet decay	$^1S^* \Rightarrow {}^1S + h\nu'$ (fluorescence)
▪ Nonradiative singlet decay	$^1S^* \Rightarrow {}^1S$
▪ Intersystem crossing	$^1S^* \Rightarrow {}^3S^*$
▪ Radiative triplet decay	$^3S^* \Rightarrow {}^1S + h\nu''$ (phosphorescence)
▪ Nonradiative triplet decay	$^3S^* \Rightarrow {}^1S$
Type I reactions	
▪ Hydrogen transfer	$^3S^* + RH \Rightarrow SH^{\cdot} + R^{\cdot}$
▪ Electron transfer	$^3S^* + RH \Rightarrow S^{\cdot -} + RH^{\cdot +}$
▪ Formation of hydrogen dioxide	$SH^{\cdot} + {}^3O_2 \Rightarrow {}^1S + HO_2^{\cdot}$
▪ Formation of superoxide anion	$S^{\cdot -} + {}^3O_2 \Rightarrow {}^1S + O_2^{\cdot}$
Type II reactions	
▪ Intramolecular exchange	$^3S^* + {}^3O_2 \Rightarrow {}^1S + {}^1O_2^*$
▪ Cellular oxidation	$^1O_2^* + cell \Rightarrow cell_{ox}$
Carotenoid protection	
▪ Singlet oxygen extinction	$^1O_2^* + {}^1CAR \Rightarrow {}^3O_2 + {}^3CAR^*$
▪ Deactivation	$^3CAR^* \Rightarrow {}^1CAR + heat$

[1] A chromophore is the part (atom or group of atoms) of a molecular entity in which the electronic transition responsible for a given spectral band is approximately localized. (Glossary of terms used in physical organic chemistry (IUPAC Recommendations 1994))

Mechanisms presented here are summarized in Figure 2.8, which was created from experimental observations. The boxes enclose points that correspond to optimal variables determined experimentally obtained from several published reports [45] on a large variety of medical applications. Two important conclusions can be drawn from this figure. The first is that for producing an effect, it is necessary an energy dose between 10 and 1000 J/cm^2. The data are not scattered through the graph but aligned along the diagonal inside the band limited by the lines corresponding to those doses. This indicates a correlation between radiant power and interaction time, which is valid for 12 orders of magnitudes of these variables but occurs for a small range of energy doses of just two orders of magnitude, showing that the specific energy dose for achieving a biological effect based on any of the previously described interaction mechanisms is almost constant. The second is that for any dose between 10 and 1000 J/cm^2, it is possible to obtain any of the four mechanisms of interaction, as shown by travelling along the diagonal lines of constant dose. It is the interaction time that defines the interaction mechanism. Continuous and quasi-continuous wave irradiations (long interaction time) are able to trigger thermal and photochemical mechanisms. Photoablative and electromechanical mechanisms require very high irradiances, only achievable with very small interaction times. This means short pulsed lasers (nano, pico and femtosecond pulsed lasers).

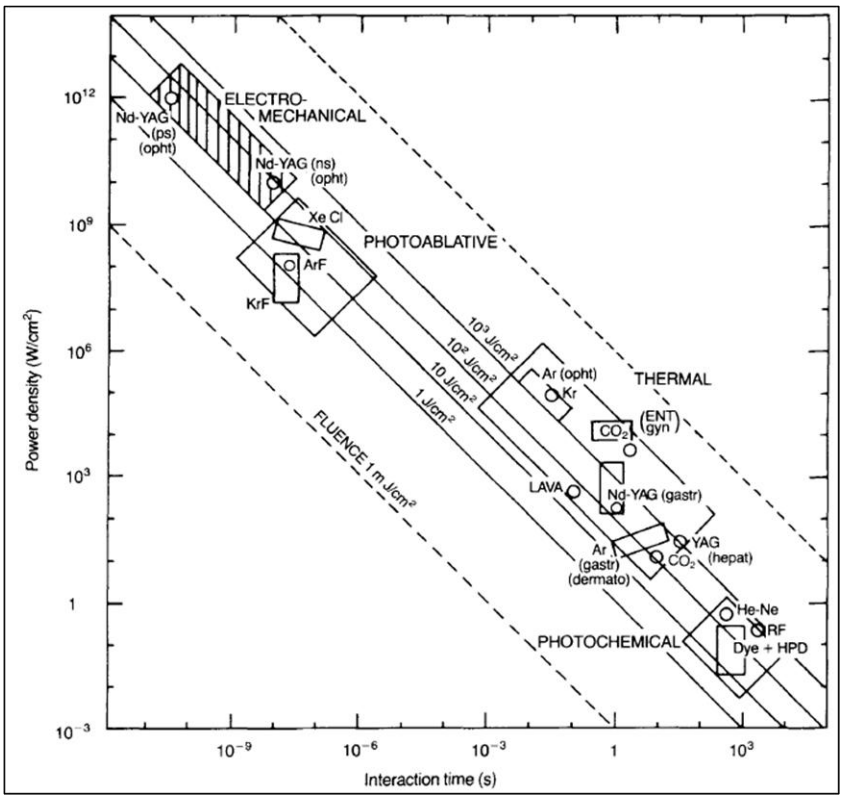

Figure 2.8– Medical laser interaction map. Diagonals lines represent a constant fluence (energy dose). The boxes enclose experimental points corresponding to reported optimal values of variables in applications of lasers in medicine (Retrieved from [45]).

In LLLT, cells or tissue are exposed to low powers of red and near infrared (NIR) radiation. The term ‘‘low level’’ is used because the radiant powers are below those required for ablation, cutting, and tissue coagulation. This means that the powers used in LLLT are lower than those required by thermal mechanisms. LLLT is based on a photochemical mechanism.

The current view is that LLLT acts by inducing a photochemical reaction in the cell after photon absorption by components of the cellular respiratory chain within the mitochondria [46]. The chromophore involved in this process can be identified through the comparison of the action spectra for the response to red and NIR radiation with the absorption spectra of membrane-bound complexes in the inner membrane of the mitochondria [47]. This process resulted in the indication of complex IV, also known as cytochrome c oxidase (CCO), as the chromophore responsible for starting the cellular response to LLLT [48]. CCO is a component of the respiratory electron transport chain [49]. The electron transport chain generates a proton gradient that is used to produce ATP. The absorption of light by CCO results in increased ATP production and electron transport. From here a cascade of cell and molecular events takes place that result in the treatment effects obtained with LLLT. These events will be detailed ahead, in section 2.5.

2.2 Inflammatory process on skeletal muscle

Inflammation is an early response to muscle tissue injury or infection and involves coordination between the immune system and the injured tissue.

Injuries of skeletal muscle, such as contusions and strains, are frequently found in contact sports, especially in rugby and football, and also in no-contact sports as athletics [50-52]. Many studies say that more than 90% of the injuries are caused by traumas in legs and arms [53,54]. Depending on the severity of the affections it is important a correct election of the adequate treatment.

The severity of injury and the vascularization of the affected zone can give us information on the magnitude of the inflammatory response, and some studies [55,56] have showed that by limiting the inflammation during the neutrophil phase, damage, pain and swelling will also be limited, promoting a more quick rehabilitation. This fact is one of the main reasons of our focus in this study.

If we consider the time-course of the skeletal muscle injury response, we verify that the healing process is long and includes different phases, as we can see on Figure 2.9 and Figure 2.10, where it is possible to identify three overlapping events in muscle regeneration. The first one is the destruction phase, also known as the neutrophil phase for the important role of these white blood cells. The repair is the second event and is focused on macrophages. The final event is remodeling through scar apoptosis and scar maturation [57].

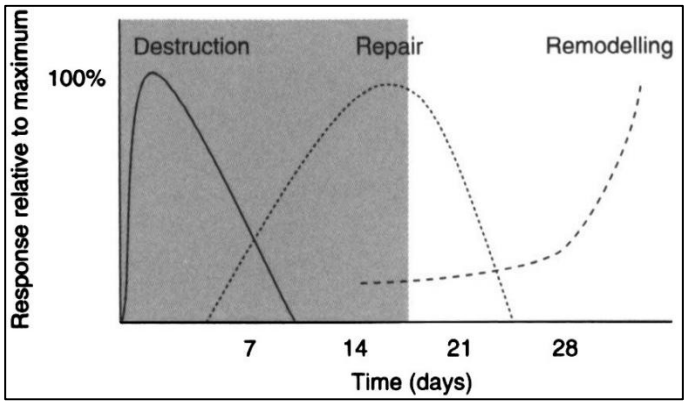

Figure 2.9– Three overlapping events in the muscle regeneration after injury (Retrieved from [57]).

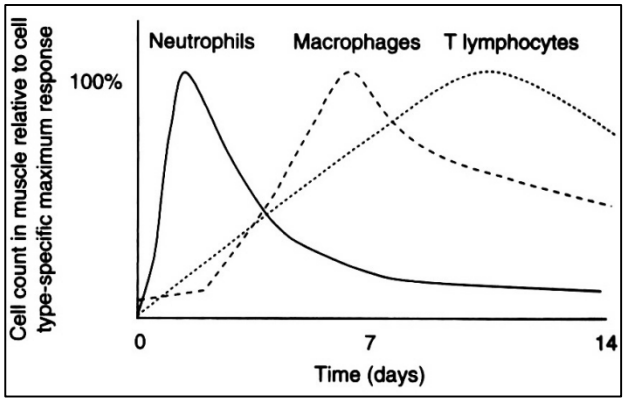

Figure 2.10– Muscle regeneration events following a trauma with indication of the most intervening peripheral immune cells (Retrieved from [58]).

Neutrophils have two functions after the trauma: clear the necrotic debris [57] and release pro-inflammatory cytokines (IL-1β, IL-6 and TNF-α) [58]. Macrophages help muscle regeneration by supplying inflammatory and growth-related mediators and finally T lymphocytes attack antigens directly and help control the immune response [59,60].

2.2.1 Acute inflammation

The acute inflammatory reaction begins with vascular coagulation and the detection of pathogens or cellular injury by pattern recognition receptors (PRR). The signaling through PRR induces inflammatory mediators which act on blood vessels to promote the recruitment of leucocytes and exudation of plasma into the damaged tissue. Inflammation is mediated by soluble proteins (cytokines and growth factors) acting between leucocytes and nonhaematopoietic cells, such as fibroblasts and vascular endothelial cells, within the injury. After elimination of microorganisms and necrotic tissue, leucocyte recruitment ceases and apoptotic neutrophils are phagocytized by macrophages. Finally tissue repair and remodeling involves the development of new blood vessels (angiogenesis), resurfacing of the wound (re-epithelialization) and collagen deposition [61]. Figure 2.11 presents these stages of the acute inflammatory response.

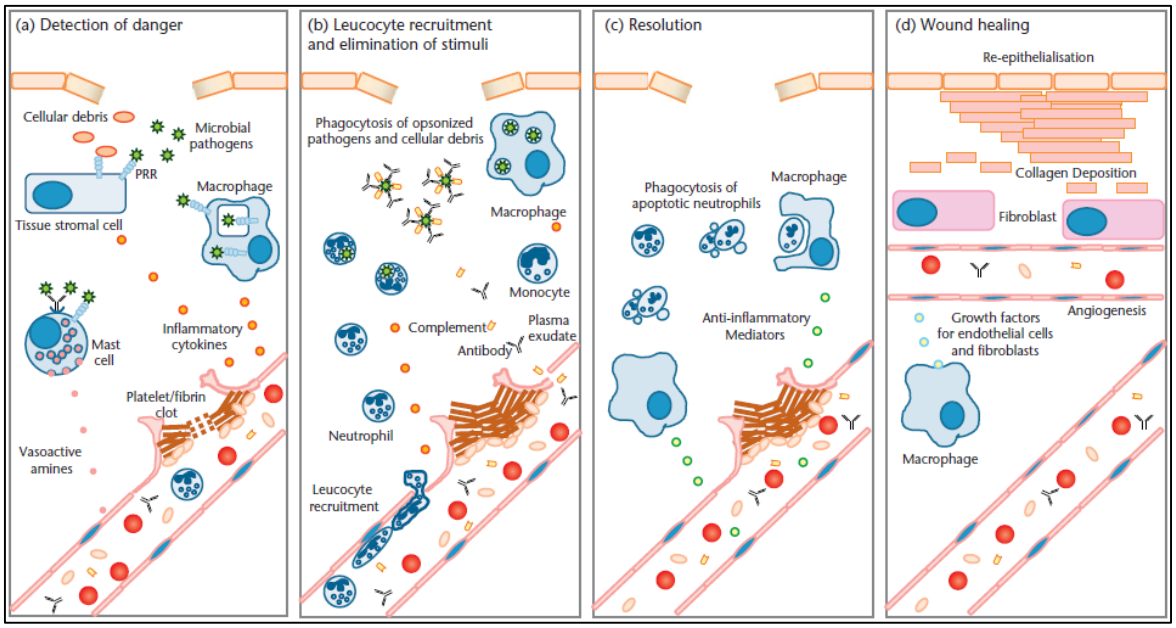

Figure 2.11– Stages of the acute inflammatory response: detection of infection or injury; leucocyte recruitment and suppression of pathogens and cellular debris; resolution of inflammation and wound healing (Retrieved from [61]).

Tissues inflammation is a process that includes a set of molecular, cellular and vascular events that have as aim to defend the body against physical, chemical or biological attacks. Inflammatory process has some fundamental characteristics: First, the response is focused in order to limit the combat area with offending agent. Secondly, inflammatory response is immediate and urgent, and therefore predominantly non-specific, but may encourage the development of a specific response. Third, inflammatory focus attracts immune cells from surrounding tissues. Vascular changes will also promote the arrival of such cells [62,63]. Summarizing:

1. Mediators release. These are molecules, most of them elementary structure, synthesized or released by cells that are already present in all tissues (mast cells, macrophages, dendritic cells, histiocytes). These mediators are responsible for inflammation clinical signs (heat, redness, and tumor pain).

2. Effect of mediators. Once released, these molecules cause vascular changes (vasodilation and increased permeability) and chemotactic effects and help to recruit immune cells to the inflammatory focus. Vascular changes allow fluid and protein exudation (fibrin and immunoglobulin) from plasma into tissue.

3. Arrival of immune system cells. Vascular changes enable leukocytes transfer from blood vessels into tissues. The first cells to arrive at the inflammatory focus are neutrophils that will remove the pathogen by phagocytosis. At a later stage, monocytes also arrive at the inflammatory focus. In addition to differentiate into macrophages, the monocytes act as antigen presenting cells to specific T and B cells, initiating specific inflammatory response [37,64]. Macrophages and lymphocytes are responsible for the synthesis of several cytokines involved in inflammation process.

4. Inflammatory process regulation. Like most immune responses, the inflammatory process integrates inhibitory mechanisms aimed at balance or ending the process. Inflammatory process should end when it is no longer necessary to prevent damage to adjacent tissues. Leucocytes present in inflamed tissue release inflammatory mediators that ensure inflammatory process regulation. Various cytokines are included in these mediators.

5. Reparation. This phase includes processes aiming at full or partial repair of tissue damaged by pathogens or by inflammatory response. These processes emphasize the recruitment of fibroblasts to produce collagen, epithelial cell proliferation and angiogenesis. In this stage it is also important to mention the skeletal muscle satellite cells or Mauro´s cells [65]. They are mononucleated cells [66] and have one surface in contact with the myfiber basal lamina and the other one in contact with its plasmalemma with a narrow gap of about 15 nm between the two cells [67]. They proliferate following muscle trauma [68] and develop new myofibers. After several cell divisions, the satellite cells begin to combine with the damaged myotubes and undergo further differentiations and maturation, with peripheral nuclei as in hallmark of the skeletal muscle regenaration. Upon minimal stimulation, they might continue the myogenic differentiation process [69].

2.2.2 Expression of cytokines anti- and pro-inflammatory regulation

Several studies have demonstrated an effect of low power laser light in the expression of pro- and anti-inflammatory cytokines. Most of these studies were performed with cell cultures with only a small number of animal studies reported [13,70]. Almost nothing is known about the influence of laser irradiation (wavelength, dose, power and interaction duration) parameters in the regulation of the expression of these cytokines.

Cytokines are low molecular weight proteins produced by different types of immune cells. Cytokine production is triggered when these cells are activated by stimuli such as pathogens. Cytokines act in communication between cells, promoting induction and regulation of immune response [71].

As mentioned, the cellular component of the inflammatory process results in the regulation of the expression of several cytokines with pro-inflammatory and anti-inflammatory action, with particular emphasis on various interleukins. These agents perform different activities such as recognition of foreign antigens by T cells, proliferation and amplification of activated T cells, attraction of macrophages and promotion of phagocytosis. Among cytokines are emphasized [72,73]:

Interleukin 1β (*IL-1β*) - is an inflammation mediator synthesized by monocytes and macrophages. Its most important action occurs (in combination with TNF-α) during the systemic response known as acute phase response and translates into vascular endothelium (modifications of endothelial cell surface thrombogenicity and leukocyte adhesivity, resulting in the induction of new endothelial cell proteins), hypothalamus (fever) and hepatocytes effects (induction of acute phase proteins). It also plays roles in inflammation specific response, such

as leucopoiesis regulation during an infectious process. The IL-1β leads to TNF-α release, and then it stimulates T lymphocytes to produce specific antibodies.

Tumor Necrosis Factor Alpha (*TNF-α*) - Like IL-1β and in association with it, is involved in stimulating the acute phase response. TNF-α induces cell death by apoptosis and promotes neutrophils activation.

Interleukin 2 (*IL-2*) - Originally known as T Cell Growth Factor (TCGF), is the major cytokine responsible for T lymphocytes progression from G1 phase into S phase of cell cycle. IL-2 is produced by CD4+ T cells, and in a lesser extent, by CD8+ cells. It functions as an autocrine growth factor, acting on the same cells that produce it. IL-2 also stimulates NK cells growth, facilitating their cytolytic action, and B lymphocytes proliferation.

Interleukin 6 (*IL-6*) - IL-6 is secreted by T cells and macrophages to stimulate immune response to trauma or other tissue injury leading to inflammation. It promotes synthesis of proteins on the acute phase. Its role as an anti-inflammatory cytokine is mediated through its inhibitory effects on TNF-α and IL-1 β [74].

2.2.3 Muscle inflammation models

There are mainly three muscle injury models, overtraining, carrageenan injection and drop-mass weight.

Overtraining model is based in excessive exercise, with inadequate rest or progressive load training, which can result in acute inflammation [75-77]. This model is useful to compare the action of different types of drugs. According to published studies, there is a large number of inflammation injuries concerning excessive training or exercise, making this processes an important topic in healing treatments. K. Ostrowski et al. [78] suggest that the balance between anti- and pro-inflammatory cytokines limits the magnitude and duration of the inflammatory response in strenuous exercise. At the same time, F. Zaldivar [79] showed that exercise increase the numbers of circulating pro- and anti-inflammatory cytokines and growth factors, preparing the organism for the post-exercise period or for possible tissue injuries and adaptation.

The injection of carrageenan is a well-known model of inflammation with local response, which can produce acute inflammation and hyperplasia [80]. R. Radhakrishnan et al. [81] tried to demonstrate the capacity of carrageenan to also produce chronic inflammation in the gastrocnemius muscle, and concluded that with 3% carrageenan injected, the inflammation transforms from acute to chronic.

In our case, a drop-mass weight model was chosen since it satisfies the requirements of reproducibility and invasiveness. In 2004, J. R. Bunn et al. [82] presented biomechanical, histomorphological and immunohistochemical evidences of the effectiveness of the drop-mass weight model, namely reliability in the energy transmission, proportions between inflammatory infiltration and damaged muscle, and release of pro-inflammatory cytokines.

F. A. Facio and V. Balisardo Minamoto [83] published another assessment of the model, based on morphological muscle analyses in short and long-term after contusion. They concluded that, after 28 days of the trauma, muscle fibers were still damaged, suggesting more attention in muscular activities, to avoid and prevent risk of re-injuries.

2.2.4 Inflammation cytokines in serum

Measurements of cytokines concentration and cytokines expression have been used extensively as markers of inflammation process and for assessing the efficacy of LLLT. In the majority of LLLT studies, cytokines concentrations are measured in a muscle sample homogenate, either by enzyme immunoassay technique (ELISA) test or by measuring the cytokines mRNA expression through reverse transcription polymerase chain reaction (RT-PCR). However, it is possible to measure cytokines concentration on the systemic blood serum for the same purpose. This quantification method allows sampling during treatment without sacrificing animals and can be applied to human studies. In our experiments we choose to measure the cytokines concentration in the serum.

It was proposed that the systemic effects of optical radiation are in part due to rapid (first 30–60 min) changes of cells and plasma components of circulating blood after local irradiation of the body surface [84]. These changes happen in the structural and functional state of all types of peripheral blood cells. The same study showed that these changes are also observed by after direct irradiation *in vitro* of blood samples of the same volunteers and subsequent mixing of these samples with a larger volume of non-irradiated autologous blood. This lead the authors to postulate that the systemic effects observed after transcutaneous irradiation are a consequence of the modification of small amounts of blood and the posterior action of this blood on the circulating volume.

In a posterior study [85], the authors were able to show, through a randomized, placebo-controlled, double-blind trial, that exposure of a small area of the body surface to light resulted in changes in the concentration of cytokines in the human peripheral blood. In particular, they observed a rapid decrease in the pro-inflammatory cytokines, namely TNF-α, IL-6 and IFN-γ, and an increase in the anti-inflammatory cytokines IL-10 and TGF-β.

The use of systemic blood samples to assess the effects of LLLT is supported by the above mentioned studies. This methodology was already used in the assessment of LLLT effectiveness. One good example is the study reported by De Marchi et al. [86]. The authors did a randomized double-blind placebo-controlled crossover trial where volunteers followed a progressive intensity running protocol on a motor-drive treadmill until exhaustion. LLLT was performed 5 minutes before this protocol. Systemic blood samples were collected before and 5 minutes after the exercise protocol. These samples were used to assess the effect of LLLT by quantifying the levels of oxidative damage to lipids and proteins, the activities of superoxide dismutase and catalase and the markers of muscle damage creatine kinase and lactate dehydrogenase.

Focusing in the evaluation of LLLT using inflammation cytokines, we can mention a study [87] where the authors evaluated the effect of LLLT in the inflammation profile of Wistar rats with heart failure. LLLT was applied on the gastrocnemius muscle of the rats. Its effect was measured on systemic blood samples and on muscle tissue homogenates through the quantification of cytokines (TNF-α, IL-6 and IL-10). The quantification of cytokines concentrations in systemic blood was also used in a study where laser phototherapy was applied to Wistar rats immediately after cryogenic brain injury [88]. The levels of IL-1β, IL- 6, IL-10 and TNF-α were measured by ELISA, in brain and blood samples. We can also cite a very recent study [89], where the effect of LLLT on the severity of oral mucositis in patients undergoing hematopoietic stem cell transplantation was evaluated by measuring the levels of inflammatory mediators (TNF-α, IL-6, IL-1β, IL-10, TGF-β, metalloproteinases, and growth factors) in saliva and blood.

2.3 LLLT effects on inflammatory processes: animal and clinical studies review

In the recent years, six systematic reviews have found clear evidence for the positive effects of LLLT:

1. A systematic review of surgical and conservative interventions for frozen shoulder found "strong evidence" for LLLT [3].
2. The International Association for the Study of Pain (IASP) found "strong evidence" for Low Level Laser Therapy on myofascial pain syndrome. The IASP fact sheet on myofascial pain now includes lasers as an evidence-based treatment for trigger points [90].
3. The British medical Journal clinical evidence recommendations for tennis elbow 2011 now include LLLT [4].
4. The American Physical Therapy Association guidelines recommend LLLT for treating Achilles tendonitis [9].
5. A systematic review published in Lancet found that "LLLT reduces pain immediately after treatment in acute neck pain and up to 22 weeks after completion of treatment in patients with chronic neck pain" [7].
6. The World Health Organization (Bone and Joint Task Force) found LLLT for neck pain "more effective than no treatment, sham, or alternative interventions" [6].

None of these reviews focus on the use of LLLT for treating muscle inflammation. However, there are many published studies showing a positive effect of LLLT on inflammation treatment. Here we will review those studies. We will include in the review the use of LLLT on systemic inflammation processes, like rheumatic diseases, and also on muscle fatigue and injuries caused by exercise. Regardless of the mechanism that causes muscle damage, the recovery process always follows the same path involving degeneration, inflammation, repair and remodeling [91].

In 2007 it was published a literature review on the effects of LLLT on inflammatory and rheumatic diseases [92], listing 82 laboratory tests, performed in cell cultures or in animals, and 11 randomized controlled clinical trials on the effects of laser therapy in inflammatory process and

metabolic disorders of ligaments, tendons and muscles. Seventy-one of the laboratory tests produced positive results in one or more parameters evaluated, while 7 of the 11 trials showed positive results in reducing the levels of Prostaglandin E2 (PGE2), edema, infiltration of inflammatory cells and erythrocyte sedimentation rate.

In seven tests performed in animal models of rheumatoid arthritis, levels of PGE2 inflammatory marker were significantly reduced with LLLT application. These studies have produced some contradictory results. While three studies [13,93,94] observed inhibition of tumor necrosis factor release (TNF-α), another study [95] showed no anti-inflammatory effect of LLLT in blood monocytes and endothelial cells of veins, or no effect on TNF-α. For the authors of the literature review, this contradiction shows that there is a narrow therapeutic range for inhibiting the release of TNF-α by LLLT action.

A similar conflict occurs with the reduction of levels of interleukin-1β: while a test shows a partial reduction in the levels of interleukin-1β [96], another study, where LLLT was applied in patients for periodontal inflammation treatment, found no effect on interleukin-1β, despite it observed a significant inflammation modulation in gingival crevicular fluid and plaque [97].

Others results reported in animal models studies were reduced PGE2 level in blood serum [98], significant reduction of cyclooxygenase 2 (COX2) mRNA levels [99,100] and reduced levels of plasminogen in periodontal ligament cells [101]. The literature review also found five studies in animal models reporting a reduction of infiltration of inflammatory cells after LLLT [94,102-105]. The same result was obtained in a clinical trial, where LLLT was applied in specific areas of knee synovial membrane of patients with rheumatoid arthritis [106]. In what concerns edema, all animal studies that evaluated edema volume showed a significant reduction after LLLT. The same occurs in two clinical trials where LLLT was used for treating ankle sprains [107] and after flexor tendon surgery [108]. In both cases LLLT was applied in multiple points since single point application, has proven to be unable to produce clinical effects, particularly in ankle sprains treatment [64].

There are animal studies comparing LLLT action with non-steroidal anti-inflammatory drugs (NSAIDs). The results consistently show that doses equivalent to clinical doses of NSAIDs produce the same kind of effects obtained with LLLT application [94,109-111].

The methods used on LLLT anti-inflammatory efficiency trials are summarized in Table 2.3. It is clearly shown that there is a large variability in the power density (irradiance) and dose (radiant exposure) values between different studies. This is one of the issues that most contributes to the controversy around LLLT as a therapy. An LLLT treatment requires the choice of several treatment and irradiation parameter (wavelength, radiant exposure, power density, pulse structure and treatment timing). If these parameters are not chosen adequately the effectiveness of the treatment is reduced and may even result in negative outcomes. It is now clear that many LLLT studies resulted in negative results just due to inappropriate selection of wavelength and energy dose [49]. From the literature analysis, authors of this review were able to identify a window of energy dose

for LLLT anti-inflammatory effect. According to the authors, this window lies between 2 and 14 J.

Table 2.3– Used methods in laboratory tests assessing LLLT anti-inflammatory (Adapted from [92]).

First Author, Model	Inflammatory Induction by	Laser Type, Mean Output Power	Power Density [mW/cm^2]	Dose [Joules/cm^2]
Campana, arthritis animal	Urate crystals	633nm, 5 mW	6	0,72
Honmura, rat paw edema	Carrageenan	830 nm, 60 mW	32	9,6
Honmura, rat paw edema	Carrageenan	830 nm, 60 mW	32	9,6
Shimizu, ligament cells	Mechanical stretch	830 nm, 30 mW	12	2,3 – 7,4
Ozawa, ligament cells	Mechanical stretch	830 nm, 700 mW	6 – 13	3,9
Sattayut, myofibroblast cells	Carrageenan	820 nm, 200 mW	22	4 – 19
Campana, arthritis animal	Urate crystals	633 nm, 30 mW	30	8
Sakurai, fibroblast cells	Lipoly-saccharide	830 nm, 700 mW	21	1,9 – 6,3
Nomura, fibroblast cells	Lipoly-saccharide	830 nm, 50 mW	6 – 13	4 – 7,9
Dourado, mice	Snake venom	904 nm, 50mW	90	2,8
Albertini, rat paw edema	Carrageenan	660 nm, 2,5 mW	31	7,5
Ferreira, rat paw edema	Carrageenan PGE_2	633 nm, 12 mW	171	7,5
Pessoa, rat wound	Excised skin flap 0,5 cm^2	904 nm, 2,8 mW	5	0,66
Lopes-Martins, mice pleurisy	Carrageenan	660 nm, 2,5 mW	31	7,5
Aimbire, rat lung injury	Bovine serum	660 nm, 2,5 mW	31	7,5
Aimbire, rat skeletal muscle	TNF-α	655 nm, 2,5 mW	31	7,5
Rizzi, rat skeletal muscle	Blunt trauma	904 nm, 45 mW	118	5
Lopes-Martins, rat paw edema	Carrageenan	820 nm, 200 mW	4750	142,5
Median results		**825 nm, 30 mW**	**31 mW/cm^2**	**7,5 J/cm^2**

After the publication of this literature review the number of published animal and human studies considering LLLT action in inflammatory processes increased substantially. Here, we present representative studies looking in more detail the methodology used, namely the used inflammation model and the applied treatment and irradiation parameters.

One study [112] compared therapeutic effect of 904 nm GaAs laser (150 mW, dose 60 J/cm2, area 1 cm^2) with 1 MHz pulsed ultrasound (0.3 W/cm^2, area 1 cm^2), when applied to inflamed skeletal muscle of Wistar rats. Animals received an intramuscular hydrochloride bupivacaine injection in tibialis muscle in order to induce an inflammatory process. Application of laser therapy and ultrasound started 24 hours after the injection. Muscle samples were retrieved from 35 animals for histological analysis. The results show that both treatments can act as anti-inflammatory. However, while the laser seems to have anti-inflammatory effect during all periods observed, the ultrasound was only able to induce reduction of inflammatory response after seven days.

Another study [113], used two different wavelengths in a paw rat edema induced by carrageenan.

Thirty-two male Wistar rats were divided into four groups. One group received sterile saline injection, while the three other groups received a sub-plantar injection of carrageenan (1 mg/paw) to induce inflammation. After one hour, LLLT was applied in two groups injected with carrageenan, using 30 mW lasers with continuous emission. One group was treated with a 660 nm laser while the other was irradiated at 684 nm. The energy doses were 7.5 J/cm^2. Measurements 4 hours after injection showed that the groups subjected to LLLT developed significantly less swelling than the control group. Similarly, a significantly lower number of inflammatory cells was found in muscle tissue and sub-plantar conjunctive in LLLT groups than in the control group. The results are shown in Figure 2.12. Authors concluded that for the administered doses, both lasers are effective in reducing edema and migration of inflammatory cells.

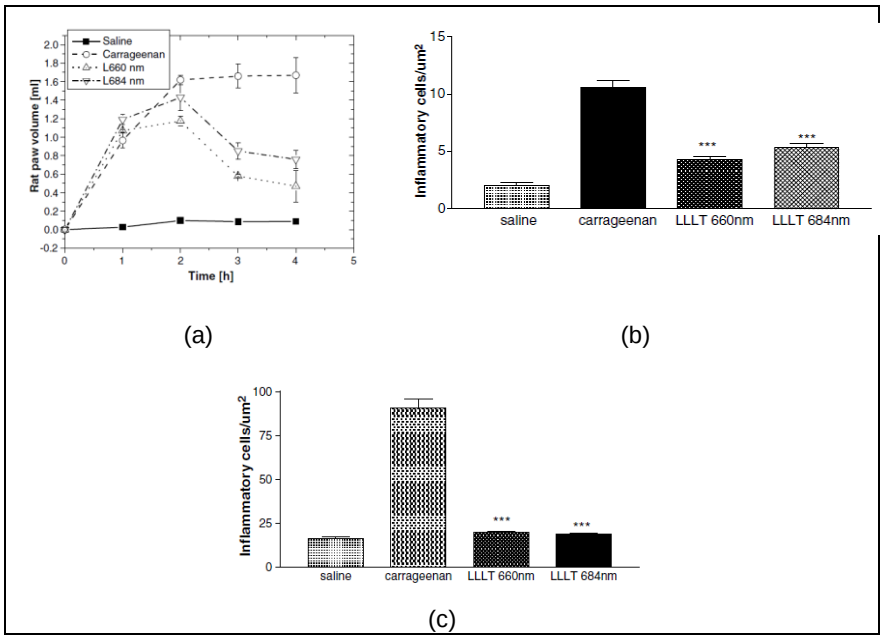

Figure 2.12– (a) Volume evolution of rats paw edema in Albertini et al. study [113]. (b) Inflammatory cells density in plantar muscle tissue. (c) Inflammatory cells density in sub-plantar.

On studies on humans, we can refer a study performed on seven patients with bilateral tendinitis in Achilles tendon. In this case, an irradiation device was used, consisting in three laser diodes placed in a linear arrangement, separated by intervals of 9 mm. Lasers emitted at 904 nm, the peak power for each pulse was 10 W and pulse duration was 200 ns, with a frequency of 5 kHz. The irradiated area was 0.5 cm^2 resulting in a power density of 20 mW/cm^2. Each patient was treated for 180 seconds, and the dose of active treatment was 1.8 J for each of three points along the Achilles tendons, giving a total of 5.4 J per tendon [114]. Treatment results were evaluated by measuring PGE2 concentration in surrounding tendon tissue and blood flow by Doppler ultrasound. Pain was measured using an algometer, an instrument to determining sensitivity to pain produced by pressure.

The PGE2 concentration decreased after 1 hour of treatment and continued to decline until the last inspection carried out at 105 minutes. Doppler ultrasound showed changes in very small blood flow, almost imperceptibles. After treatment it was observed that pain threshold increased in pressure algometry (it was necessary to exert more pressure to obtain pain response) in patients treated with laser. The conclusion exposed in this publication was that LLLT is an effective in treatment for Achilles tendinitis rehabilitation by reducing tendon inflammation, as evidenced by PGE2 concentration decrease. Authors also emphasized that PGE2 measurement is an objective assessment of the treatment effect of laser therapy in inflammatory processes [114].

A very large study [115] makes a comparison between a control patients group, treated with classical therapeutic means (NSAIDs), a patients group treated with a "placebo laser" (in this case corresponded to an off-laser treatment) and patients groups in which LLLT was applied using a GaAs laser diode or a HeNe and GaAs lasers combination.

The authors treated 583 patients with osteoarthritis (cervical and lumbar intervertebral, spondylosis, knee osteoarthritis, coccyx osteoarthritis and others), 445 patients with non-articular rheumatism (shoulder tendinopaty, sciatica, Dupuytren disease, elbow tendonitis, etc.) and 106 patients with inflammatory arthritis (rheumatoid arthritis, ankylosing spondylitis, gout, etc.). These patients were divided into four homogeneous groups according to the type of treatment, each containing the three types of rheumatic diseases mentioned above. As shown in Figure 2.13, there were significant differences among the four treatment regimens, with laser therapy getting better results than conventional therapies.

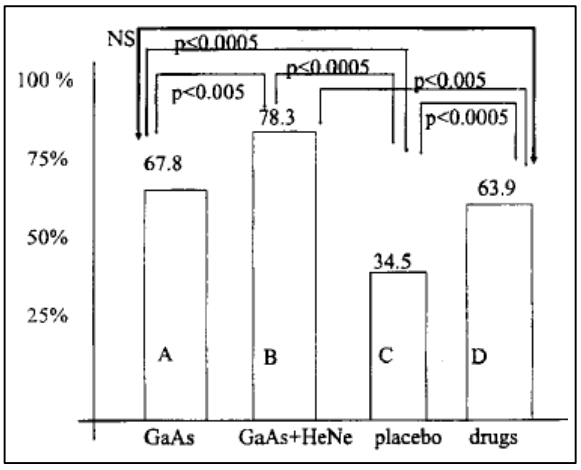

Figure 2.13– Results obtained with four treatment groups for rheumatic diseases patients. The results indicate the significant differences among the four treatment regimens (Retrieved from [115]).

These results were compared with results obtained from a clinical evaluation performed 6 months after laser therapy, with patients not undergoing any treatment for during those six months. The comparison between these two sets of results (see Figure 2.14) lead the authors to conclude that LLLT immediate efficiency is similar for different rheumatic diseases, except osteoarthritis of the

coccyx (the authors also indicate that results for elbow tendonitis were low). They also concluded that after six months a decrease was noted in the effectiveness of the treatment, although this decrease is considered by the authors as not significant, except for inflammatory rheumatism treatment. For this condition, the authors noted that it is necessary to irradiate specific areas for a few months, once or twice a week.

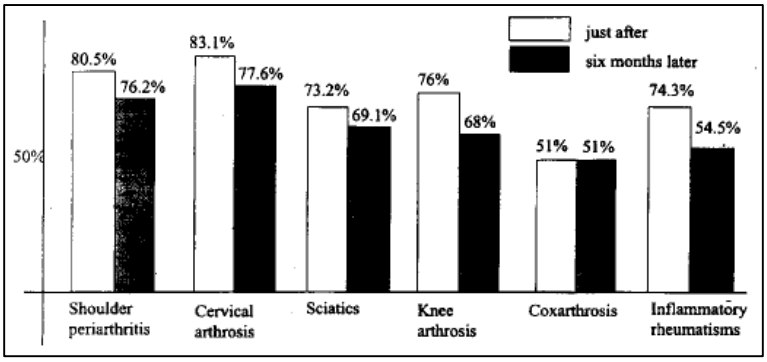

Figure 2.14– Laser therapy in rheumatic diseases, immediately after treatment and six months later (Retrieved from [115]).

Another study [116] reported reduction of the inflammatory process after GaAs laser irradiation (λ = 830 nm) in molar surgery. In this work, surgeries were performed conventionally in one dental element of five patients (considered as control elements). In a second step, starting 21 days after the first surgery, when inflammation has resolved completely, surgeries took place in the same dental element but in opposite side, using low intensity laser irradiation (in application of 4J on 4 points in the immediate postoperative period). It was observed, on the laser application side, a significant reduction of the inflammatory process, with statistically significant differences for swelling, pain and color. The temperature, which proved to be proportional to edema size, also showed lower values on the treated side. The authors concluded that LLLT allows a more suitable postoperative rehabilitation.

If we focus on muscle injury or fatigue we find a variety of recent studies confirming the positive effects of LLLT. The effects of LLLT on skeletal muscle repair were recently reviewed [117].

There are several animal and clinical studies concerning the effect of LLLT on the recovery from muscle fatigue induced by exercise or by neuromuscular electrical stimulation.

Vieira et al. [118] presented a study on rats addressing the action of LLLT on energy metabolism related to muscle fatigue. The animals were trained for 30 consecutive days on a treadmill at the anaerobic threshold. Continuous irradiation at 780 nm was performed after each training session, on a single point on the femoral quadriceps, tibialis anterior, soleus and gluteus maximus. For each irradiation, the energy dose was 3.8 J/cm^2 and the radiant power was 15 mW. The irradiation time of each session and the irradiated area were not reported, making impossible to determine the delivered energy per session. The authors found that LLLT provided greater inhibition of lactate dehydrogenase activity. This result was also observed in the heart muscle, which was not

irradiated, suggesting the existence of systemic effects triggered by LLLT.

On a different study [119], rats were trained, until the exhaustion, on a treadmill in declined plane. LLLT was applied on single point on gastrocnemius muscle. Irradiation was continuous, at 632.8 nm. The rats were divided in low-, medium- and high-dose groups (12, 28, and 43 J=cm^2 - 4, 9, and 14 mW, 20, 46, and 71 mW/cm^2, irradiation time: 10 minutes). The authors found that LLLT had therapeutic effects by enhancing muscle anti-oxidative capacity and reducing the inflammatory reaction. The creatine kinase activity in blood serum and the muscle levels of malondialdehyde were reduced while the activity of the antioxidant enzyme superoxide dismutase increased. The LLLT effect was dose-dependent, being 43 J/cm^2 the most efficient dose.

Sussai et al. [120] used the levels of creatine kinase on the blood and the muscle cell apoptosis to measure the effects of LLLT (660 nm) on rats with muscle fatigue induced by resistance swimming. LLLT (100 mW, wavelength 660 nm, 133.3 J/cm^2) was applied during 40 s on a single point of the gastrocnemius muscle immediately after swimming. The irradiation resulted in lower levels of creatine kinase and apoptosis 24 h and 48 h after swimming.

There are several animal studies on the use of LLLT for muscle fatigue, where this fatigue was not induce by exercise but by neuromuscular electrical stimulation. Chronologically, the first study was reported by Lopes-Martins et al. [121]. The study addressed the effect of LLLT on tibialis anterior muscle fatigue. The assessment was based on the measurement of blood levels of creatine kinase and on the time required for the muscle force to fall to 50% of the initial value for each contraction. LLLT (655 nm, continuous power of 2.5 mW; irradiation during lasted 32, 80, and 160 s, with fixed irradiance of 31.25 mW/cm^2; total energy: 0.08, 0.2, and 0.4 J.) was applied at a single point of the muscle before electrical stimulation. The results included reduced fatigue at 0.5 J/cm^2 and decreased muscle damage at 1.0 and 2.5 J/cm^2.

A different study from the same research group [122] used a similar experimental model and protocol. LLLT (infrared irradiation at 904 nm, with mean output power of 15 mW; spot size: 0.2 cm^2; irradiation times: 7, 20, 67 and 200 s; fixed irradiance of 75 mW/cm^2; total delivered energy: 0.1, 0.3, 1.0 and 3.0 J.) was applied on a single point on the tibialis anterior muscle also before fatigue induction. Muscular fatigue was quantified by the maximal force elicited at beginning of each induced muscle contraction, the time taken for a contraction force to reduce to 50% of the initial value and the work done by each contraction. The blood levels of creatine kinase and lactate were measured. Groups irradiated with 1 and 3 J showed the highest force peak. The blood lactate levels were lower in all irradiated groups. The creatine kinase level in blood was also lower in irradiated groups, with the exception of group 3 J.

A third similar study, [123] with the same irradiation protocol of [120], showed that LLLT decreased significantly the level of creatine kinase in the blood and reduced the mRNA expression for protein cyclooxygenase (COX)-2 and increased the expression of COX-1.

In what concerns human trials, there are several published papers concerning LLLT and exercise.

As with the animal studies, it is possible to find studies where fatigue is induced by mechanical exercise as well as studies using neuromuscular electrical stimulation for fatigue induction.

In one of the first published studies [124], the authors used pulsed laser irradiation (50 mW at 808 nm adjusted to deliver a total energy of 7 J for 10 min or 3 J for 5 min; pulse repetition between 1 and 10 kHz) to study the effect of LLLT on skeletal muscle fatigue. LLLT was applied to the dominant knee extensor muscle group before electrical stimulation. The study failed to find any statistically significant difference in muscle fatigue between treated and non-treated participants, a result that was attributed by the authors to the selection of LLLT parameters.

A set of double-blind placebo-controlled trials used similar methodologies for inducing muscle fatigue (Scott bench exercise performed with 75 % of the load corresponding to maximum voluntary contraction until exhaustion) and investigating the effects of LLLT on the biceps brachii performance [125-127]. Irradiation was done at 655 nm with a total energy of 5 J and a radiant exposure of 500 J/cm^2 at each of four points along the biceps. The effect of LLLT was assessed by the number of repetitions done in the exercise, the total time to complete the effort, and by the blood levels of lactate. The results showed a significant increase in number of repetitions of the LLLT group but no increase in time of exercise. No difference was found between groups I the lactate concentrations. The same results were obtained for an identical trial using infrared irradiation (830 nm) [127]. One study using LED irradiation (commercial device with a cluster with 5 diodes of 810 nm; continuous output of 200 mW each diode; irradiance 5.495 W/cm^2, radiant exposure 164.85 J/cm^2, for each laser spot; 30 J on each point, 30 s on each point; 2 irradiation points per muscle) found increases in number of repetitions and time of exercise, and lower levels lactate, creatine kinase and c-reactive protein after exercise, for LLLT treated participants [128].

The use of the same commercial LED device is also reported in another two human studies. One aimed to investigate the effects of LLLT on energetic metabolism, muscle damage and delayed onset muscle soreness after 5 sets of 15 eccentric contractions of the femoral quadriceps performed on the isokinetic dynamometer [129]. The second study was meant to verify the effects of LLLT on fatigue, oxidative stress, muscle damage and human physical performance on treadmill [86]. Both studies included irradiation of six points of the femoral quadriceps before exercise, with the second study adding of four points on the hamstrings and two points on gastrocnemius muscles. Each point was irradiated during 30 s. The first study found that LLLT lead to a lower increase of lactate dehydrogenase activity and of creatine kinase concentration in the blood, as well as a lower loss of maximum voluntary contraction. The results of the second study showed, for the irradiated participants, lower lactate dehydrogenase activity, less muscle and lipid damage and higher levels of superoxide dismutase, as well as an increase absolute and relative maximal oxygen uptake and time of exercise.

A randomized, controlled clinical trial demonstrated that LLLT can modulate gene expression of human muscle [130]. The authors used a near-infrared device (808 nm) with six diodes of 60 mW

power each, operating in continuous wave mode. The energy per point was 0.6 J, with a total energy per-session in each lower limb of 25.2 J. The radiant exposure per diode was 214.28 J/cm^2 and the irradiance was 21.42 W/cm^2. The application time in each lower limb was 70 s (for a total time of 140 s, both lower limbs). Biopsies from the vastus lateralis muscle were performed before and after the strength training program. The results showed that the volunteers that had undergone LLLT immediately after each training session had a higher increase of load at the strength test as well as significant up-regulation of the genes PPARGC1-α (mitochondrial biogenesis), mTOR (protein synthesis) and vascular endothelial growth factor (tissue angiogenesis) and down-regulation of MuRF1 (protein degradation) and IL-1β (inflammation).

Another study [131] showed the efficiency of LLLT in muscle fatigue rehabilitation in elder people. In this work, twenty-four subjects were divided in two groups: control (placebo). LLLT (808 nm wavelength, 100 mW, energy 7 J) was administered on the rectus femoris muscle immediately before a session of voluntary isotonic contractions of knee flexion-extension performed with a load corresponding to 75% of 1-MR (Maximum Repetition) during 60 s. The therapy was evaluated by surface electromyography. The number of repetitions of flexion-extension during fatigue protocol was also compared between groups. The conclusion showed no difference in the slope comparing placebo LLLT and active LLLT groups. However, after active LLLT, subjects demonstrated significantly higher number of repetitions. The authors concluded that LLLT was efficient in increasing the mean number of repetitions during knee flexion-extension exercise, although results have not shown delayed electromyographic fatigue.

If we focus on muscle injury caused bay trauma we find a small number of published studies that confirm the positive effects of LLLT in decreasing inflammation. These studies present a considerable variety of irradiation and treatment parameters and protocols. Laser wavelengths vary between 632.8 and 904 nm. Therapeutic effects are reported [132,133] for radiant exposures from 1 J/cm^2 to more than 300 J/cm^2. Protocols show a large variation in the number of treatment days and of daily treatment sessions.

A study published in 2006, [134] investigated the effects of LLLT on the activation of nuclear factor kappa B (NF-κB) and on the expression of inducible nitric oxide synthase (iNOS) using rats with inflammation induced by single impact trauma by a falling mass on the gastrocnemius muscle (exactly the experimental model we used in our studies). LLLT (904 nm CW laser; radiant power, 45 mW; radiant exposure, 5 J/cm^2; exposure time, 35 s). While in non-treated animals, it was observed activation of NF-κB, up-regulation of iNOS expression and decrease in the expression of protein IκBα, all these events related to acute inflammatory response were blocked by LLLT, in the treated animals. LLLT reduced the inflammatory response and blocked the effects of reactive oxygen species release.

The use of LLLT for alleviating pain and edema of the rat calcaneus tendon was evaluated in a study that also used single impact by a falling mass to induce muscle trauma [135]. The authors

treated, during 5 consecutive days, three groups of animals with distinct exposures (2, 4 and 8 J/cm^2) with a 670 nm laser. The exposure time was 3 s for each 1 J/cm^2 of exposure. Treatment evaluation was done by measuring the paw elevation time of the animal, while walking on a 30 cm diameter cylinder at 3 rpm, and by measuring the edema size with caliper. The results showed that LLLT decreased edema and the pain (lower paw elevation time), in a dose-dependent manner, with the best results achieved for the lower dose.

There are several studies using an experimental model of muscle trauma based in cryolesion. Two studies from the same research group address the effect of LLLT on the expression of TNF-α and TGF-β [136] and IL-1β [137]. In both studies, LLLT was applied three times a week by continuous irradiation with a red laser (660 nm; output power of 20 mW; irradiance of 500 mW/cm^2 and energy dose of 5 J/cm^2 during 10 s). The animals were analyzed at 1, 7, and 14 days following injury. The protocol implied animal sacrifice at these occasions to remove the tibialis anterior muscle for measuring the mRNA expression of the cytokines through RT-PCR. The results showed that LLLT was able to modulate cytokine expression during muscle repair, inducing a decrease in TNF-α, TGF-β and IL-1β expression.

Two papers reported on the effect of LLLT using infrared laser light (808 nm) for reducing the inflammatory response [138] and contribute to muscle regeneration [139], after trauma induced by cryolesion of the tibialis anterior muscle in rats. In both studies, the injured region was irradiated daily during 4 consecutive days (radiant power 30 mW; exposure time 47 seconds; radiant exposure 180 J/cm^2; irradiance 3.8 mW/cm^2). The animals were sacrificed on the fourth day after injury. The first study showed that LLLT was able to LLLT decrease oxidative and nitrative stress, lipid peroxidation, nitrotyrosine formation and nitric oxide production, a result that the authors attributed to the down-expression of iNOS protein. LLLT also up-regulated superoxide dismutase gene expression and decreased the inflammatory response (lower gene expression of NF-κb and COX-2 and lower concentration of cytokines TNF-α and IL-1β in the muscle).

LLLT also accelerates the muscle regeneration process, increasing neoangiogenesis and stimulating the expression of myogenic regulatory factors [140]. This was demonstrated in a study using LLLT (660 nm; radiant exposures: 10 J/cm^2 laser-treated group, and 50 J/cm^2) to treat animals after cryolesion in tibialis anterior muscle. Animals were sacrificed 7, 14, or 21 days after lesion for histopathological and immunohistochemical analysis of muscle tissue. These analyses revealed a lower inflammatory process in the LLLT treated groups after 7 days, with full tissue repair at 21 days. The expression of myogenic regulatory factors MyoD and myogenin was observed in both treated groups. The animals exposed to the higher dose presented a higher number of blood vessels after 14 and 21 days.

The modulation of pro-inflammatory (IL-6, TNF-α, and IFN-γ) and anti-inflammatory cytokines (TGF-β1) by LLLT was studied by Fukuda et al. [141]. The authors used isogenic mice which were submitted to a surgical procedure with three standard cutaneous incisions, followed by an

abdominal muscle incision and suture. A group of animals was irradiated after the surgical procedure (wavelength of 780 nm, radiant exposure of 10 J/cm^2, output power of 20 mW, three points per session, and exposure time of 20 s per point). Animals were treated 12, 36 and 60 hours after the surgical procedure. Twenty four hours after each treatment, a group of animals (treated and non-treated) euthanatized and evaluated. Cytokines quantification was done at spleen mononuclear cells, after isolation and culture for 48 h, using ELISA. The study revealed a significant difference between the IL-6 and TNF-α concentrations in the 60 and 84 hours evaluations, when comparing LLLT with the control group. There was a modulatory effect of TNF-α and IFN-γ in the laser treated groups, particularly in the 60 hours evaluation. No significant differences were found for TGF-β1 and for IL-6.

As an ending, is worth mentioning the existence of studies that prove the success of LLLT in muscle regeneration, namely after muscle atrophy due to disuse. This success is justified by the important role of activation of satellite cells into the cell cycle, promoting its proliferation to new muscle fibers. Studies were performed in vitro [142] and in vivo experiments [143].

From the reviewed studies, it is possible to conclude that LLLT exerts an important anti-inflammatory action, which is present on the early phases of the inflammatory response. It reduces chemical mediators (PGE2, histamine), cytokines (IL-1, IL-2, IL-6, IL -10, TNF-α, IL-1β), decreases edema and increases the expression of growth factors. The studies also make evident the lack of standardization of dose and treatment parameters, which are critical for successful laser therapy. This fault is responsible for some negative results and complicates the choice of parameters to be used when applying LLLT. There is a large variation in the parameters reported for LLLT application in muscle injuries. Additional studies are required to determine which treatment protocols are most effective.

One major problem found when studying the LLLT scientific literature is the incorrect reporting of dose and treatment parameters namely due to omissions when submitting papers for publication. Many reports have missing data and no verification of beam parameters namely spot size and beam profile. This makes reproducibility very hard.

This situation led to the publication of an article [15] with the objective of becoming a reference document for adequate reporting of LLLT studies and trials in what concerns treatment and irradiation parameters (including beam parameters). It provides a checklist to help researchers to report all the necessary parameters for a repeatable scientific study. The most important beam parameters are: wavelength, power, irradiation time, beam area at the target surface, pulse parameters, anatomical location, number of treatments, interval between treatments, exposure time, energy and energy density (radiant exposure). A more complete reporting would also include coherence, application technique, beam profile and spectral width.

2.4 Clinical practice

The previously published studies show the clinical value of LLLT in the treatment of inflammatory processes. That technique is now used extensively in Physical and Rehabilitation Medicine and Veterinary Medicine.

The variety of LLLT clinical applications can be witnessed by the query tables of doses recommended for treatment, which were published by the World Association of Laser Therapy (WALT). These tables can be found in Appendix 1 of this document. The tables include recommended doses for treatment of various tendinopathies and arthritis. We can add to these conditions strains and sprains treatment, applications for relief of postoperative pain and tissue healing. LLLT is still applied in nerves diseases [144] (facial nerve palsy, neuralgia, etc.), dermatology (decubitus ulcers, psoriasis, eczema, thrush), otorhinolaryngology [145,146] (pharyngitis, acute tonsillitis, sinusitis, otitis, otitis media) and dentistry treatment (dental hypersensitivity, pulpitis, oral herpes, oral mucositis, mandibular paresthesia) [147].

The International Association for the Study of Pain, a well-known organization in musculoskeletal pain studies, issued a guideline for the diagnosis and treatment of myofascial pain syndrome [5]. This condition involves a musculoskeletal local and referred pain, characterized by the presence of myofascial trigger points in any part of the body. One of the recommended treatments for trigger points is LLLT

Based on moderate evidence, the Orthopaedic Section of American Physical Therapy Association clinical guidelines recommend LLLT to decrease pain and stiffness in the treatment of Achilles Tendinitis, and others tendinitis [8].

The World Health Organization (Bone and Joint Task Force) [6] recommends the LLLT for neck pain treatment.

In Veterinary Medicine, LLLT is used to treat various dogs, cats and horses diseases. It is used to relief arthritic pain, for healing wounds, to treat various inflammatory conditions (ear infections, inflammations of the anal glands, periodontitis, lick granuloms, idiopathic cystitis, sinusitis, rhinitis) and for treating tendinopathies [148]. Other pathologies treated are: degenerative disc disease, corneal diseases, head trauma, muscle and ligament injuries, pain management for trauma and post-surgical wounds, inflammation, swelling and wound healing including degloving injuries [149].

2.4.1 Equipment

There are several commercial devices currently available for LLLT application. Table 2.4 presents the most significant equipment, indicating some technical characteristics and certifications.

Table 2.4– LLLT commercials equipment.

Manufacturer	Model	Type	Wavelength [nm]	Output Power	Mode	Certifications
Biocare Systems [150]	LumiWave	LED	880, 893	60 mW x 4	CW	FDA
K-Laser [151]	Cube 4	GaAlAs	660, 800, 905, 970	15 W (max)	CW and PL	FDA, ISO, CE
Kondortech [152]	Bio Wave LLLT Infra	GaAlAs	830	40 mW	CW	BPF
LaserLight [153]	Compact CombiLaser	GaAlAs	650, 808	100 mW x 2 500 mW x 2	CW	CE
Laserex Technologies [154]	LaserTENS 2000 IR	GaAlAs	830	35 mW	CW and PL	ISSO, CE
Medicom [155]	Maestro CCM	GaAlAs, GaAlInP	635 , 670, 830	450 mW	CW and PL	ISO, CE, EN
MedX Health [156]	LPS200	GaAlAs	808	200 mW	CW	ISO, CE
Meridian Medical [157]	LAPEX-200	GaAlAs	830	30 mW x 3	CW and MCW	FDA, Health Canada, CE e SSA
MicroLight [158]	*ML830*	GaAlAs	830	30 mW x 3	CW and MCW	FDA
MKW Lasersystem [159]	Laserdusche PowerTwin 21	GaAlAs	785	50 mW x 21	CW and PL	ISO, CE
Sunny Technology [160]	MDL500	GaAlAs	808	500 mW	CW and PL	FDA, ISO, CE
Terraquant [161]	MQ2000	GaAlAs e LED	850, 900	60 mW	CW and PL	FDA, ISO, CE
THOR Photomedicine [162]	LX2 Cluster 810	GaAlAs	810	200mW x 5 400mW x 5	CW and PL	FDA, Health Canada, TGA and CE

CW - Continuous Wave
MCW - Modulated Continuous Wave
PL- Pulsed Laser
FDA - Food and Drugs Administration
ISO - International Organisation for Standardisation
CE - Conformité Européenne
BPF - Boas Práticas de Fabricação de Produtos Médicos, Brazil
Health Canada - Health Department of Canada.
SSA - Health Department of Mexico.
EN - European Norm
TGA - Therapeutic Goods Administration, Australia.

Figure 2.15 shows some of LLLT equipment listed in Table 2.4.

Figure 2.15– Examples of LLLT equipment.

As it can be seen, all the equipment has emission in infrared region, between 800 nm and 1000 nm, within the so-called human body therapeutic window. As we have seen, optical radiation penetration in biological tissues is maximal in this region.

2.5 Cellular mechanisms triggered by LLLT

Several cellular mechanisms are thought to be responsible for the observed effects in the different applications of LLLT (inflammation, pain, wound healing). The current view on the LLLT action involves various cellular mechanisms interconnected in an arrangement that may be called cascade, well evidenced in Figure 2.16, which concerns LLLT application for inflammation treatment.

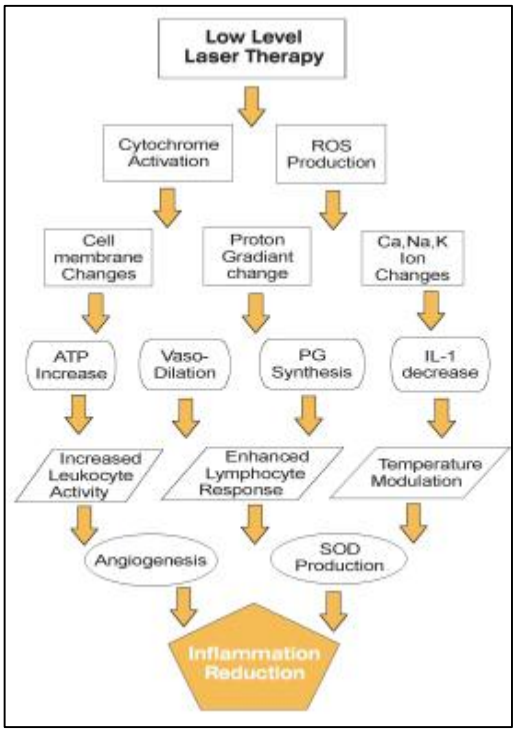

Figure 2.16– Cellular cascade mechanisms that promotes inflammation reduction in LLLT response (Retrieved from [163]).

It is known that almost all cells increase their metabolism when irradiated with light of certain wavelengths, particularly on the red and infra-red region. There is also a lot of evidence pointing to mitochondria as responsible for cellular response induced by LLLT. Observed effects include an increase of protons electrochemical potential, an increase in synthesis of ATP, RNA and proteins and also an increase of oxygen consumption and in membrane potential.

The initial event leading to the action mechanisms of LLLT has to be absorption of radiation photons by a photoacceptor. The current view is that cytochrome c oxidase (CCO) is the molecular photoacceptor involved in LLLT [164]. CCO is an enzyme of the respiratory chain in eukaryotic cells (Figure 2.17). It mediates the transfer of electrons from cytochrome c to molecular oxygen [164]. CCO contains transition metals centers, namely two iron centers (haem a and haem a3, sometimes called cytochromes a and a3), and two copper centers (Cu_A and Cu_B). When CCO is fully oxidized, both iron atoms are in the Fe(III) oxidation state, with the copper atoms in the Cu(II) oxidation state. A fully reduced CCO presents the iron centers in Fe(II) oxidation state and the copper atoms in Cu(I) oxidation state. CCO can also assume many intermediate mixed-valence forms.

The identification of CCO as the primary photoacceptor was obtained from the analysis of the action spectra for photostimulation of diverse cellular processes [165], identifying their bands by comparison with the absorption spectra of metal-ligand systems. The current knowledge on LLLT assigns the band centered at 825 nm to the oxidized Cu_A center of the CCO molecule, the 760 nm band to the reduced Cu_B center, the 680 nm band to the oxidized Cu_B center and the 620 nm band to the reduced Cu_A center. The analysis of the action spectra also demonstrated that CCO does not

act as a primary photoacceptor when is fully oxidized or fully reduced but only in an intermediate form [164,165].

CCO role as primary cellular photoacceptor for red and infrared light was confirmed by additional studies. Pastore et al. [166], studied the effect of He-Ne laser illumination on the purified CCO and found increased oxidation of CCO and higher electron transfer. Another study [167] shows an increased enzyme activity of catalase with the application of He-Ne illumination.

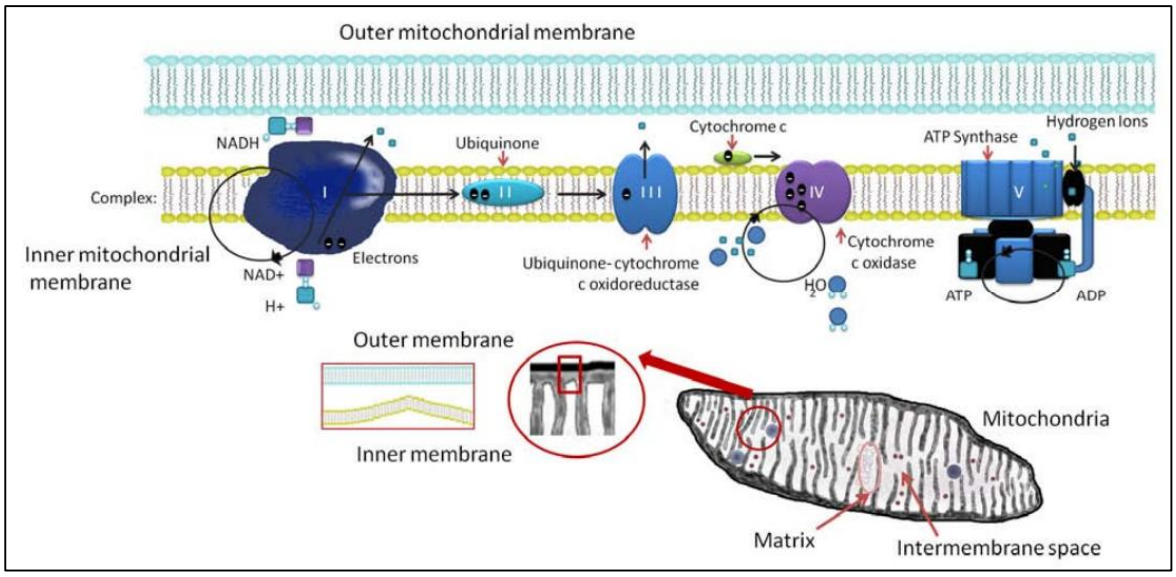

Figure 2.17– Mitochondria and Mitochondrial respiratory chain (Retrieved from [168]).

After photon absorption, four types of primary processes may occur:

1. acceleration of the electronic transfer in the respiratory chain due to the excitation of chromophores in CCO.
2. reversion of the partial inhibition of CCO catalytic center by nitric oxide (NO), through the activation of the electron flow.
3. increased production of superoxide anions.
4. transient local heating of the absorbing chromophores in CCO molecules.

The first process is a consequence of light absorption by CCO chromophores (Cu_A, Cu_B and hemes a and a3). The photo absorption processes change the redox state of these CCO centers, which in turn increases the rate of the electron flow in the CCO molecule leading to increased ATP synthesis [169].

NO regulates CCO activity through reversible inhibition of mitochondrial respiration by binding to CCO, especially in situations of cellular stress. In fact, several studies have measured increases in NO concentration after LLLT application [170-172]. The proposed mechanism is the NO photodissociation of CCO. It is possible that the activation of the electron flow in the CCO molecule reverses the partial inhibition of CCO by NO leading to an increase in O_2 binding and respiratory rate [171], and to increased production of Reactive Oxygen Species (ROS). The idea is depicted in

Figure 2.18. Experimental work using NO modulators did not reject this hypothesis, which, in turn, may explain the observed increase in the concentration of the oxidized form of Cu_B. As already said, it is also known that NO concentration is increased in several pathological conditions, leading to a higher probability of inhibition of cell's respiration. One possible mechanism for LLLT positive effects may reside in the attenuation of NO inhibitory action.

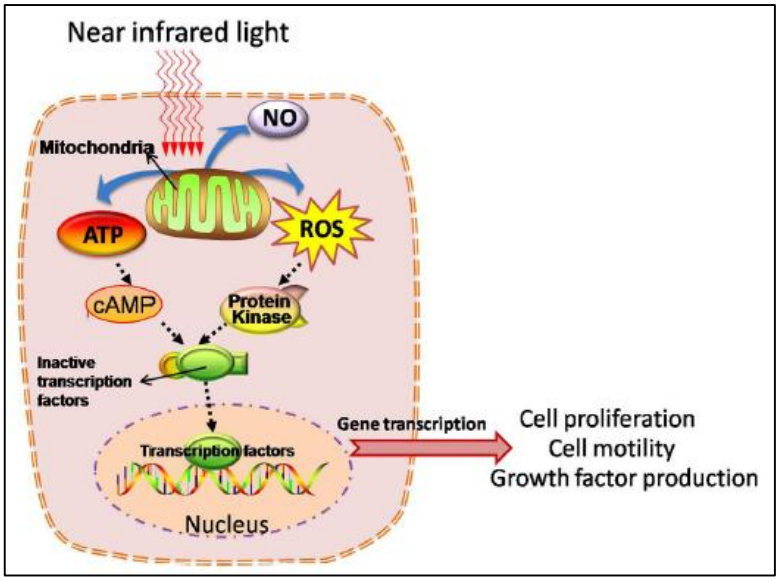

Figure 2.18– Mechanisms of LLLT (Retrieved from [170]).

The activation of the respiratory chain can lead to increased production of superoxide anions, $O_2^{\cdot-}$. It was demonstrated that the production of superoxide anions depends mainly on the metabolic state of the mitochondria. LLLT can also activate other redox chains in cells. Various studies showed that He-Ne laser irradiation induces a non-mitochondrial respiratory burst of neutrophils. It was shown that protein tyrosine kinases play a role in this process. NADPH-oxidase is also involved in this process. This enzyme is capable of generating superoxide anions through the transfer of electrons from intracellular NADPH and their coupling to molecular oxygen. The generation of superoxide anions can lead to the production of high amounts of ROS can be induced [173,174].

The primary processes presented above are not mutually exclusive. They can occur simultaneously when cells are irradiated. However, although all the processes may lead to a modulation of the redox state of the mitochondria, it is reasonable to assume that some processes may be more significant than others, depending on the used energy dose and irradiance.

As said, the primary processes triggered by photon absorption lead to changes in the redox state of the cells. These in turn induce the activation of several cellular signaling pathways, regulate nucleic acid and protein synthesis, as well as enzyme activation and cell cycle progression.

The experimentally observed stimulation of DNA and RNA synthesis by LLLT requires cellular signaling between mitochondria and the nucleus. Several experiments used the cDNA microarray technique to analyze gene expression profiles in irradiated cells. The experiments showed that cell

irradiation lead to the up-regulation of genes that play roles in increasing cell proliferation and decreasing apoptosis [175]. Three regulation pathways have been proposed: (1) control of the level of intracellular ATP by the photoacceptor and mediation through the cell redox state involving (2) redox-sensitive transcription factors and (3) cellular signaling cascades from cytoplasm via cell membrane to nucleus.

Experimental data from several studies in the last 25 years suggest strongly that the activation of cellular metabolism after light absorption is a redox-regulated phenomenon. Stabilization of Ca^{2+}, Na^{+} and K^{+} concentrations in the cell membrane and changes in the mitochondrial membrane potential are positively influenced by LLLT action. This is achieved, at least in part, by the already mentioned increased production of ROS. These ROS modulate Ca^{2+} intracellular concentrations improving the uptake of Ca^{2+} in mitochondria [169,176,177]. The three mentioned regulation pathways suggest a shift in the cell redox potential in the direction of greater oxidation due to the irradiation [164,178]. It is important to note that as different cells have distinct redox states, the effects of LLLT can vary considerably. Cells at a more reduced state (low intracellular pH) have higher potential to respond to LLLT that cells near the optimal redox state, which may no respond to LLLT.

Finally it is necessary to mention that other mechanisms may be operating in LLLT in addition to CCO mediated increase in ATP production. One of such mechanisms is known as the “singlet-oxygen hypothesis.” After photon absorption, certain molecules, like porphyrins without transition metal centers [179] and flavoproteins [180] can be converted, by intersystem crossing, into a metastable triplet state. This triplet state can transfer energy its energy to ground-state oxygen leading to the production of excited singlet oxygen, which is a reactive species.

The secondary reactions following the primary processes triggered by photon absorption lead to several cellular mechanisms that are responsible for the LLLT effects:

LLLT stimulates vasodilatation primarily due to the increase of NO concentration. We have already seen that LLLT leads to an increase in NO production. It must also consider a laser induced release, a level of hemoglobin nitrosilades and myoglobin nitrosilades. The vasodilatation increases nutrients transport and oxygen to damaged cells and facilitates removal of cellular remains [181,182].

Proton gradient changes across mitochondrial membrane leads to increased synthesis of prostaglandins, particularly to the conversion of PGG2 prostaglandin and PGH2 peroxides into PGI2 prostaglandin (prostacyclin). PGI2 is a vasodilator and anti-inflammatory with attributes similar to inhibitors of COX (cyclooxygenase) I and II [183].

Due to increased ATP production, the acceleration of leukocyte activity leads to faster removal of cellular components and non-viable tissue, and faster regeneration and repair processes. Several in vitro studies showed that LLLT applied in a low doses regime

increases the proliferation of fibroblasts [184], keratinocytes [185], endothelial cells [186] and lymphocytes [187].

Laser irradiation lowers the concentration of interleukin 1 (IL-1), a pro-inflammatory cytokine that has been implicated in rheumatoid arthritis pathogenesis and other inflammatory conditions [188]. This regulation effect of a cytokine involved in inflammation was also observed with several other cytokines.

Laser irradiation also results in increased angiogenesis and regeneration of blood and lymphatic capillaries. Consequently, LLLT improves circulation and increases perfusion which results in an improvement of the efficacy of repair and healing processes. The increased concentration of NO and growth factors, particularly IFN-γ cytokines, caused by laser irradiation contributes to this process [189,190].

Another LLLT effect observed is the acceleration of temperature normalization in inflamed areas. Areas of inflammation generally have higher temperature.

LLLT also stimulates increased levels of SOD. This enzyme acts on inflammatory processes where free radicals formation is very high, being present in synovial fluid. Interactions between SOD and ROS production, subsequent to LLLT, balance the activity of free radicals, stimulating ROS beneficial effects [191].

Finally, it is known that LLLT leads to decreased serum levels of inflammatory markers C-reactive protein and neopterin, particularly in patients with rheumatoid arthritis. The lower level of inflammatory markers decreased level indicates that the combined effects of all anti-inflammatory actions induced by LLLT actually result in a reduction of the inflammatory process.

2.6 Open questions in LLLT

Although many studies and reports from LLLT experiments conducted *in vitro* or *in vivo*, in animals or humans give positive results, the mechanisms of interaction between different light sources and biological tissues remain not fully understood. There are still controversial issues concerning the processes triggered by light absorption in LLLT as well as the adequate irradiation and treatment parameters. This is a consequence of the complexity in the interpretation of the amount of scientific data generated in those studies and of the diversity on the selection and reporting of the different parameters used in the treatment protocols, like wavelength, polarization, total power, power density, pulse structure, total energy, fluence, coherence, area of exposure, illumination time and treatment repetition [15]. The next subsections present the main questions that are still focus of debate in LLLT.

2.6.1 Biphasic dose response

Many of the published studies in LLLT have presented evidence of a biphasic dose response, with low levels of light having more positive effects than high levels [192-194]. The delivered dose is measured as a radiant exposure (J/m2). Therefore controlled experiments should either vary the irradiance while keeping the irradiation time constant, or varying the irradiation time for a constant irradiance. This biphasic dose response behavior is often described using the “Arndt-Schulz Law” [195-197] which has its origin when Hugo Schulz published, in 1887, a paper showing that various low doses of poisons could stimulate the metabolism. Later he developed with Rudolph Arndt, in 1923, the principle that while weak stimuli increase metabolism and stronger stimuli raise it further, there is a limit to this behavior: after reaching a maximum, the effects start to decrease. Increasing further the stimuli leads to suppression of its effect and even to negative responses [198]. Figure 2.19 shows how the response to LLLT varies depending on the combination of irradiance and application time [49]. Very low irradiance or very short irradiation time will result in no effect. The same will happen for a very high irradiance or irradiation time.

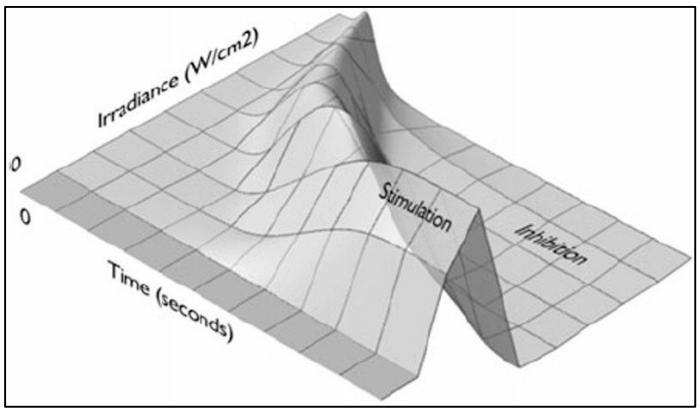

Figure 2.19– Biphasic dose response in LLLT (Retrieved from [49]).

Although the biphasic dose behavior in LLLT is well established, it is still necessary to know better the extent of its application and how it depends on the irradiation parameters and on the redox state of the target tissue, in order to optimize the treatments. Some explanations have been proposed for the cellular mechanisms responsible for the biphasic behavior. One of the proposals is based on the existence of two peaks of ROS production with different effects. Low levels of light would result in an initial production of ROS that will stimulate of mitochondrial electron transport and lead to the activation of transcription factors such as NF-κB. A second peak in ROS production would occur for higher doses of light. This ROS can start apoptosis by the mitochondrial pathway including cytochrome c release. It was hypothesized that the ROS produced for low levels of light is mainly superoxide while the second peak has more damaging ROS like hydroxyl radicals [199].

2.6.2 Laser vs non-coherent light

The question of whether coherent sources produce better treatment effects than monochromatic non-coherent sources with the same wavelength and radiant power is currently much discussed. While it is considered that, for the range of power densities used in LLLT, coherent properties of light do not play a role during molecular level light-tissue interaction [47], there are several documented clinical cases where the therapeutic effect of coherent light is higher. In fact, although several published works, concerning cellular level experiments, concluded that coherent and non-coherent light with the same wavelength, intensity, and irradiation time produce the same biological effect [48,200], it appears that the coherence longitudinal length of the light source has an important role when irradiating bulk tissue. It was hypothesized that the speckle intensity pattern, resulting from the coherent radiation field established for the full penetration length, causes a spatially non-homogeneous energy deposition, leading to statistically non-homogeneous photochemical processes [48], which could justify the advantages of coherent sources in LLLT. When light is applied in a non-transparent tissue, scattering will spread the irradiated volume. This will decrease tissue irradiance and, therefore, the depth at which the irradiance is no longer enough to initiate the biochemical processes of photobiomodulation (a typical threshold value is 5 mW/cm^2). The laser speckle pattern, resulting from interference processes, could provide localized spots with irradiances high enough to produce a therapeutic effect beyond the threshold depth obtained with a non-coherent source. This hypothesis is illustrated in Figure 2.20.

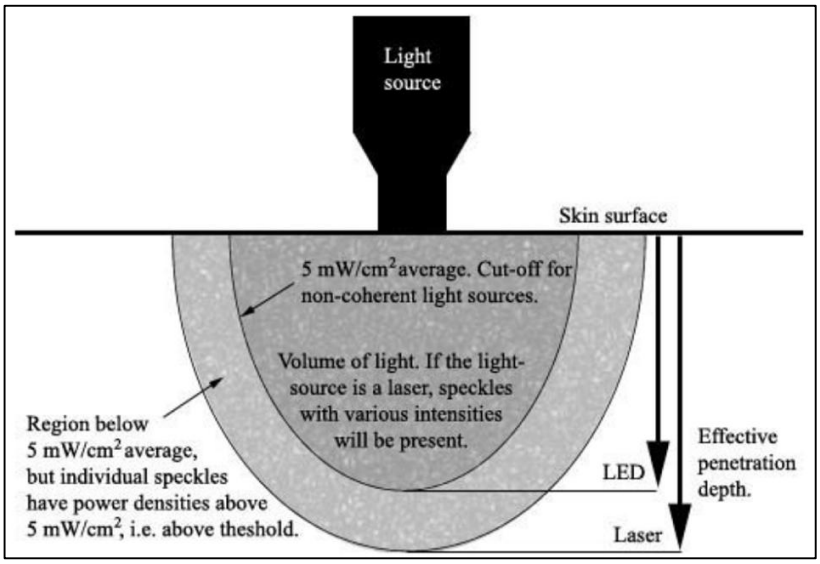

Figure 2.20– Effective penetration of coherent and non-coherent light-sources (Retrieved from [201]).

In monolayers of cells or optically thin layers of cell suspensions (Figure 2.21 A, B) with a longitudinal size of irradiated sample Δl less than the coherence length L_{coh}, the biological effect is the same for any source of monochromatic light with the same wavelength and radiant power (laser, LED, etc), as shown by some studies [182,202]. On the other hand, when the irradiated sample is a bulk tissue (Figure 2.21 C), the biological responses are different between coherent

and non-coherent sources. This was also confirmed by our studies, as it will be presented in section 4.3.

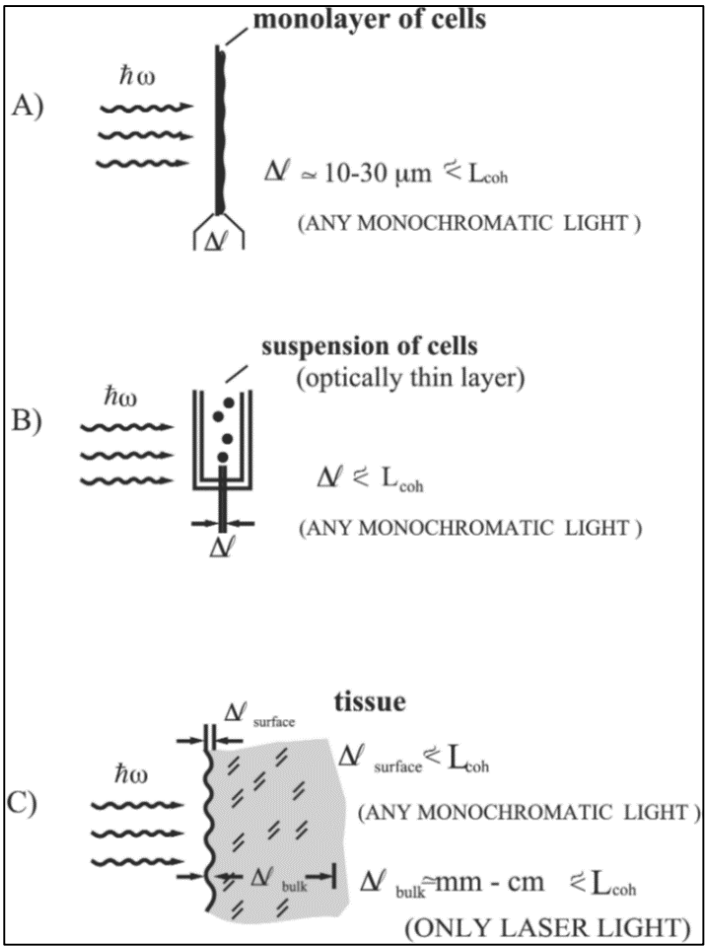

Figure 2.21– Light interaction with monolayer of cells, optically thin layers of cell suspensions and bulk tissue (Retrieved from [203])

2.6.3 Pulsed or CW irradiation

There is published evidence that pulsed irradiation produces different effects than CW irradiation. Hashmi et al. recently reviewed the effects of pulsing in LLLT [204] reporting nine studies comparing CW and PW irradiations, none of them on muscle inflammation. Of those, seven found beneficial effects from pulsed irradiation with only one study finding a higher treatment effect with CW irradiation, although by a minimal margin. Biological reasons are usually proposed for the increased efficiency of PW irradiation. One of the proposed mechanisms is the modulation of ion channels kinetics in the milliseconds time range, namely for potassium and calcium channels in the mitochondria. Another mechanism is the promotion of multiple nitric oxide photodissociation events from a protein binding site [204]. As we said, one of the effects triggered by LLLT is the photodissociation of nitric oxide from a protein binding site cyctochrome c oxidase. It was suggested that there is a high probability of the NO rebinding to the same site even in the presence of CW light, while PW light would promote multiple photodissociation events.

It was also proposed that the use of pulsed light reduces tissue heating and allows the safe use of higher peak irradiances, resulting in higher penetration in the tissue and therefore greater treatment depths. However it was pointed out that this proposal violates linear behavior of optics, observed up to peak powers many orders above the low levels used for LLLT, and that the data supporting it was just the result of limited understanding of the technology involved and awkwardly performed experiments with misinterpreted results.

Currently, there is still no consensus on whether CW or PW light is more suitable for a given LLLT application.

2.6.4 Polarized or non-polarized light

Other controversial topic is the difference of positive results when it is applied polarized or non-polarized light. Some studies claim the advantage of using linearly polarized light, stating that it propagates deeper in biological tissue, and interacts more efficiently with the chromophores in the respiratory chain, than non-polarized light.

The photon absorption cross-section for a given chromophore depends on the angle between the light wave electrical field and the chromophore excitation dipole, being maximal when the two vectors are aligned. Therefore, there is a theoretical basis supporting the use of linearly polarized light. However, in most tissues the absorbing molecules are not aligned in a particular direction. In fact, in most tissues the orientation of the dipoles of the absorbing species can be considered as random. In this case, the use of linearly polarized light does not bring any advantage in what concerns the efficiency of light absorption. So, from the theoretical point of view, the use of linearly polarized light in LLLT should only provide better results when applied to tissues where the target molecules have a defined orientation. That can be the case of tissues composed mainly by fibers and fibrils of collagen, as is the case of the skin.

Ribeiro et al. [205], presented a comparison between polarized and non-polarized laser (at 632.8 nm, with 10 mW of output power) in the treatment of skin burns. The authors concluded that the treatment results were directly linked with the relative direction of the laser polarization, explaining these results with the orientation of the collagen fibers in the dermis. It was observed that, when light is polarized in the adequate plane, scattering is reduced and the polarization will be preserved, resulting into an acceleration of cutaneous wound healing. Another study [206] also showed an increase of collagen deposition and myofibroblasts in healing wounds when using polarized light (685 nm, 20 J/cm^2). The effects of polarized light on the immune system were also observed in *in vitro* tests [207].

L. Hode, J. Tunér [208] reported good results of non-coherent light treatment but not more effective than laser therapy. They also showed that the laser coherence was still by tissue due to scattering.

3. Methodologies

The aim of this study is to determine the influence of irradiation parameters on the LLLT treatment of the acute phase of skeletal muscle inflammation, through the measurement of cytokines expression in systemic serum. Although our experiments were not designed to validate any of the LLLT action mechanisms, we intended to evaluate and discuss their results in the framework of the currently most accepted LLLT cellular-level mechanism, which is based on the role of CCO as a primary photo-acceptor to red-NIR radiation. This was achieved by conducting studies in animals (Rattus norvegiccus, Wistar strain) which were induced in a controlled inflammatory state.

A discussion of our methodology was published on SPIE Proceedings [209]. It takes into consideration the animal welfare, housing, anesthesia protocols, as well as blood sampling techniques and quantities, euthanasia methods and serum and muscle tissue analysis. The methodology proved to be suitable for measuring LLLT treatment effects on injured skeletal muscle. Its main drawback is to be limited to the treatment of superficial muscle traumas. As we choose to keep constant the irradiation time and the size of the laser spot size on the animal, our experiments evaluated the influence of laser irradiation parameters (wavelength, energy, dose and light delivery: continuous or pulsed) in the expression of anti-inflammatory and pro-inflammatory cytokines in systemic blood. We did a small pilot experiment [210], to define the treatment schedule, blood sampling times and analysis methods.

During the development of our work, we found that following the three Rs principle (Reduction, Replacement, and Refinement) [211] of animal experimentation was of key importance, since it enabled us to minimize the quantity of animals used for the experiments while preserving statistical relevance. It was also equally important to follow the ARRIVE guidelines [212].

3.1 Laser and LED instrumentation and irradiation parameters

Laser radiation was administered using a Thorlabs ITC4001 - Benchtop Laser Diode/TEC Controller, with a single HL8338MG GaAlAs Laser Diode emitting at 830 nm or a L9805E2P5 Laser Diode emitting at 980 nm (Thorlabs, Newton, New Jersey, USA) capable of providing at least 50 mW of radiant power. The specifications of both laser diodes can be found in Appendices 2 and 3. The controller (driver) for these lasers, in addition to ensuring an accurate and stable radiant power control, allows continuous power adjustment in the range 0 to 50 mW and emission in the pulsed mode for a range of pulse widths between 1 s and 100 µs, with rates up to 1 kHz. The laser controller also controls the operating temperature of the laser diodes.

The 830 nm wavelength was selected for being a wavelength located in the band of highest transmission through the combination of skin and muscle (770 – 850 nm) [213], for being one of the two most common wavelengths used in therapeutic light sources (the other is 632.8 nm) and also for being a peak of CCO absorption spectrum, understood as due to the relatively oxidized Cu_A chromophores [164]. It is important to remember that the absorption spectrum of CCO is similar to

the action spectra for biological responses to light, like DNA and RNA synthesis, a fact that supports the role of CCO as primary photoacceptor for red-NIR radiation in LLLT.

One of the reasons for selecting the 980-nm wavelength was the fact that it does not correspond to any CCO absorption band. At this wavelength there is a large water absorption band making 980-nm photons more likely to produce tissue heating than photochemical effects. The fact that reported results for 980-nm-based LLLT are mixed also lead us to choose this wavelength. The literature presents conflicting results in wound healing [214,215], positive effects on neuropathic pain relief [216], and no effects on traumatic brain injury [217]. Published data on the effectiveness of 980 nm in the treatment of skeletal muscle inflammation are very scarce, a fact that also prompted us to use this wavelength.

Laser beam profile and shape were measured with a BeamStar PCI-PAL 100345 beam profiler (Ophir, Jerusalem, Israel) at a plane corresponding to the animal leg. The 830 nm beam presented an elliptical shape, with horizontal and vertical profiles whose correlation coefficients to Gaussian shape were 78.5 % and 90.7%, respectively. Profiles widths at $1/e^2$ were 9.74 ± 0.003 mm, for the horizontal profile, and 8.31 ± 0.001 mm, for the vertical profile, resulting in a beam spot size at target of 0.80 cm2. The 830 nm beam 2D and 3D shapes are shown in Figure 3.1, along with its horizontal and vertical profiles.

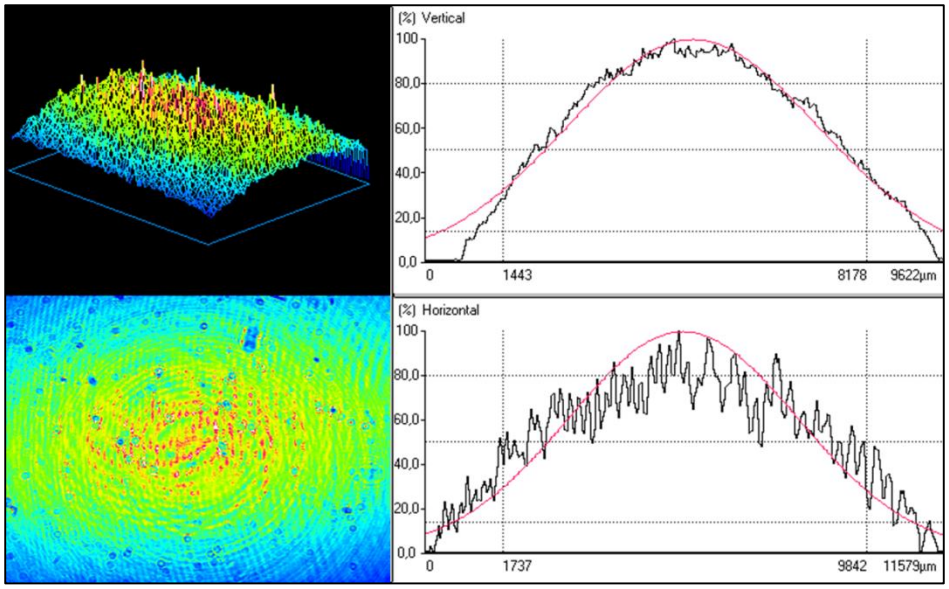

Figure 3.1– Beam shape and profile for the 830 nm laser beam. The smooth line indicates a Gaussian profile.

The 980 nm laser also presented an elliptical shape. The correlation coefficients between the horizontal and vertical profiles and a Gaussian profile were 80.1 % and 82.2 %, respectively. The measured profiles widths at $1/e^2$ were 9.26 ± 0.001 mm, for the horizontal profile, and 7.42 ± 0.001 mm, for the vertical profile, resulting in a beam spot size at target of 0.69 cm^2. Figure 3.2 presents the 2D and 3D shapes and horizontal and vertical profiles for the 980 nm laser beam.

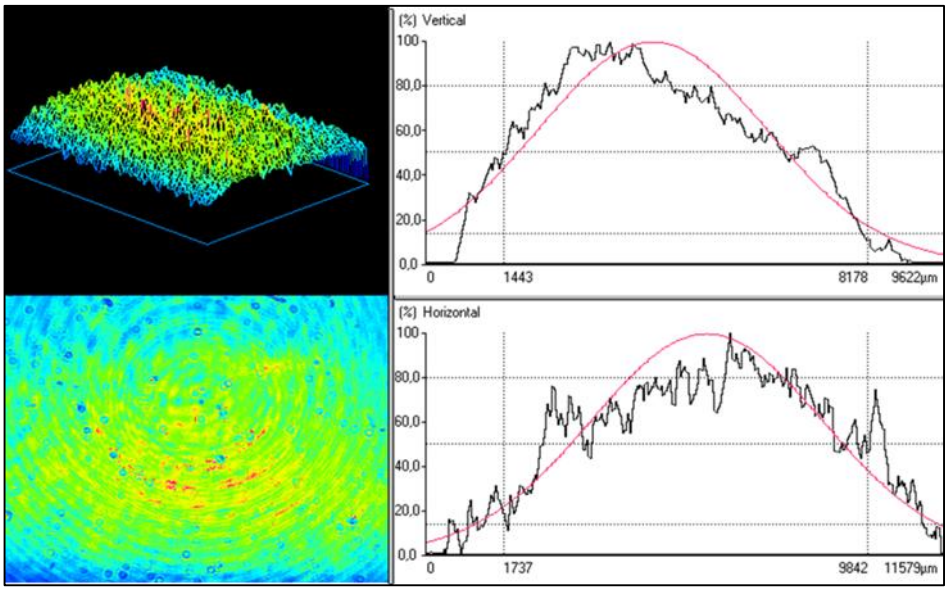

Figure 3.2– Beam shape and profile for the 980 nm laser beam. The smooth line indicates a Gaussian profile.

These measurements required the use of neutral density (ND) filters to prevent CCD saturation. Speckle is not evident in the actual treatment conditions. The large ring patterns visible in Figure 3.1 and Figure 3.2 probably result from interference effects due to reflections on the ND filters. The small circular patterns are most probably due to dust on the filters.

Non-coherent LED light was administered through a Thorlabs T-Cube LEDD1B Driver with a M850L3 LED with the central wavelength at 850 nm. This LED source can emit a radiant power of 50 mW; Appendix 4 contains the data sheet for this LED.

The laser system performance was evaluated by measuring the radiant power and by optical pulses characterization. To measure the radiant power, we used a Melles Griot 13PEM001/J 2-Watt Broadband Power/Energy Meter (Melles Griot, Rochester, New York, USA).

3.2 Animals

For this study, we used Rattus norvegiccus (Wistar strain) male adult rats, with an average body mass of approximately 250 g and 8 weeks of age.

All procedures were approved by the Commission of Ethics of the Faculty of Medicine of the University of Coimbra, which follows the Directive 2010/63/EU of the European Parliament and of the European Council [218].

3.2.1 Housing

The rats were housed in collective standard cages, with dimensions of 395 x 346 x 213 mm and floor area of 904 cm^2 (Tecniplast S.p.A., Varese, Italy), with two or three animals per cage, depending on the experiment, with a period of 12 hours light and 12 hours dark and receiving *ad libitum* water and standard food [219,220].

3.2.2 Whether conditions and bedding

The environment conditions were: a controlled room temperature of 21ºC, cage ventilation rates of about 75 air changes per hour, a relative humidity of 70%. Bedding was replaced once a week [219,220].

3.2.3 Number of animals

The number of animals was calculated using the resource equation [221]:

$$E = N - T \quad (3.1)$$

which takes in account the main factors in experimental animal research: number of animals (N), number of treatment groups (T) and error degrees of freedom (E). For a good statistical relevance without unnecessary increase in the number of animals, E should be between 10 and 20.

Although the resource equation method does not allow to determine in advance the experiment efficiency for detecting a given treatment effect, since it does not specify statistical power, standard deviation or minimum detectable difference, it is known that little additional information is retrieved when using a substantially higher number of animals than the necessary to obtain error degrees of freedom equal to 20 [221].

For example, in our first experiment, where we wanted to evaluate different laser delivered doses, we used 6 treatment groups (control, 10 mW, 20 mW, 30 mW, 40 mW and 50 mW) [222,223].

For T = 6 the number of animals per group should be between 3 (E = 12) and 4 (E = 18).

In order to reach at least E equal to 20, with equal number of animals between treatment groups, we choose to use 5 animals per group. This results in a value of 24 for E and a total number of animals equal to 30.

3.2.4 Cage position randomization

We needed to carry out two randomizations: the first one was inside the cages to avoid errors in social behavior and the second was with respect to the light environment and its influence in daily rat behavior.

For both randomizations, the Microsoft Excel (Microsoft, Redmond, Washington, USA) function RANDBETWEEN was used. For the randomization Inside the cages, the used function was **RANDBETWEEN(0;5),** where each number between 0 and 5 was a group number.

Regarding the daily light environment, the randomization function was **RANDBETWEEN(1;10)**. In this case we used ten cages.

3.2.5 Controlled inflammation in animals

In order to study the effects of LLLT in the treatment of inflammatory diseases, it is necessary to have a group of animals with inflammatory processes of identical characteristics, to allow

establishment of a control sample and ensure that observed effects in treated animals do not depend on their initial condition. Thus, it is mandatory to use a process of muscle damage capable of creating a controlled and reproducible inflammation condition between different animals. To this purpose, we used the model of muscle trauma proposed by Rizzi et al. [134].

Following our reasoning, the muscle selection was pointed on gastrocnemius since this muscle has important characteristics for our study: two types of fibers are involved (type I, highly vascularized, and type IIb, with lower vascularization), large dimension (avoiding bone lesion), and rapid and easy access to histological evaluation [58,224,225].

Gastrocnemius injury was induced by a single impact in a press developed by Industrias Mantineo, Mendoza, Argentina (Figure 3.3), after shaving the rat right leg. Injury was done by a metal mass (0.300 kg) falling through a metal guide from a height of 30 cm. The impact kinetic energy was 0.889 J. During the procedure, rats were anesthetized with a mixture of isoflurane (2.5%) and oxygen (97.5%) with a flow of 1.5 l/min. This process was executed during Day 0, starting at 9:00 a.m. The average duration of the process was 3 minutes per rat.

Figure 3.3– Equipment for inflammation induction.

Isoflurane was chosen because it has a rapid induction and recovery, cardiovascular stability and muscle relaxation [226]. This anesthesia was administered using a VetEquip 901806 Laboratory animal anesthesia system (VetEquip, Inc., Pleasanton, California, USA).

3.2.6 Treatment parameters

The treatment was applied daily, using continuous wave or pulsing wave, with excitation at 830 nm, 980 nm or 850 nm (LED) depending on the experiment. Exposure time was 3 minutes. Laser treatment was applied, under artificial light, at the same time of the day (9:00 a.m.), during five

days, directly to shaved skin by transcutaneous application, with a working distance of 1.2 cm. An area of 0.5026 cm2 was irradiated with a spot size of 8 mm. Beam incidence was kept perpendicular to the irradiation area. Only one spot was irradiated. During irradiation, animals were anesthetized with a mixture of isoflurane (2.5%) and oxygen (97.5%) at a flow of 1.5 l/min. Control rats were also anesthetized to ensure standardization, but did not receive laser treatment.

For continuous wave irradiation, energy delivered was 0 J (control group), 1.8 J, 3.6 J, 5.4 J, 7.2 J and 9 J taking into account the output power chosen (radiant powers between 10 and 50 mW, at 10 mW steps, for both 830 nm and 980 nm). Pulsed wave irradiation was performed only with peak power of 50 mW, and duty cycle equal to 80%, which corresponds to an average power of 40 mW. The used frequencies were 5, 25, 50, 100 and 200 Hz.

Regarding the used irradiation parameters, total energy was selected according to the World Association for Laser Therapy (WALT) recommended treatment doses, for Low Level Laser Therapy, which vary between 4 and 16 J. The radiant powers were selected in order to obtain irradiances in the higher half of the common range of values used for stimulation and healing (5 to 50 mW/cm^2) [199] and are similar to those reported for modulation of cytokines expression in skeletal muscle following acute injury [134,136,137].

For PW repetition rates, due to the lack of reference values for the treatment of skeletal muscle inflammation, we choose to use values similar to those reported for pain reduction, since pain relief seems to be obtained by the anti-inflammatory action of LLLT.

It is important to stress that we made the experiments sequentially. First we did the CW treatments. The PW measurements were done afterwards and using only the wavelength and average power that yielded the best results with CW irradiation. The same procedure was followed for the non-coherent LED irradiation experiments. This way we complied with one of the principles on animal experimentation, reduction, minimizing the number of used animals.

3.2.7 Blood Sampling

Blood was collected on days 0 (5 hours after inflammation induction), 3 and 6 (before animal sacrifice), always at 2:00 p.m. A blood volume of 1 ml was taken through the jugular vein. Rats were anesthetized with isoflurane (2.5%) and oxygen (97.5%) with a flow of 1.5 l/min [227].

All blood samples were placed in BD Vacutainer Plastic SST II Advance tubes (BD, Franklin Lakes, New Jersey, USA) for subsequent centrifuging during 15 minutes at 3500 rpm at 4ºC. The serum was removed and the samples were stored at -20 °C. Figure 3.4 summarizes the followed work schedule.

	Day 0	Day 1	Day 2	Day 3	Day 4	Day 5	Day 6
Since 9:00 a.m.	Inflammation induction	Treatment	Treatment	Treatment	Treatment	Treatment	
Since 2:00 p.m.	Blood Sampling			Blood Sampling			Blood Sampling Sacrifice

Figure 3.4– Experiment work schedule.

3.3 ELISA analysis

As we focused our studies on the acute phase (neutrophils or destruction phase) of skeletal muscle inflammation, we choose to measure the serum concentrations of TNF-alpha (TNF-α), IL-1 beta (IL-1β), IL-2 and IL-6 cytokines, which area more present in that phase [56,57]. Tumor necrosis factor (TNF)-α and interleukin IL-1β are two key cytokines, produced in response to trauma, that promote inflammatory responses, including the recruitment of immune cells to the injured area. IL-6 is also a pro-inflammatory cytokine that is responsible, with TNF-α and IL-1β, for increasing the liver synthesis of most acute-phase proteins. IL-2 has both pro- and anti-inflammatory roles. It is a potent inducer of T-cell proliferation but also has regulatory roles, namely in the development and function of regulatory T cells. Thus, IL-2 contributes both to the induction and the end of acute inflammatory responses. The concentration of these cytokines in the blood was measured by ELISA, using Peprotech ELISA Kits [228] (PeproTech EC Ltd., London, United Kingdom).

Counting was done using a BioTek Synergy HT (BioTek Instruments, Inc., Winooski, Vermont, USA) microplate reader, with reading at 405 nm with and a wavelength correction set at 650 nm. The plate was monitored at 5-minute intervals during 45 minutes [228]. The concentrations of samples were calculated by interpolation of the regression curve formula through four parametric regression.

3.4 Animals sacrifice, sample preparation and examination

Rats were killed on day 6 for histological analysis of muscle tissue. The animals were anesthetized with a mixture of isoflurane (2.5%) and oxygen (97.5%) with a flow of 1.5 l/min before blood sampling and cervical dislocation [229]. The gastrocnemius muscle was rapidly removed from the injured legs, snap-frozen in cryopreservation resin, and stored at -80ºC until analysis. The surgical procedure took less than 5 minutes.

The gastrocnemius muscle was rapidly removed from the injured legs, snap frozen in cryopreservation resin, and stored at -80ºC until analysis. The surgical procedure took less than 15 minutes.

The cuts were made transversely to the muscular fibers with a thickness of 5 µm, with a glass knife using a Leica Microsystems CM3350S cryostat (Leica Microsystems, Wetzlar, Germany). After this process, sample dewaxing and hydration, the samples were colored with hematoxylin-eosin and fixed with DPX mountant for microscopy, in order to observe the hematoma area and other visible changes.

The cross sections were observed with Motic AE 31 inverted microscope (Motic Ltd. Hong-Kong, China), using 10X, 20X and 40X objectives. The muscles images were captured using a high resolution camera Motic Moticam 2 for later analysis. The most representative cuts were selected. Hematoma areas were identified through microscopic visual inspection.

These cuts were be used to measure the degree of muscle inflammation by quantifying predominant cells in an acute inflammatory reaction (neutrophils) and evaluating the presence of interstitial edema and vascular congestion.

We compared the number of inflammatory cells between different rats groups (different laser power), on images obtained with the 20X objective. Cells were counted using an unbiased counting frame [230]. For each animal, a minimum of three images were used for inflammatory cell counting [231].

3.5 Statistical Analysis

Comparisons between different cytokines concentrations and concentrations decrease were done using a one-way ANOVA procedure, with post hoc between-group comparisons by the Tukey test [232], if the samples meet the criteria of normality as measured by the Shapiro-Wilks test or Kolmogorov-Smirnov test. When samples do not meet the criteria of normality, the results are analyzed using the Kruskal-Wallis with post hoc comparison between groups by non-parametric Nemenyi test. A significance level of 0.05 was considered in all cases.

The same statistical tests were used to compare between groups the number of inflammatory cells. For each animal, ten images were used for inflammatory cell counting.

Results comparisons between animals groups will be performed by variance analysis (ANOVA), unifactorial or multifactorial, with *post-hoc* comparison between groups by Tukey's test, if the samples meet the criteria of normality as measurement by the Shapiro-Wilks test or Kolmogorov-Smirnov test. When samples do not meet the criteria of normality, the results are analyzed using the Kruskal-Wallis with *post hoc* comparison between groups by non-parametric Nemenyi. It will evaluate statistical power of tests and a minimum detectable difference in order to define statistical significance to use.

3.6 Monte-Carlo simulation of light transport in tissue

The expected dose in muscle tissue was evaluated through computer Monte-Carlo (MC) simulation of light transport in a heterogeneous medium. MC simulations were done with the mcxyz.c code developed and made available by Steven Jacques, Ting Li and Scott Prahl [233]. We used a two-layer tissue model: skin (thickness: 2.1 mm) and muscle. The laser beam was modeled as a Gaussian beam with a diameter of 8 mm at the 1/e2 contour. The optical parameters were obtained from published research work [234] and are summarized in Table 3.1.

Table 3.1– Optical parameters for the tissue model used in Monte-Carlo simulation of light transport.

Layer	μ_a (cm^{-1})		μ_s (cm^{-1})		g	
	830 nm	**980 nm**	**830 nm**	**980 nm**	**830 nm**	**980 nm**
Skin	0.17	0.35	74.49	72.05	0.82	0.84
Muscle	1.15	1.15	91.82	89.79	0.88	0.89

4. Results

Here we present the results of our set of experiments. The first experiment evaluated the effect of energy dose delivered on the treatment of gastrocnemius muscle inflammation with continuous LASER irradiation at 830 nm. The second experiment was identical to the first but the irradiation was done at 980 nm.

Taking into account the results of these two experiments and their comparison, we selected the wavelength, radiant power and energy that produced the largest treatment effect and performed a third experiment using non-coherent LED illumination, with that wavelength, radiant power and energy. The objective was to compare treatment efficacy between coherent and non-coherent irradiation.

Finally, on our last experiment, we used the irradiation parameters (wavelength, output power and energy) with the largest treatment effect on CW irradiation on an experiment using pulsed irradiation. We kept wavelength and average power equal to those that yielded the best results with CW irradiation, and made measurements for a set of five frequencies and pulse widths.

4.1 CW laser irradiation at 830 nm

In the first experiment we evaluated the influence of delivered energy dose, for CW irradiation at 830 nm, on the expression of the previously mentioned inflammatory cytokines. Animals were divided in 6 sub-groups. Five groups are irradiated with a laser emitting at 830 nm, while the remaining group receives no treatment (control group). The irradiated groups received distinct values of radiant power: 10 mW, 20mW, 30 mW, 40 mW and 50 mW. Irradiation time was the same for all animals (3 minutes). By maintaining constant irradiation time while varying the radiant power we ensure a delivered dose variation, according with:

$$\mathrm{Dose[J]} = \mathrm{Power[W]} \times \mathrm{Time[s]} \quad (4.1)$$

Sample number of animals was obtained following the resource equation [221]. The total number of rats for the experiment was 30 rats, 5 for each group.

4.1.1 Serum cytokines concentration measurements by ELISA

Table 4.1 shows the results obtained for TNF-α (mean concentrations and standard deviations). Figure 4.1 and shows the concentration of TNF-α on irradiated and control groups serum. Figure 4.2 shows the concentration relative decrease at day 6, expressed as percentage of the concentration at day 0.

Table 4.1– Serum concentrations of TNF-α measured by ELISA for CW irradiation at 830 nm.

Rat Group	TNF-α concentrations [pg/ml]			Rel. Conc. Decrease day 6 [%]
	day 0	day 3	day 6	
Control	280.956 ± 44.47	257.909 ± 47.98	237.235 ± 50.43	16.046 ± 4.82
10 mW	229.029 ± 22.58	201.107 ± 17.53	165.590 ± 22.77	27.696 ± 7.51
20 mW	220.137 ± 9.09	177.675 ± 20.37	131.982 ± 12.21	40.107 ± 3.97
30 mW	303.320 ± 31.98	209.163 ± 18.41	140.588 ± 15.49	53.089 ± 8.06
40 mW	263.123 ± 33.39	200.737 ± 8.82	158.591 ± 15.97	39.163 ± 7.77
50 mW	255.560 ± 34.97	224.418 ± 31.86	197.447 ± 31.85	22.424 ± 9.56

Results are mean ± SD of 5 rats per group.

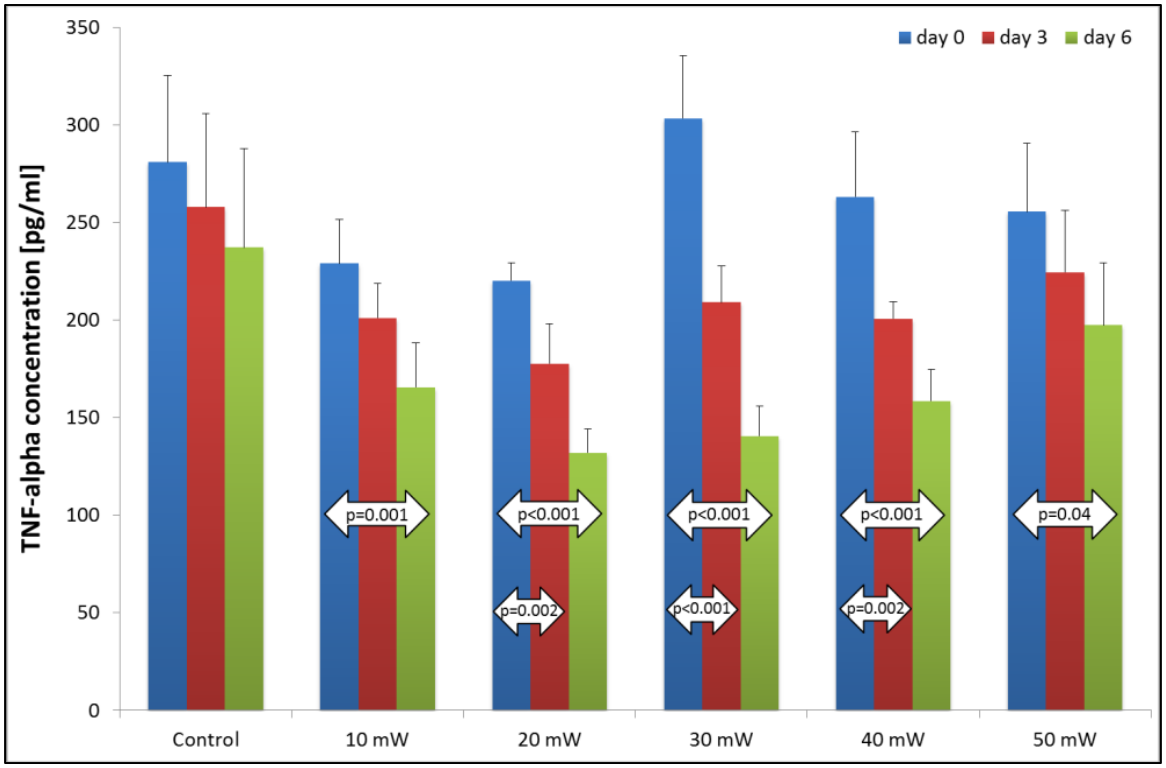

Figure 4.1– TNF-α concentrations for different laser powers (830 nm), observed before inflammation and at days 3 and 6 after inflammation. Error bars indicate standard deviations (SD ±).

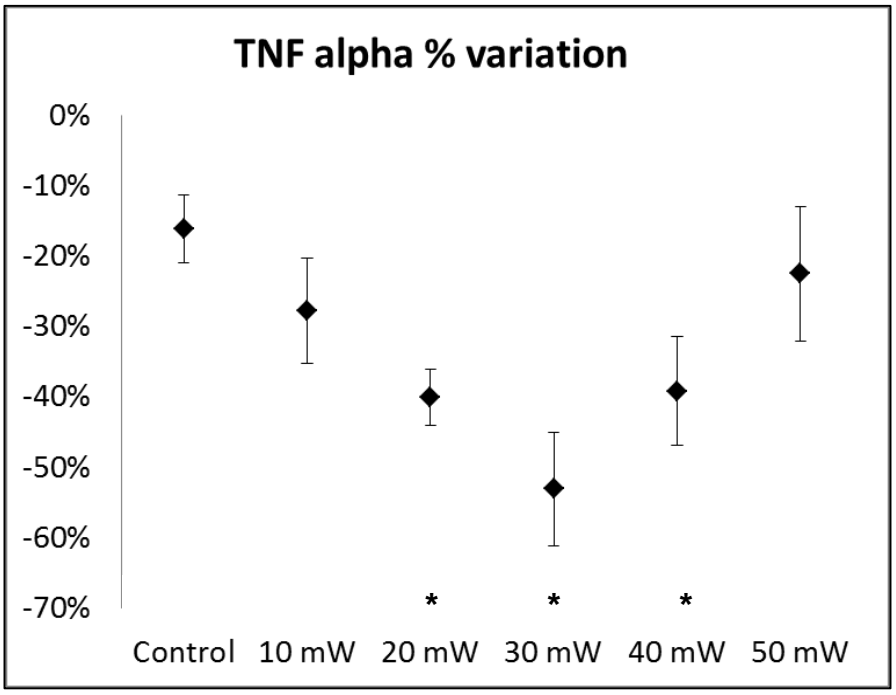

Figure 4.2– Percentage variation of TNF-α concentration from day 0 to day 6 for CW irradiation at 830 nm. Error bars indicate standard deviations (SD ±). Significant difference in relative cytokines concentration decrease for comparisons with control group: * $p < 0.0005$.

There were significant concentration decreases between day 0 and day 3 for 20, 30 and 40 mW while for 10 and 50 mW the concentration decrease was only significant at day 6 (see Figure 4.1). For each group, we also tested if the measured cytokines relative concentration decrease was different than that measured for the control group. Significantly different concentration decreases are identified in Figure 4.2. The TNF-α concentration decrease was significantly higher for the 20, 30 and 40 mW treated groups, when compared with control group. This higher TNF-α decrease could be already observed at day 3 for the 30 and 40 mW groups. The highest variation between day 0 and day 6 was found in the 30 mW group (see Figure 4.2) and it was significantly higher than the observed decrease for the 10 mW and 50 mW groups ($p<0.0005$). The differences for the 20 mW and 40 mW groups were not significant for a 95% level of confidence ($p=0.084$ and $p=0.054$, respectively).

Table 4.2 contains the data on IL-1β measurements. Figure 4.3 and Figure 4.4 show the concentration of IL-1β on irradiated and control groups serum and the concentration relative decrease at day 6. There are significant concentration differences between day 0 and day 6 for control group and all treatment groups, except the 20 mW group. At day 6, the highest concentration relative variation was observed for the 40 mW groups, significantly different from the decrease observed for the control group ($p<0.001$) and the other treatment groups ($p<0.007$), except the 50 mW group ($p=0.57$). The concentration relative variations observed in the 30 mW and 50 mW groups were also significantly higher than that measured for the control group ($p=0.028$ and $p=0.0001$, respectively). This could be clearly observed already at day 3, for the 40 and 50 mW

groups (p<0.001). IL-1β was the only cytokine for which we observed a significant concentration decrease in the control group. (p=0.043 at day 3; p=0.001 at day 6). For the other cytokines, the decreases were not statistically significant, even at day 6.

Table 4.2– Serum concentrations of IL-1β measured by ELISA for CW irradiation at 830 nm.

Rat Group	IL-1β concentrations [pg/ml]			Rel. Conc. Decrease day 6 [%]
	day 0	day 3	day 6	
Control	938.974 ± 48.82	878.404 ± 22.73	832.195 ± 26.93	11.292 ± 2.15
10 mW	1090.544 ± 83.85	966.384 ± 91.03	911.232 ± 77.09	16.481 ± 1.00
20 mW	1046.655 ± 213.14	951.514 ± 148.42	854.059 ± 118.55	17.358 ± 8.74
30 mW	1096.662 ± 71.40	962.524 ± 61.92	867.796 ± 50.19	20.801 ± 2.76
40 mW	1168.729 ± 66.28	954.677 ± 58.60	793.277 ± 51.26	32.100 ± 2.89
50 mW	1154.145 ± 70.77	952.661 ± 37.21	835.537 ± 33.32	27.415 ± 4.71

Results are mean ± SD of 5 rats per group.

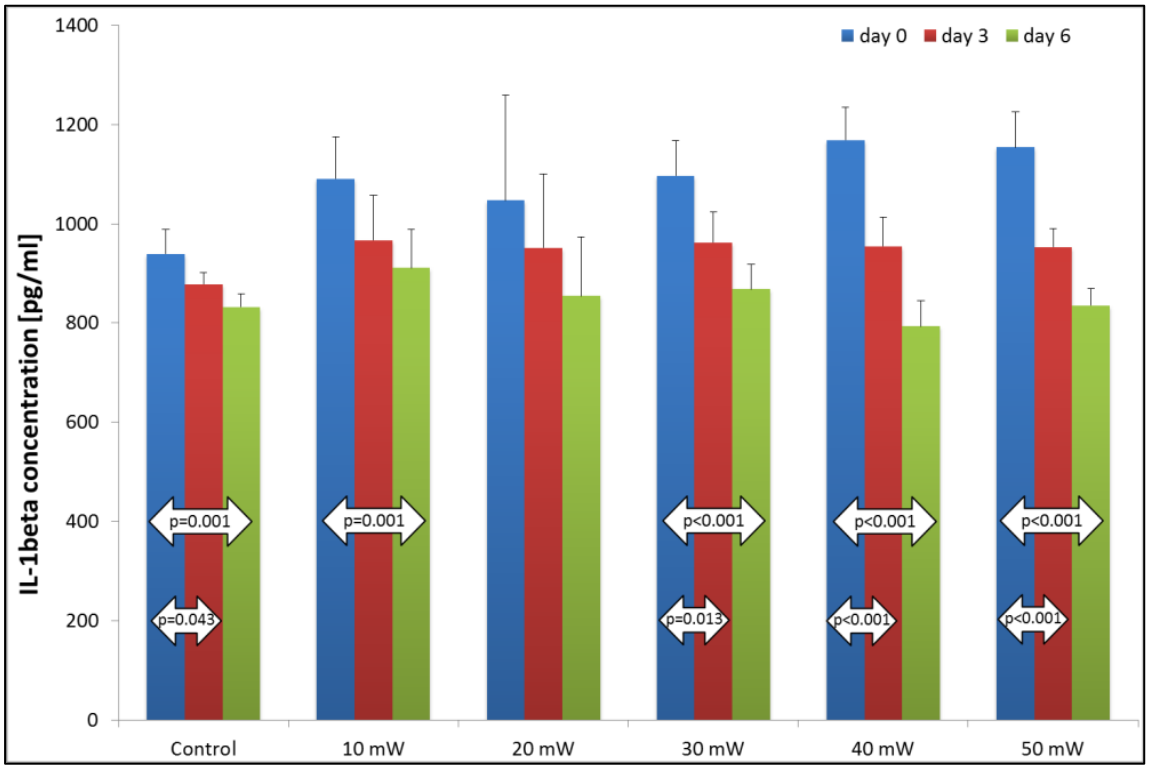

Figure 4.3– IL-1β concentrations for different laser powers (830 nm), observed before inflammation and at days 3 and 6 after inflammation. Error bars indicate standard deviations (SD ±).

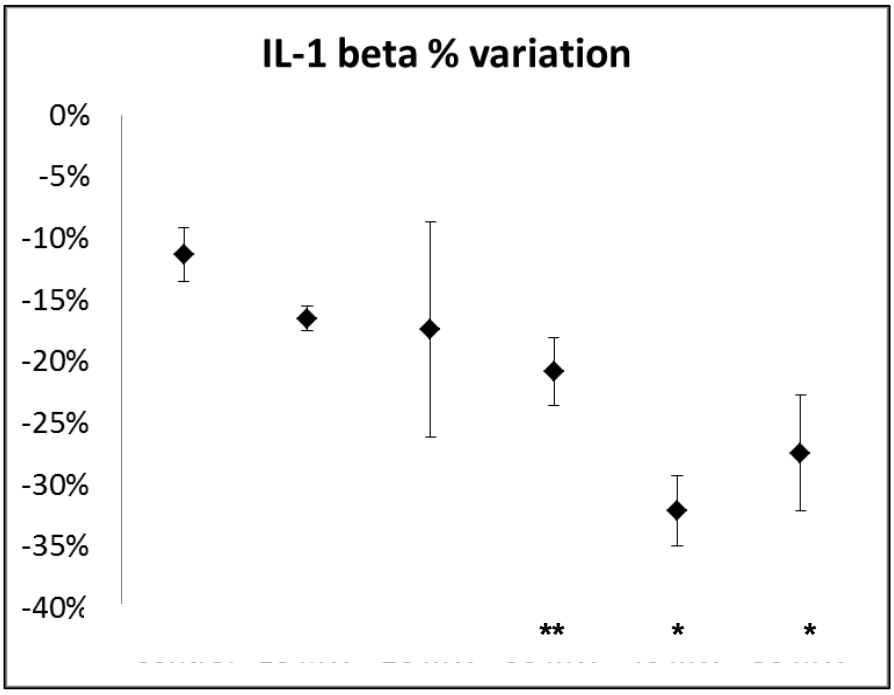

Figure 4.4– Percentage variation of IL-1β concentration from day 0 to day 6 for CW irradiation at 830 nm. Error bars indicate standard deviations (SD ±). Significant difference in relative cytokines concentration decrease for comparisons with control group: * $p < 0.0001$; ** $p < 0.03$.

In the case of IL-2, the concentration decrease between day 0 and day 6 was not statistically significant for any treated group, when considering a confidence level of 95%. The highest differences were observed for 20 mW (p=0.064) and 30 mW (p=0.061). At day 6, the IL-2 concentration relative variation was highest for the 40 mW group. This concentration decrease was significantly higher than that observed for the control group ($p < 0.0003$), for the 10 mW group (p=0.014) and for the 50 mW group (p=0.017). The concentration decrease measured for the 30 mW group was also significantly higher than that obtained for the control group ($p = 0.008$). IL-2 results are shown on Table 4.3, Figure 4.5 and Figure 4.6.

Table 4.3– Serum concentrations of IL-2 measured by ELISA for CW irradiation at 830 nm.

Rat Group	IL-2 concentrations [pg/ml]			Rel. Conc. Decrease day 6 [%]
	day 0	day 3	day 6	
Control	126.418 ± 5.23	122.992 ± 4.74	119.793 ± 4.29	5.222 ± 0.66
10 mW	132.073 ± 12.54	125.863 ± 11.63	122.905 ± 12.20	6.973 ± 0.98
20 mW	134.099 ± 8.35	128.098 ± 7.19	123.005 ± 4.79	8.148 ± 3.11
30 mW	121.970 ± 7.72	116.176 ± 7.06	110.526 ± 6.40	9.357 ± 0.85
40 mW	121.840 ± 9.08	114.600 ± 7.91	108.673 ± 9.44	10.871 ± 1.34
50 mW	124.615 ± 8.31	119.917 ± 8.78	115.781 ± 7.76	7.078 ± 1.84

Results are mean ± SD of 5 rats per group.

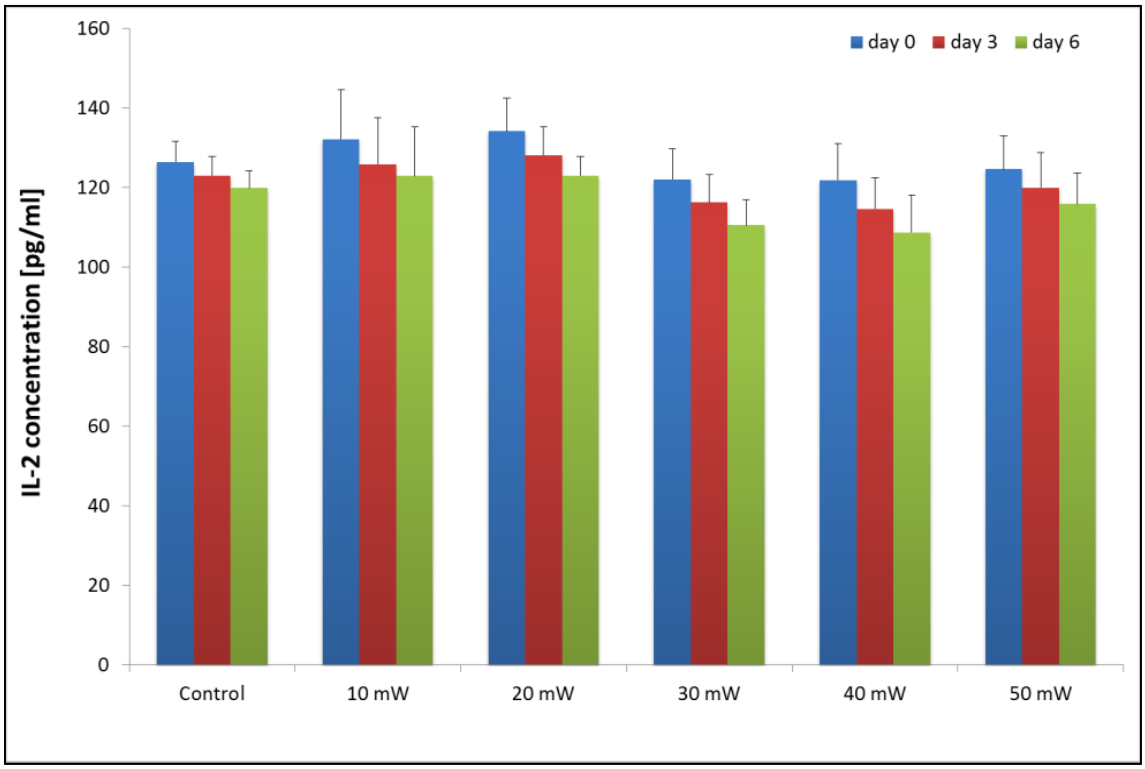

Figure 4.5– IL-2 concentrations for different laser powers (830 nm), observed before inflammation and at days 3 and 6 after inflammation. Error bars indicate standard deviations (SD ±).

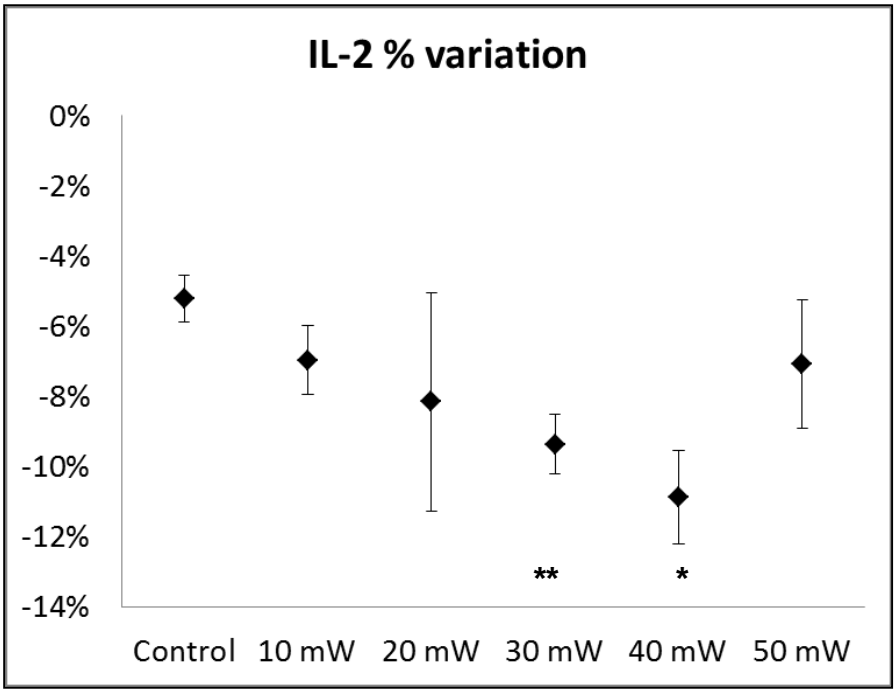

Figure 4.6– Percentage variation of IL-2 concentration from day 0 to day 6 for CW irradiation at 830 nm. Error bars indicate standard deviations (SD ±). Significant difference in relative cytokines concentration decrease for comparisons with control group: * $p < 0.0003$; ** $p < 0.01$.

The results for IL-6 are presented on Table 4.4, Figure 4.7 and Figure 4.8. For IL-6, we found significant concentration differences between day 0 and day 6 for the 40 mW group ($p = 0.02$). For the other groups, the concentration differences were not significant. The highest relative decrease at day 6 was observed for the 40 mW. It was significantly higher than relative decreases observed for the control group ($p<0.0001$) and the other treatment groups (10 mW: $p<0.0005$; 20 mW: $p=0.005$; 30 mW: $p=0.042$; 50 mW: $p=0.009$). At day 6, all treatment groups showed concentration decreases significantly higher than that measured for the control group (see Figure 4.8).

Table 4.4– Serum concentrations of IL-6 measured by ELISA for CW irradiation at 830 nm.

Rat Group	IL-6 concentrations [pg/ml]			Rel. Conc. Decrease day 6 [%]
	day 0	day 3	day 6	
Control	3111.381 ± 415.32	2931.402 ± 403.09	2742.575 ± 388.55	11.926 ± 0.82
10 mW	2298.405 ± 620.96	2059.389 ± 627.35	1790.663 ± 565.51	22.678 ± 8.17
20 mW	2317.961 ± 696.63	2037.327 ± 611.11	1719.165 ± 473.92	25.299 ± 2.58
30 mW	2344.619 ± 585.95	2046.220 ± 488.72	1678.280 ± 369.83	27.953 ± 3.29
40 mW	2642.701 ± 637.03	2047.368 ± 359.18	1671.596 ± 411.60	36.732 ± 3.28
50 mW	2142.222 ± 642.75	1824.716 ± 606.95	1575.661 ± 434.03	26.052 ± 4.42

Results are mean ± SD of 5 rats per group.

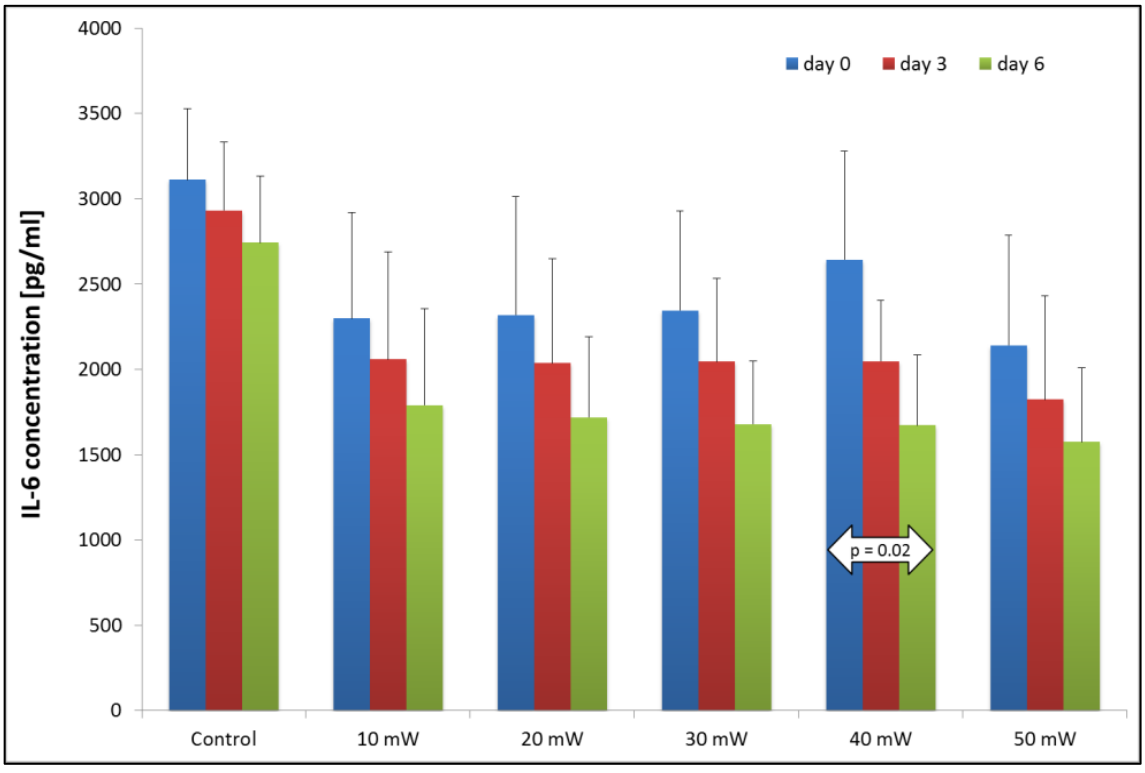

Figure 4.7– IL-6 concentrations for different laser powers (830 nm), observed before inflammation and at days 3 and 6 after inflammation. Error bars indicate standard deviations (SD ±).

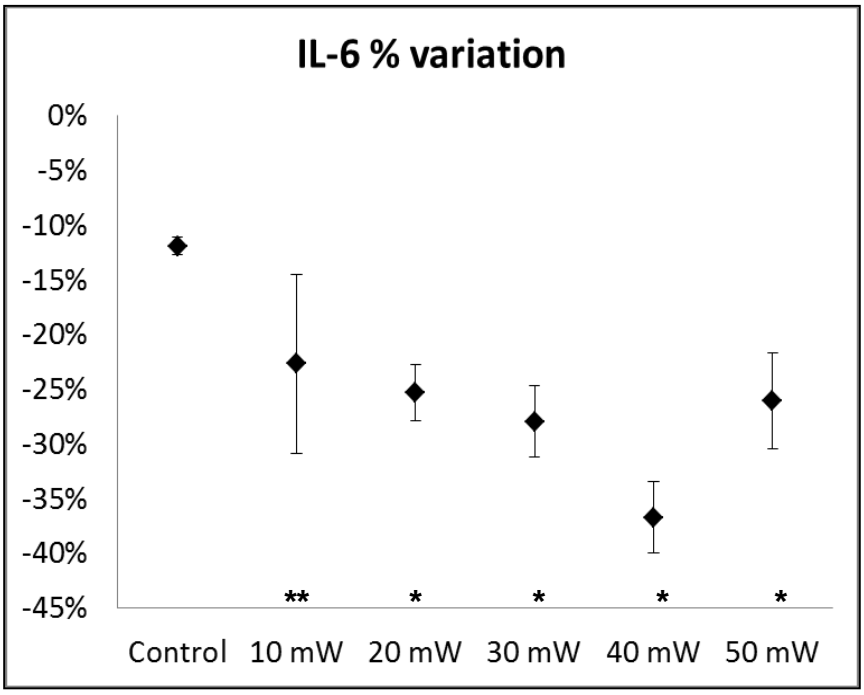

Figure 4.8– Percentage variation of IL-6 concentration from day 0 to day 6 for CW irradiation at 830 nm. Error bars indicate standard deviations (SD ±). Significant difference in relative cytokines concentration decrease for comparisons with control group: ** $p < 0.01$; * $p < 0.001$.

4.1.2 Muscle tissue analysis by optical microscopy

In the control rat, without treatment, it is possible to observe an infiltration of inflammatory cells. The other rats show an improved condition, although they also present inflammatory cells. As trauma is diffuse and considering the days that have passed since inflammation induction, it is only possible to see a slight infiltration with polymorphonuclear neutrophils and macrophages distributed separately. However, this infiltration is lower in the muscles of rats treated with laser. On observation, the best results were obtained for 40 mW group where it is seen a significant improvement of the inflammatory condition, with less inflammatory cells infiltration.

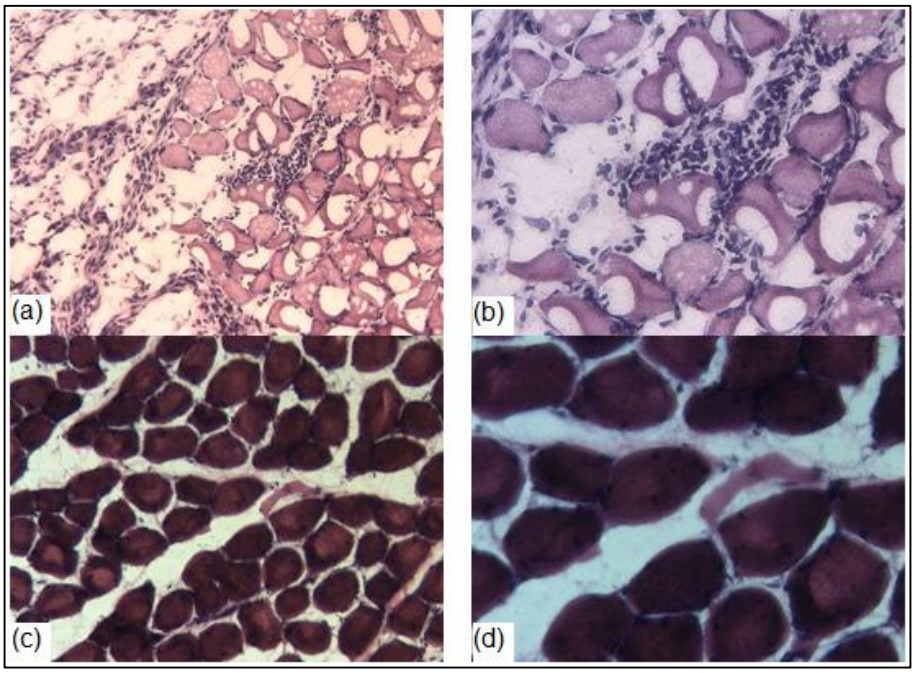

Figure 4.9– Muscle microscopy images for CW irradiation at 830 nm: Control rat (a) 20X; (b) 40X; Rat from 40 mW group: (c) 20X; (d) 40X.

Table 4.5 shows the number of counted inflammatory cells. For each animal, the counting value is the average of measurements done in 10 slides. The values presented are the average for all animals in a given group. The lowest counts of inflammatory cells were obtained at 40 mW. Statistical analysis shows statistically significant differences between the control animals and all of the treated groups ($p < 0.001$). Statistical significant differences were also found between the animals treated with 40 mW and the other groups ($p < 0.001$), except the 50 mW group ($p=0.15$).

Table 4.5– Inflammatory cell counting in images of the gastrocnemius muscle of control and 830 nm treated animals. Values are average ± SD.

Group	Cell counting
Control	17.76 ± 0.79
10 mW	14.30 ± 1.59
20 mW	13.24 ± 1.66
30 mW	12.78 ± 1.84
40 mW	10.84 ± 1.57
50 mW	12.08 ± 2.06

4.2 CW laser irradiation at 980 nm and comparison with irradiation at 830 nm

In the second experiment, we studied the influence of delivered energy dose in the expression of the tested inflammatory cytokines, for irradiation at 980 nm. The experiment was similar to the previous: 6 sub-groups of animals, being five groups irradiated at 980 nm, while the remaining control group receives no treatment; irradiated groups with different values of radiant power (10

mW, 20mW, 30 mW, 40 mW and 50 mW); continuous irradiation with equal exposure time for all animals (3 minutes).

The number of animals per group was obtained following the resource equation [221]. The total number of rats for the experiment was 30 rats, 5 for each group.

Results from this experiment are compared with those obtained for CW irradiation at 830 nm.

4.2.1 Serum cytokines concentration measurements by ELISA

Table 4.6 shows the results obtained for TNF-α (mean concentrations and standard deviations). Figure 4.10 and Figure 4.11 show the concentration of TNF-α on irradiated and control group serum and the concentration relative decrease at day 6.

Table 4.6– Serum concentrations of TNF-α measured by ELISA for CW irradiation at 980 nm.

Rat Group	TNF-α concentrations [pg/ml]			Rel. Conc. Decrease day 6 [%]
	day 0	day 3	day 6	
Control	280.956 ± 44.47	257.909 ± 47.98	237.235 ± 50.43	16.046 ± 4.82
10 mW	305.107 ± 17.85	279.995 ± 18.48	248.441 ± 16.39	18.452 ± 5.54
20 mW	298.318 ± 17.21	265.024 ± 16.42	234.011 ± 17.80	21.594 ± 3.05
30 mW	299.426 ± 13.46	250.843 ± 10.04	218.089 ± 10.53	27.100 ± 3.68
40 mW	346.748 ± 25.13	307.684 ± 15.46	260.168 ± 23.97	24.989 ± 3.75
50 mW	306.811 ± 19.69	276.043 ± 15.32	245.118 ± 20.30	20.137 ± 3.19

Results are mean ± SD of 5 rats per group.

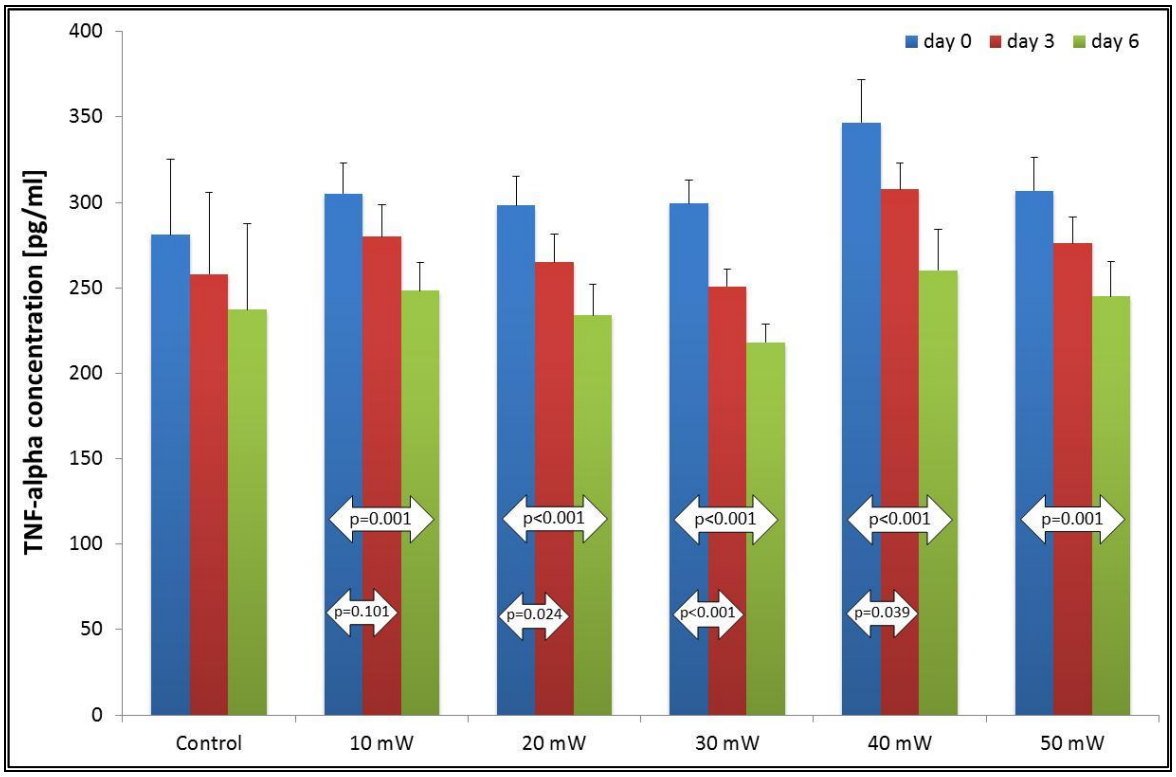

Figure 4.10– TNF-α concentrations for different laser powers (980 nm), observed before inflammation and at days 3 and 6 after inflammation. Error bars indicate standard deviations (SD ±).

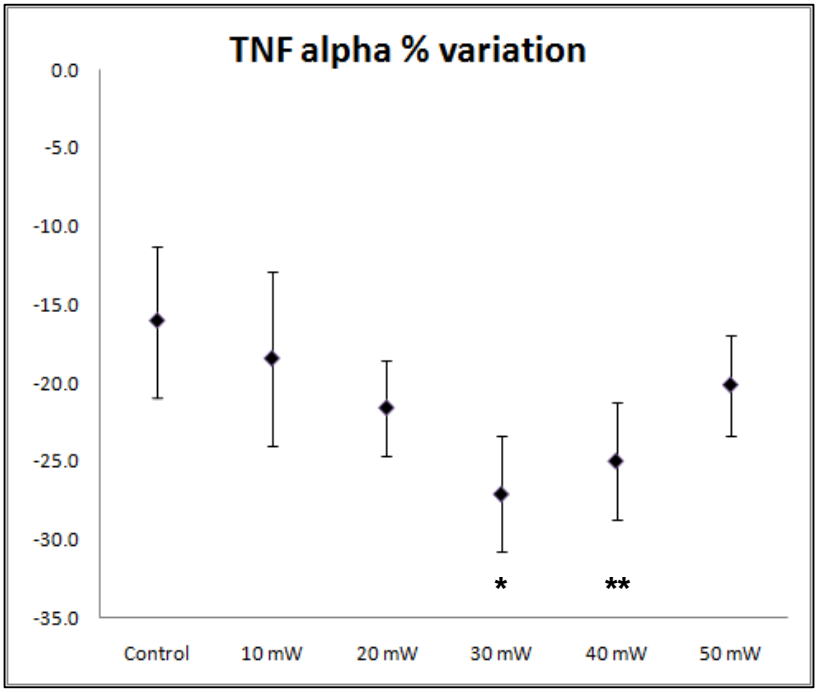

Figure 4.11– Percentage variation of TNF-α concentration from day 0 to day 6 for irradiation at 980 nm. Error bars indicate standard deviations (SD ±). Significant difference in relative cytokines concentration decrease for comparisons with control group: * $p < 0.004$; ** $p < 0.03$.

There were significant concentration decreases between day 0 and day 3 for all groups except 50 mW. At day 6, all groups presented a significantly lower concentration of TNF-α cytokine. When we compare the relative concentration decrease between treated groups and the control group, we find that, at day 6, LLLT was only effective for the 30 and 40-mW groups, with no statistically significant difference between them. The lower effectiveness of irradiation at 980 nm, when compared with 830 nm, is immediately revealed by the lower number of treatment groups that achieved a statistically higher relative decrease of TNF-α expression, when compared with that measured for the control group (2 vs. 3) and is further highlighted by Figure 4.12, which compares TNF-α relative concentration variation, between irradiation at 830 nm and 980 nm. The larger treatment effect for irradiation at 830 nm is clear. When comparing between treated groups at 830 and 980 nm, with the same radiant power and energy dose, we find that TNF-α concentration decrease is significantly higher at 830 nm, for the 20, 30 and 40 mW groups.

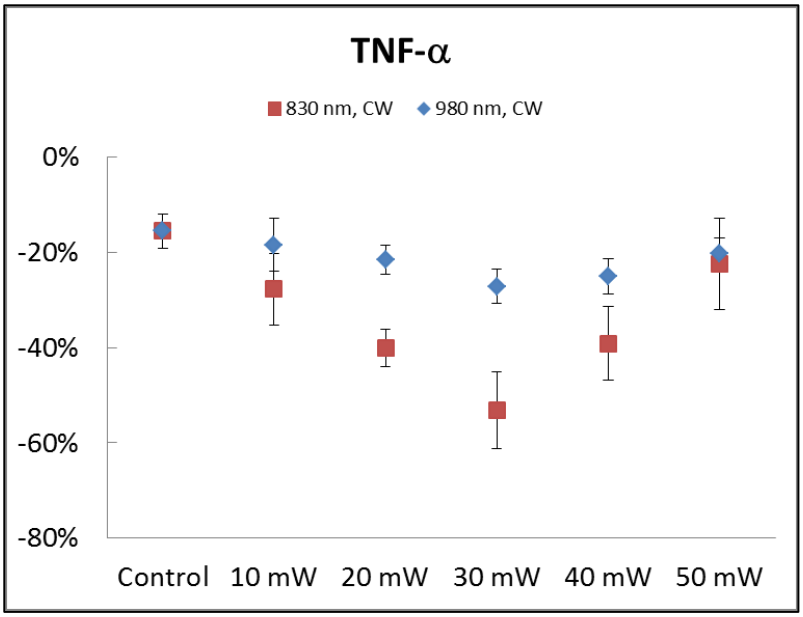

Figure 4.12– Percentage decrease of TNF-α concentration from day 0 to day 6 for irradiation at 830 nm and 980 nm. Error bars indicate standard deviations (SD ±).

Table 4.7 contains the data on IL-1β measurements. Figure 4.13 and Figure 4.14 show the concentration of IL-1β on irradiated and control group serum and the concentration relative decrease at day 6, while Figure 4.15 compares the relative concentration variations between irradiation at 830 nm and 980 nm.

All groups presented significant decreases in the concentration of IL-1β between day 0 and day 6 and even between day 0 and day 3 (here with the exception of the 10 mW group). IL-1β measurements at day 6 show higher relative concentration decreases for the 30, 40 and 50 mW groups, when compared with controls. This could be clearly observed already at day 3 for the 40 mW group ($p<0.001$). The concentration decrease was lower for animals treated at 980 nm.

Comparison between groups treated at 830 and 980 nm with equal radiant power, yielded a higher decrease at 830 nm, for the 40 (p=0.002) and 50 mW (p=0.016) groups.

Table 4.7– Serum concentrations of IL-1β measured by ELISA for CW irradiation at 980 nm.

Rat Group	IL-1β concentrations [pg/ml]			Rel. Conc. Decrease day 6 [%]
	day 0	day 3	day 6	
Control	938.974 ± 48.82	878.404 ± 22.73	832.195 ± 26.93	11.292 ± 2.15
10 mW	907.777 ± 44.26	849.048 ± 50.02	788.511 ± 51.86	13.166 ± 3.00
20 mW	953.441 ± 39.21	877.318 ± 21.52	814.503 ± 19.52	14.488 ± 3.14
30 mW	960.096 ± 49.99	869.632 ± 31.71	789.281 ± 48.33	17.772 ± 3.33
40 mW	922.032 ± 50.51	789.759 ± 34.97	739.119 ± 32.57	19.771 ± 2.50
50 mW	908.282 ± 49.42	835.378 ± 42.66	747.690 ± 35.96	17.577 ± 4.05

Results are mean ± SD of 5 rats per group.

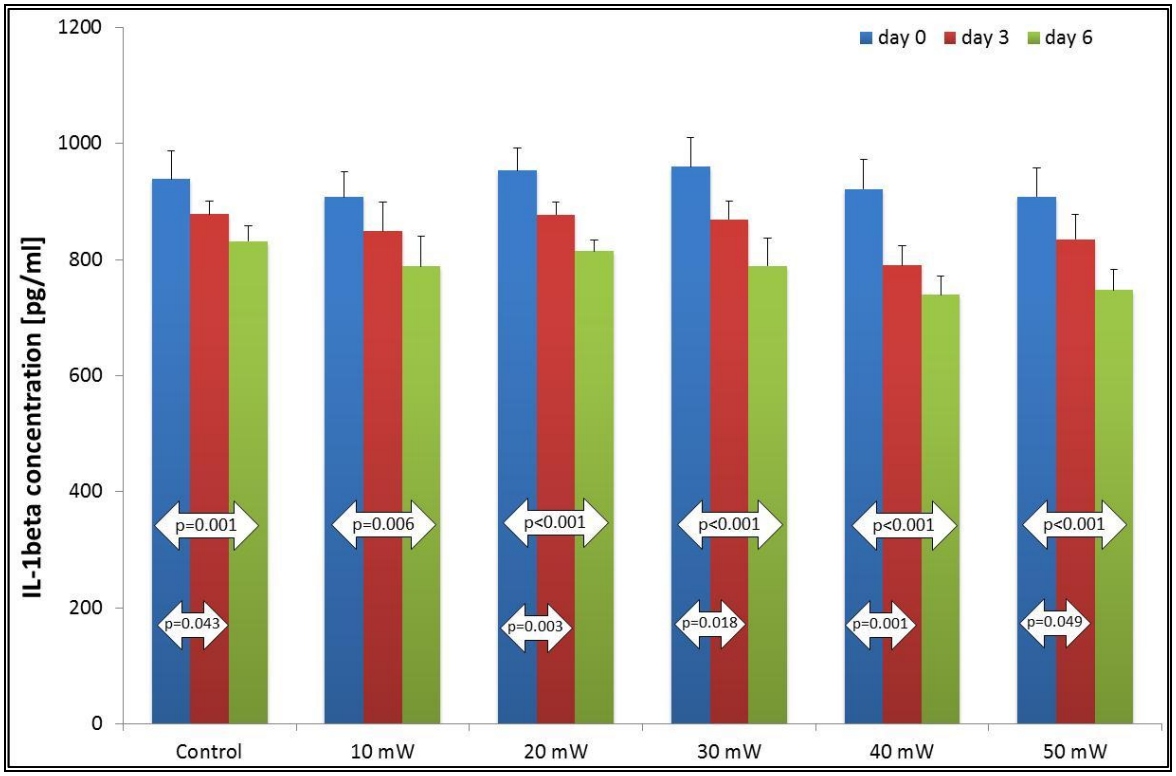

Figure 4.13– IL-1β concentrations for different laser powers (980 nm), observed before inflammation and at days 3 and 6 after inflammation. Error bars indicate standard deviations (SD ±).

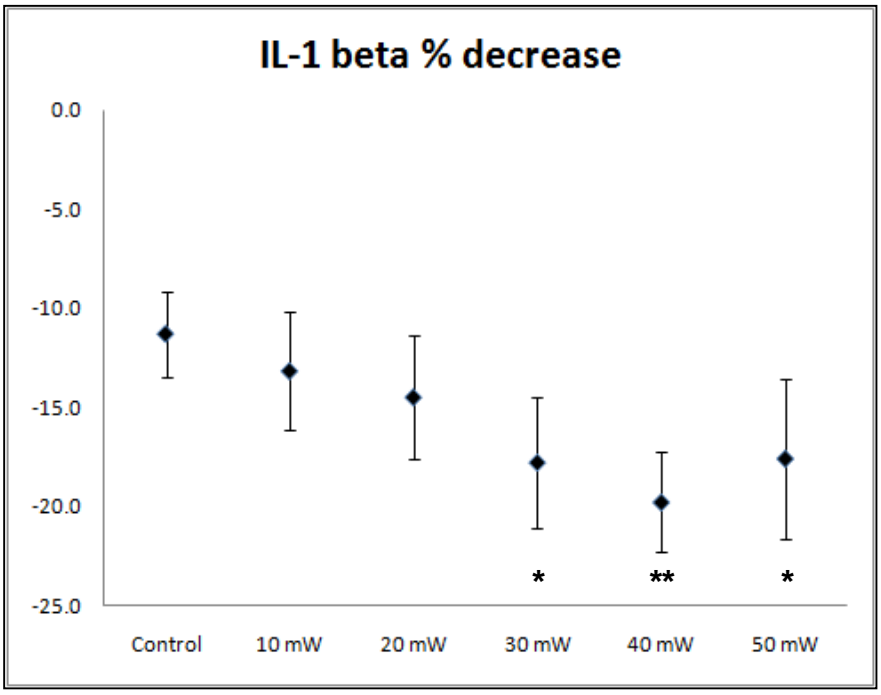

Figure 4.14– Percentage variation of IL-1β concentration from day 0 to day 6 for irradiation at 980 nm. Error bars indicate standard deviations (SD ±). Significant difference in relative cytokines concentration decrease for comparisons with control group: * $p < 0.04$; ** $p < 0.003$.

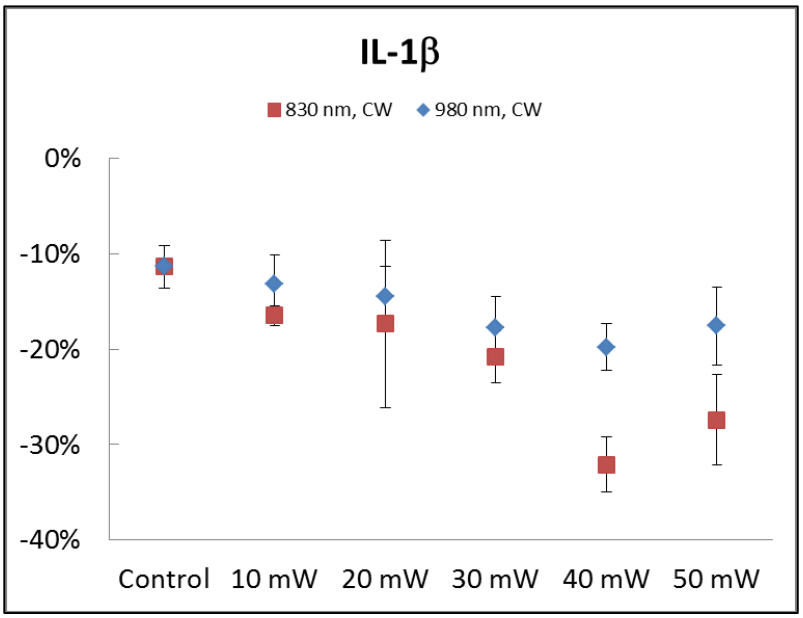

Figure 4.15– Percentage decrease of IL-1β concentration from day 0 to day 6 for irradiation at 830 nm and 980 nm. Error bars indicate standard deviations (SD ±).

IL-2 measurements at day 6 failed to show any significant concentration variation between day 0 and day 6 for the treated groups and for the control. The higher concentration decreases occur for the 30, 40, and 50 mW groups but the concentrations at day 6 are not statistically different from the corresponding concentrations at day 0. When analysing the percentage concentration decreases,

we did not find differences between treatment groups at day 6. The only significant difference was found between the relative concentration variations between the 40 mW group and the control group ($p = 0.017$). IL-2 results are shown on Table 4.8, Figure 4.16 and Figure 4.17. The comparison between LLLT groups with the same radiant power, at 830 and 980 nm, shown in Figure 4.18, yielded no differences.

Table 4.8– Serum concentrations of IL-2 measured by ELISA for CW irradiation at 980 nm.

Rat Group	IL-2 concentrations [pg/ml]			Rel. Conc. Decrease day 6 [%]
	day 0	day 3	day 6	
Control	126.418 ± 5.23	122.992 ± 4.74	119.793 ± 4.29	5.222 ± 0.66
10 mW	142.683 ± 20.67	137.994 ± 19.81	133.615 ± 19.58	6.349 ± 1.48
20 mW	142.879 ± 29.59	137.380 ± 29.95	133.100 ± 29.40	7.040 ± 1.33
30 mW	156.148 ± 20.80	149.682 ± 19.40	144.600 ± 19.80	7.430 ± 1.39
40 mW	138.943 ± 31.47	133.232 ± 32.39	127.969 ± 30.50	8.042 ± 1.63
50 mW	148.343 ± 16.80	144.161 ± 16.37	137.829 ± 16.16	7.118 ± 0.65

Results are mean ± SD of 5 rats per group.

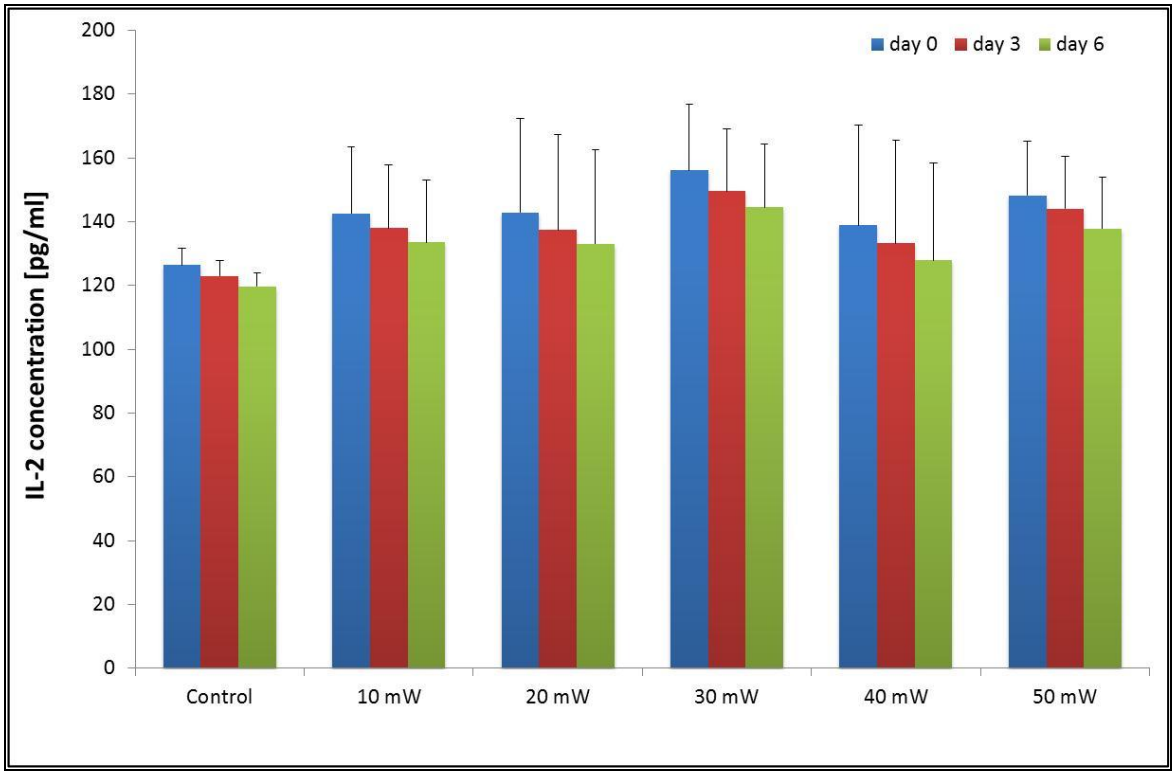

Figure 4.16– IL-2 concentrations for different laser powers (980 nm), observed before inflammation and at days 3 and 6 after inflammation. Error bars indicate standard deviations (SD ±).

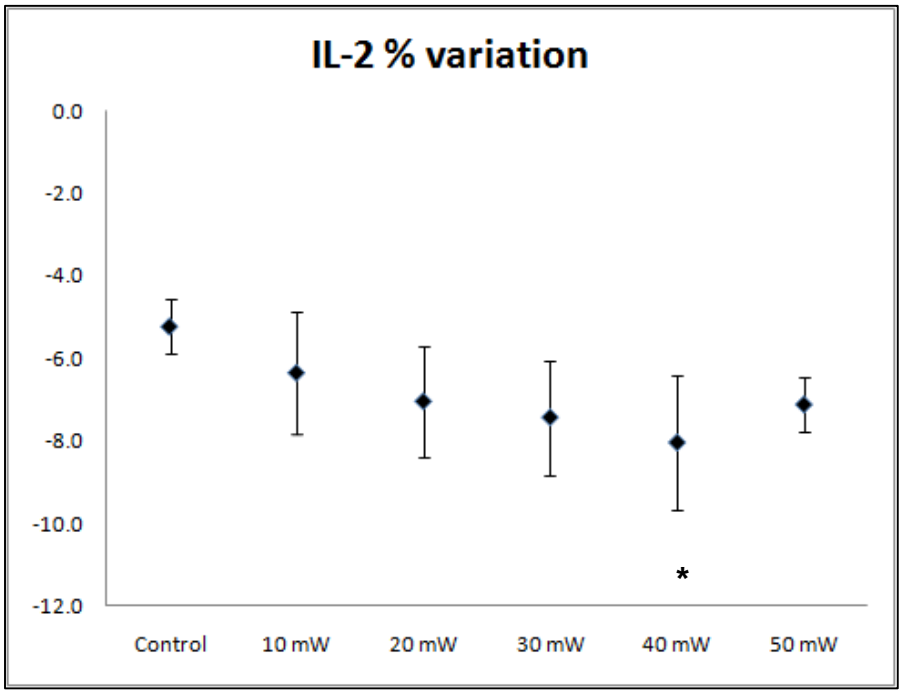

Figure 4.17– Percentage variation of.IL-2 concentration from day 0 to day 6 for irradiation at 980 nm. Error bars indicate standard deviations (SD ±). Significant difference in relative cytokines concentration decrease for comparisons with control group: * $p < 0.02$.

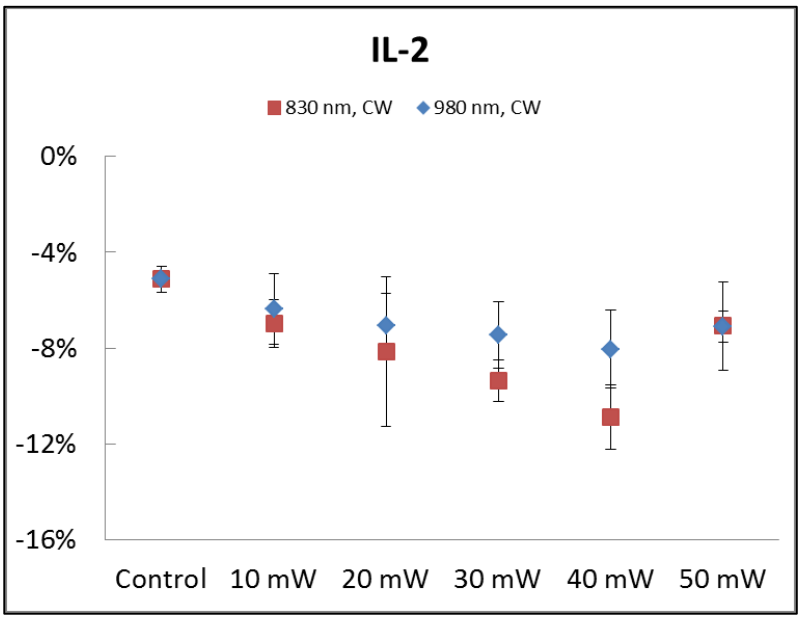

Figure 4.18– Percentage decrease of IL-2 concentration from day 0 to day 6 for irradiation at 830 nm and 980 nm. Error bars indicate standard deviations (SD ±).

The results at day 6 for IL-6 show significant concentration differences, when compared serum concentrations at day 0, just for the 40 mW group ($p = 0.04$). No significant IL-6 concentration decreases were observed at day 3. The relative percentage decrease on IL-6 concentration is significantly higher for the 30 mW ($p = 0.013$), 40 mW ($p < 0.001$) and 50 mW ($p = 0.005$) groups

than for the control group. No significant differences were found between the relative concentration variations between these groups. These results are presented on Table 4.9, Figure 4.19 and Figure 4.20.

The comparison between equivalent LLLT groups at 830 and 980 nm produced significant differences for all compared groups, being highly significant ($p<0.001$) for the 30 and 40 mW groups, For the 40 mW groups, this highly significant difference appears already at day 3. Figure 4.21 shows this comparison.

Table 4.9– Serum concentrations of IL-6 measured by ELISA for CW irradiation at 980 nm.

Rat Group	IL-6 concentrations [pg/ml]			Rel. Conc. Decrease day 6 [%]
	day 0	day 3	day 6	
Control	3111.381 ± 415.32	2931.402 ± 403.09	2742.575 ± 388.55	11.926 ± 0.82
10 mW	2929.588 ± 471.06	2736.349 ± 362.22	2529.988 ± 379.66	13.503 ± 2.80
20 mW	3144.905 ± 300.43	2897.436 ± 288.37	2676.458 ± 252.26	14.880 ± 1.17
30 mW	3024.628 ± 318.59	2774.476 ± 266.72	2529.202 ± 250.91	16.330 ± 0.99
40 mW	3078.682 ± 349.71	2785.911 ± 404.74	2516.816 ± 329.52	18.368 ± 2.62
50 mW	3215.266 ± 413.75	2913.953 ± 352.45	2676.760 ± 354.64	16.763 ± 1.89

Results are mean ± SD of 5 rats per group.

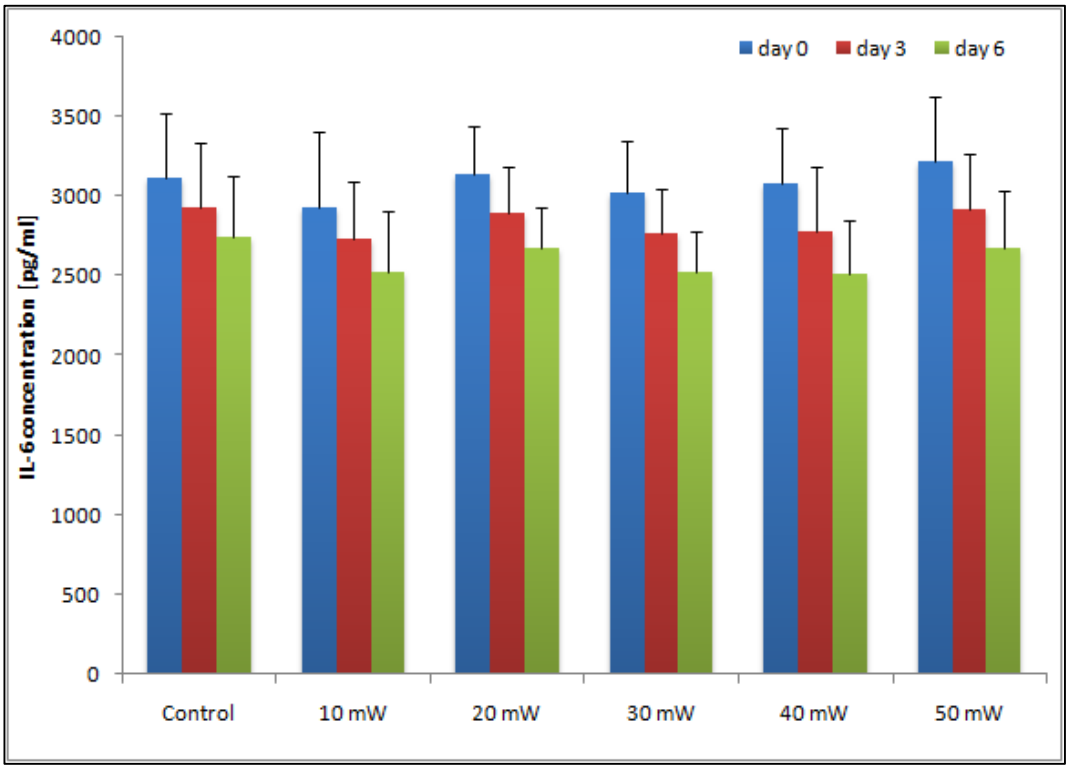

Figure 4.19– IL-6 concentrations for different laser powers (980 nm), observed before inflammation and at days 3 and 6 after inflammation. Error bars indicate standard deviations (SD ±).

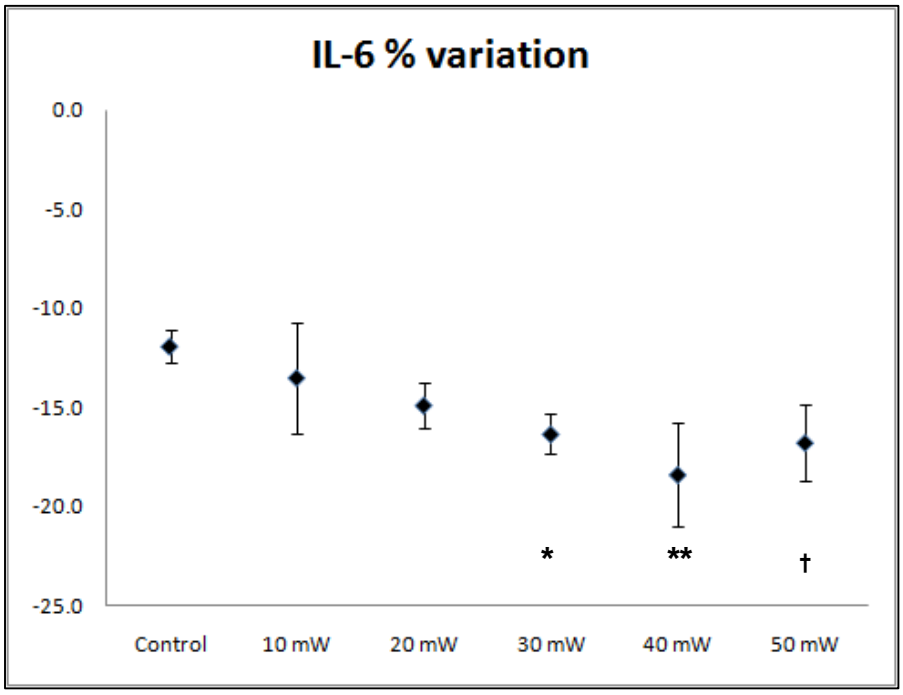

Figure 4.20– Percentage variation of.IL-6 concentration from day 0 to day 6 for irradiation at 980 nm. Error bars indicate standard deviations (SD ±). Significant difference in relative cytokines concentration decrease for comparisons with control group: * $p < 0.02$; ** $p < 0.001$; † $p < 0.005$.

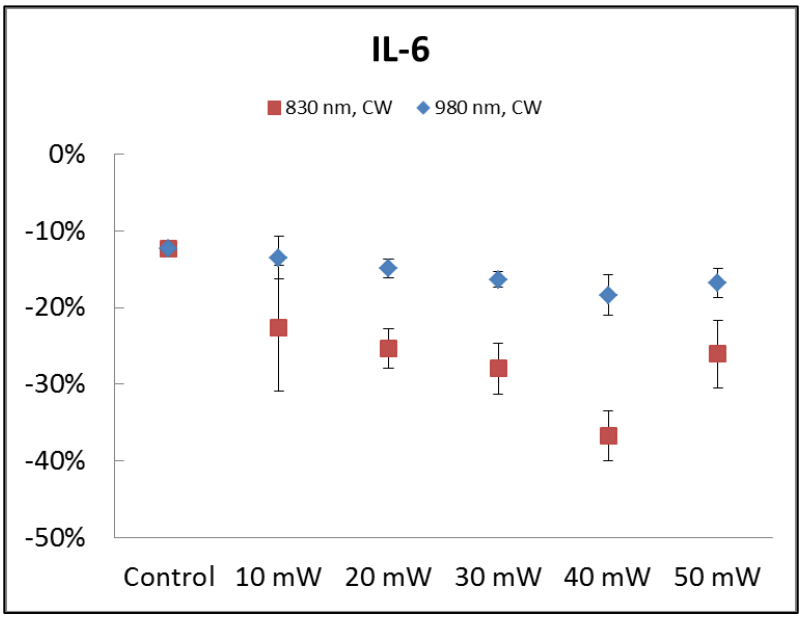

Figure 4.21– Percentage decrease of IL-2 concentration from day 0 to day 6 for irradiation at 830 nm and 980 nm. Error bars indicate standard deviations (SD ±).

4.2.2 Muscle tissue analysis by optical microscopy

In the control rat, without treatment, it is possible to observe an infiltration of inflammatory cells (Figure 4.22 and Figure 4.22b). The treated animals show an improved condition, although they also present inflammatory cells. Once again, as trauma is diffuse and considering the days that

have passed since inflammation induction, it is only possible to see a slight infiltration with polymorphonuclear neutrophils and macrophages distributed separately (see Table 4.10). However, this infiltration is lower in the muscles of rats treated with laser. Again, significant differences ($p<0.001$) were found between the control and all treatment groups, The lowest counts of inflammatory cells was obtained at 40 mW Statistical analysis found significant differences between the cell counting for the 40 mW group and both the 10 and 20 mW groups (Figure 4.22c and Figure 4.22d).

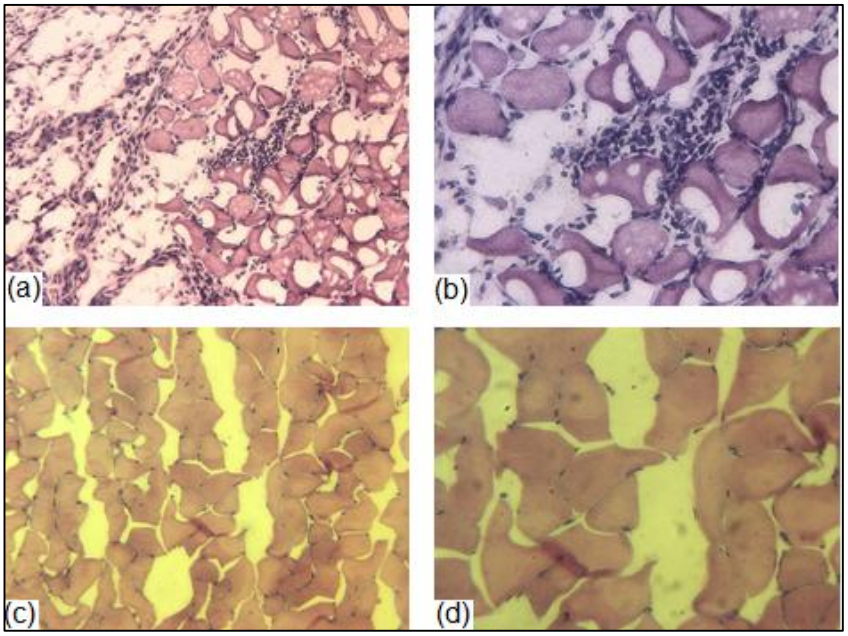

Figure 4.22– Muscle microscopy images for irradiation at 980 nm: Control rat (a) 20X; (b) 40X; Rat from 40 mW group: (c) 20X; (d) 40X.

Table 4.10– Inflammatory cell counting in images of the gastrocnemius muscle of control and 980 nm treated animals. Values are average ± SD.

Group	Cell counting
Control	17.76 ± 0.79
10 mW	14.88 ± 1.59
20 mW	14.06 ± 1.42
30 mW	13.08 ± 1.54
40 mW	12.29 ± 1.96
50 mW	13.02 ± 1.39

The images from animals irradiated with the 830 nm laser present less inflammatory cells when compared with the muscle cuts from animals treated at 980 nm. However, as Table 4.11 shows, the differences are not statistically significant for the level of confidence used.

Table 4.11–Inflammatory cell counting in images of the gastrocnemius muscle of control and CW treated animals. Values are average ± SD.

Group	830 nm Laser	980 nm Laser	p (830 nm vs. 980 nm)
Control	17.76 ± 0.79	17.76 ± 0.79	
10 mW	14.30 ± 1.59	14.88 ± 1.59	0.97
20 mW	13.24 ± 1.66	14.06 ± 1.42	0.79
30 mW	12.78 ± 1.84	13.08 ± 1.54	1.00
40 mW	10.84 ± 1.57	12.29 ± 1.96	0.09
50 mW	12.08 ± 2.06	13.02 ± 1.39	0.63

4.3 Comparison between laser and non-coherent light

In this experiment, the animals were randomly divided into four groups (5 per group): control, Laser 830nm, Laser 980 nm and LED 850 nm. Exposure time was 3 minutes. Energy dose for was 0 J (control group) and 7.2 J (irradiated groups), since our previous experiments achieved the best results for the 40 mW groups.

4.3.1 Serum cytokines concentration measurements by ELISA

For TNF-α, there were significant concentration differences for both laser irradiations. These differences were significant already at day 3 (see Table 4.12). No treatment effect was seen for LED light (see Figure 4.23). The concentration relative decrease at day 6 (see Figure 4.24) for the laser 830 nm group was significantly higher than the observed for all the other groups ($p<0.003$), while for irradiation with LED light the relative decrease was not different from the one observed on the non-treated group ($p=0.971$).

Table 4.12– Serum concentrations of TNF-α measured by ELISA.

Rat Group	TNF-α concentrations [pg/ml]			Rel. Conc. Decrease day 6 [%]
	day 0	day 3	day 6	
Control	280.956 ± 44.47	257.909 ± 47.98	237.235 ± 50.43	16.046 ± 4.82
830 nm	263.123 ± 33.39	200.737 ± 8.82	158.591 ± 15.97	39.163 ± 7.77
980 nm	346.748 ± 25.13	307.684 ± 15.46	260.168 ± 23.97	24.989 ± 3.75
LED 850 nm	433.848 ± 107.94	394.530 ± 90.53	370.967 ± 93.92	14.587 ± 3.81

Results are mean ± SD of 5 rats per group.

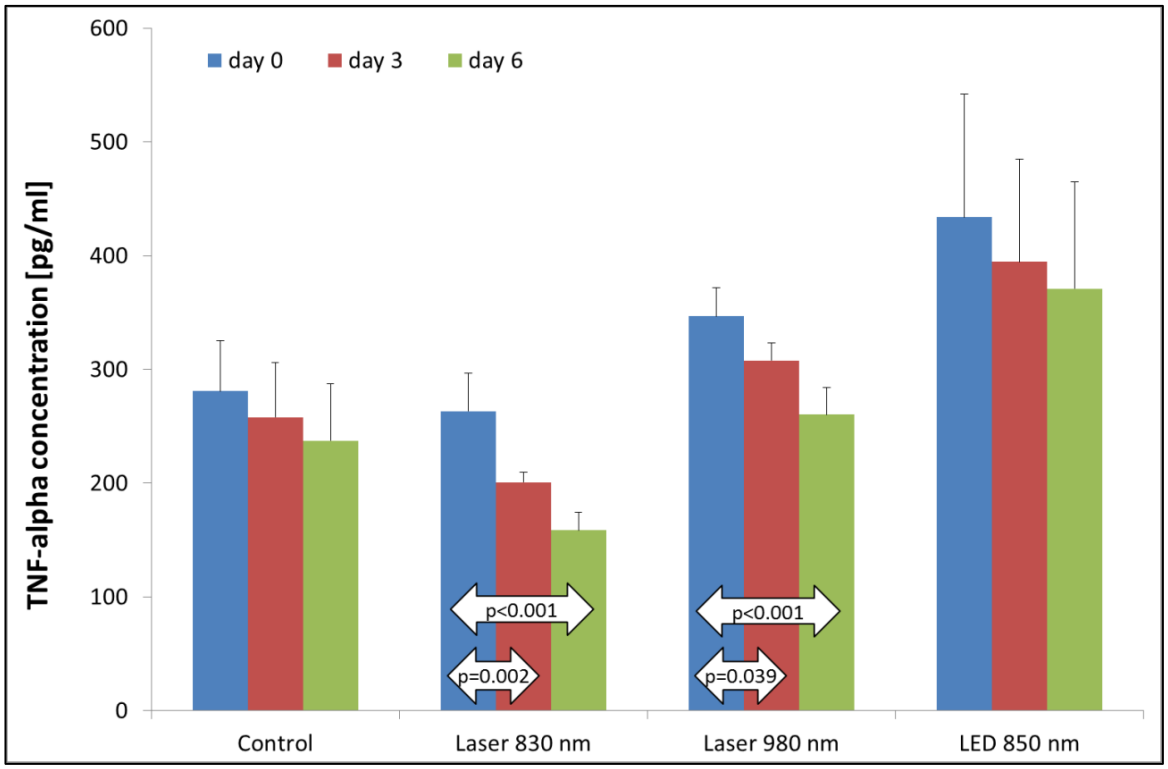

Figure 4.23– TNF-α concentrations for 40 mW laser (830 nm and 980 nm) and LED irradiation, observed before inflammation and at days 3 and 6 after inflammation induction. Error bars indicate standard deviations (SD ±).

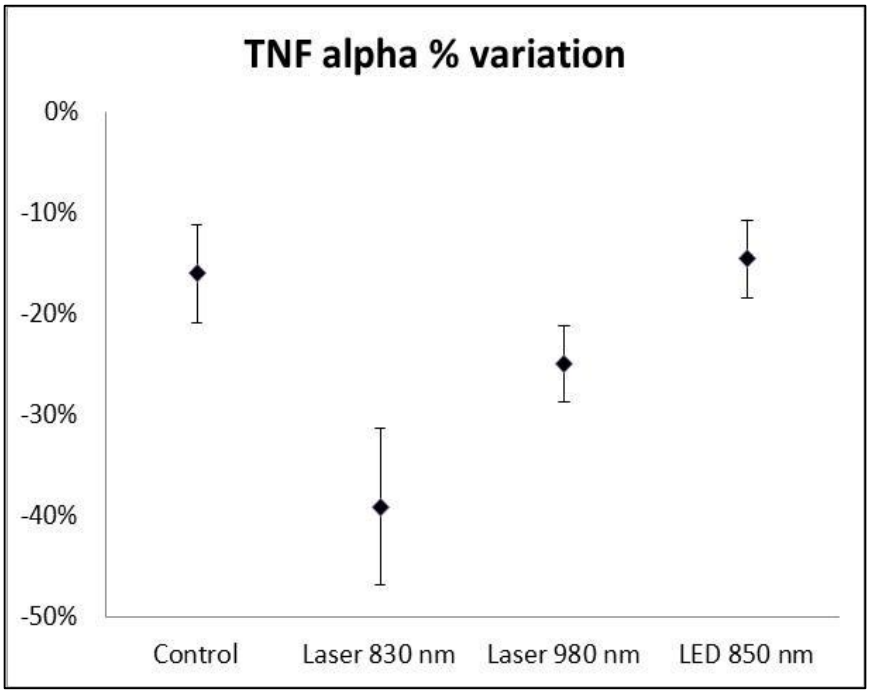

Figure 4.24– Percentage variation of TNF-α concentration from day 0 to day 6 for 40 mW laser (830 nm and 980 nm) and LED irradiation. Error bars indicate standard deviations (SD ±).

Table 4.13 contains the data on IL-1β measurements. Figure 4.25 and Figure 4.26 show the concentration of IL-1β on irradiated and control group serum and the concentration relative decrease at day 6. There are significant concentration differences between day 0 and day 6 for control group and all laser treatment groups but no differences were found for the LED treatment group (p=0.581). Again, the concentration relative decrease at day 6 (see Figure 4.26) for the laser 830 nm group was significantly higher than the observed for all the other groups (p<0.0001). For irradiation with LED light, the relative concentration decrease was not different from the one observed on the control group (p=0.312).

Table 4.13– Serum concentrations of IL-1β measured by ELISA for 40 mW laser (830 nm and 980 nm) and LED irradiation.

Rat Group	IL-1β concentrations [pg/ml]			Rel. Conc. Decrease day 6 [%]
	day 0	day 3	day 6	
Control	938.974 ± 48.82	878.404 ± 22.73	832.195 ± 26.93	11.292 ± 2.15
830 nm	1168.729 ± 66.28	954.677 ± 58.60	793.277 ± 51.26	32.100 ± 2.89
980 nm	922.032 ± 50.51	789.759 ± 34.97	739.119 ± 32.57	19.771 ± 2.50
LED 850 nm	835.202 ± 139.95	752.307 ± 114.47	675.419 ± 92.70	18.747 ± 4.27

Results are mean ± SD of 5 rats per group.

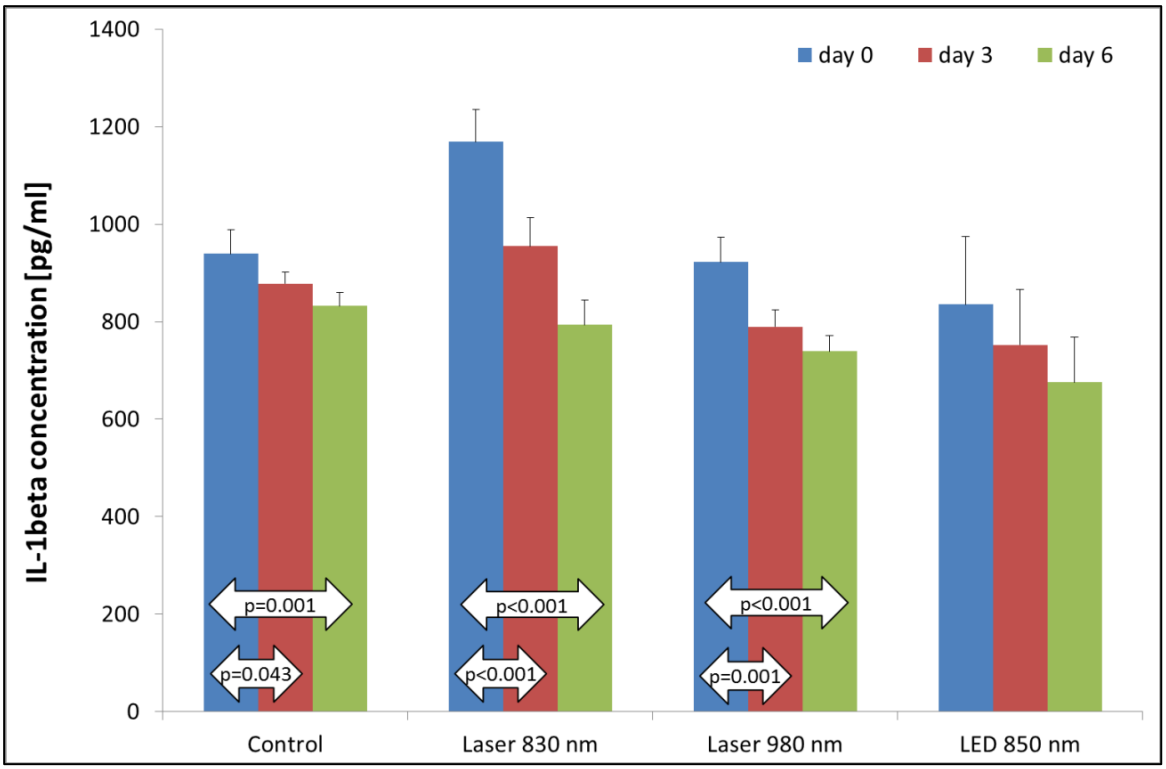

Figure 4.25– IL-1β concentrations for 40 mW laser (830 nm and 980 nm) and LED irradiation, observed before inflammation and at days 3 and 6 after inflammation induction. Error bars indicate standard deviations (SD ±).

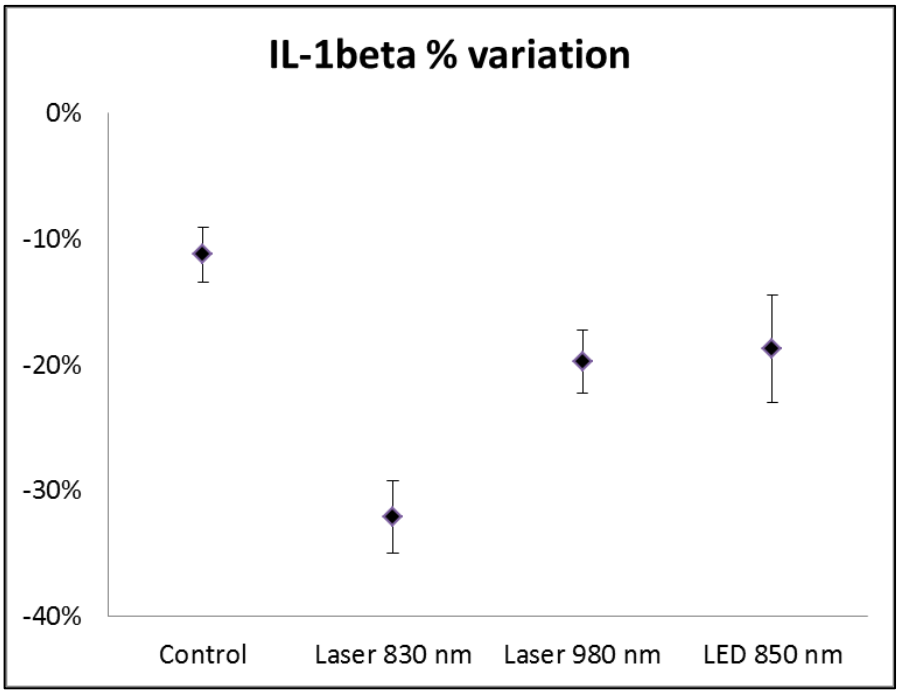

Figure 4.26– Percentage variation of IL-1β concentration from day 0 to day 6 for 40 mW laser (830 nm and 980 nm) and LED irradiation. Error bars indicate standard deviations (SD ±).

IL-2 results are shown on Table 4.14, Figure 4.27 and Figure 4.28. The concentration decrease between day 0 and day 6 was not statistically significant for any treated group and for the control group, when considering a confidence level of 95% (p=0.99). When analyzing relative concentration variations (see Figure 4.28) we found again that the relative for the laser 830 nm group was significantly higher than the observed for the other groups (p<0.025). The laser 980 nm group also presented a relative variation significantly higher than that observed for the control (p=0.022). That did not happened when comparing with the LED 850 nm group (p=0.09). Once again, irradiation with LED light did not result in a relative concentration decrease significantly different from that observed for the control group (p=0.88).

Table 4.14– Serum concentrations of IL-2 measured by ELISA for 40 mW laser (830 nm and 980 nm) and LED irradiation.

Rat Group	IL-2 concentrations [pg/ml]			Rel. Conc. Decrease day 6 [%]
	day 0	day 3	day 6	
Control	126.418 ± 5.23	122.992 ± 4.74	119.793 ± 4.29	5.222 ± 0.66
830 nm	121.840 ± 9.08	114.600 ± 7.91	108.673 ± 9.44	10.871 ± 1.34
980 nm	138.943 ± 31.47	133.232 ± 32.39	127.969 ± 30.50	8.042 ± 1.63
LED 850 nm	149.540 ± 5.55	145.025 ± 5.69	140.816 ± 6.42	5.850 ± 1.58

Results are mean ± SD of 5 rats per group.

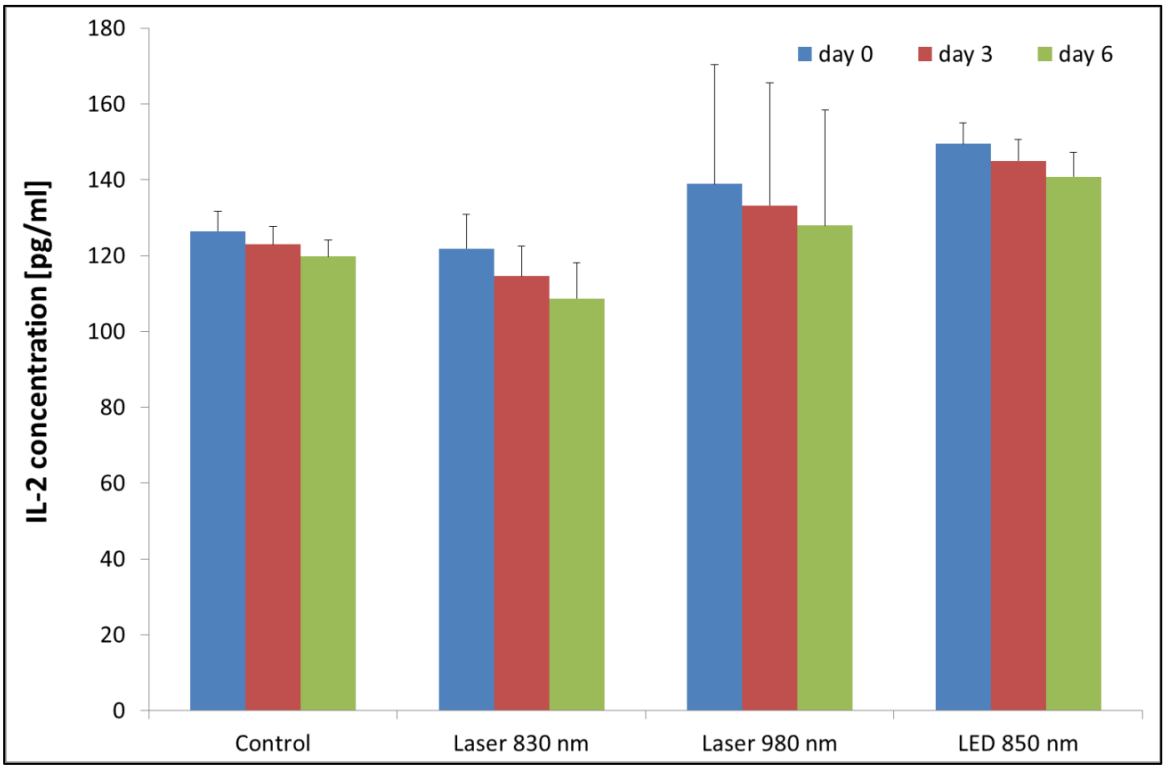

Figure 4.27– IL-2 concentrations for 40 mW laser (830 nm and 980 nm) and LED irradiation, observed before inflammation and at days 3 and 6 after inflammation induction. Error bars indicate standard deviations (SD ±).

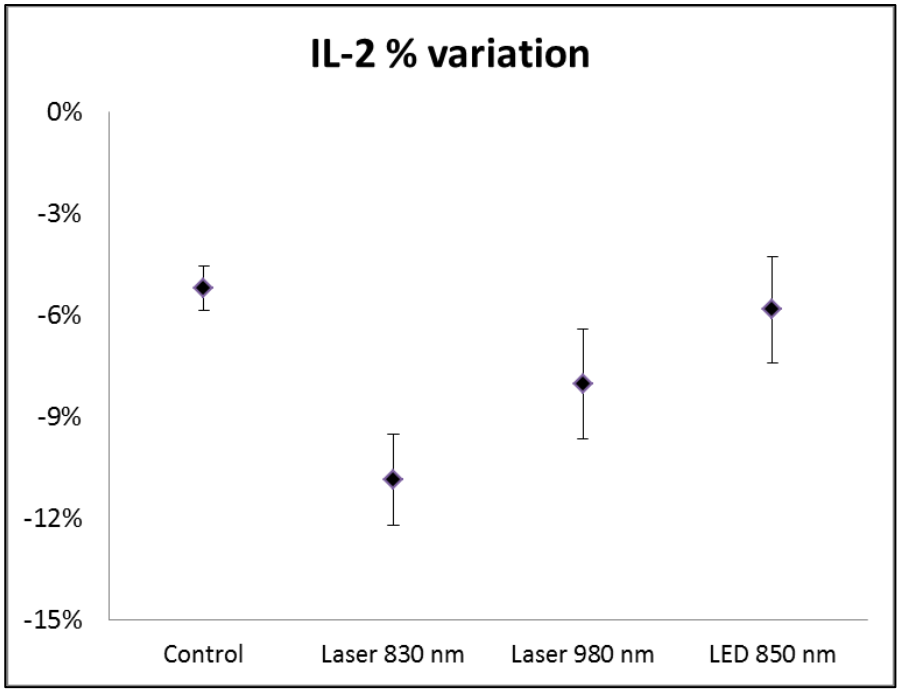

Figure 4.28– Percentage variation of IL-2 concentration from day 0 to day 6 for 40 mW laser (830 nm and 980 nm) and LED irradiation. Error bars indicate standard deviations (SD ±).

For IL-6 (results shown on Table 4.15, Figure 4.29 and Figure 4.30), the concentration decrease between day 0 and day 6 was statistically significant just for the laser treated groups. The relative

concentration decrease (Figure 4.30) was significantly higher for the laser 830 nm group than for the other groups ($p<0.001$). The laser 980 nm group also presented a relative variation significantly higher than that observed for the control ($p=0.006$), but not when compared with the LED 850 nm group ($p=0.057$). Like before, irradiation with LED light did not produce a relative IL-6 concentration decrease significantly different from that observed for the control group ($p=0.66$).

Table 4.15– Serum concentrations of IL-6 measured by ELISA for 40 mW laser (830 nm and 980 nm) and LED irradiation.

Rat Group	IL-6 concentrations [pg/ml]			Rel. Conc. Decrease day 6 [%]
	day 0	day 3	day 6	
Control	3111.381 ± 415.32	2931.402 ± 403.09	2742.575 ± 388.55	11.926 ± 0.82
830 nm	2642.701 ± 637.03	2047.368 ± 359.18	1671.596 ± 411.60	36.732 ± 3.28
980 nm	3078.682 ± 349.71	2785.911 ± 404.74	2516.816 ± 329.52	18.368 ± 2.62
LED 850 nm	3317.512 ± 412.40	3046.792 ± 400.22	2855.715 ± 333.28	13.811 ± 2.89

Results are mean ± SD of 5 rats per group.

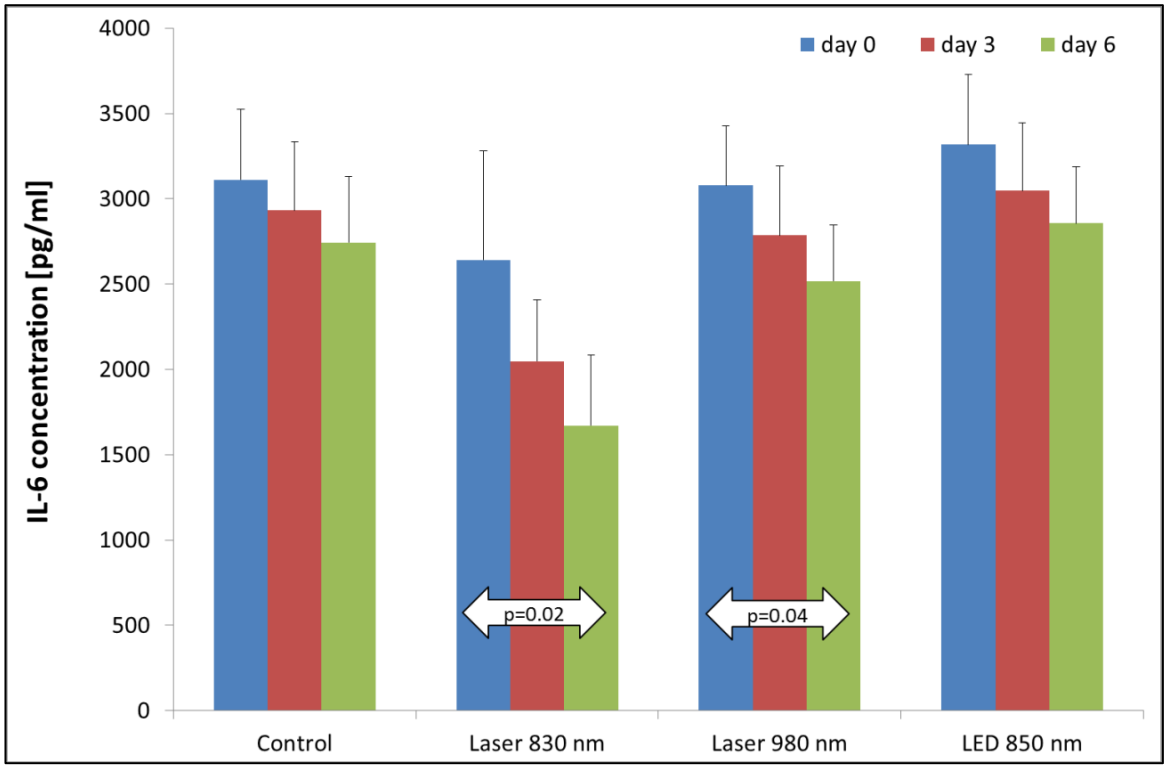

Figure 4.29– IL-6 concentrations for 40 mW laser (830 nm and 980 nm) and LED irradiation, observed before inflammation and at days 3 and 6 after inflammation induction. Error bars indicate standard deviations (SD ±).

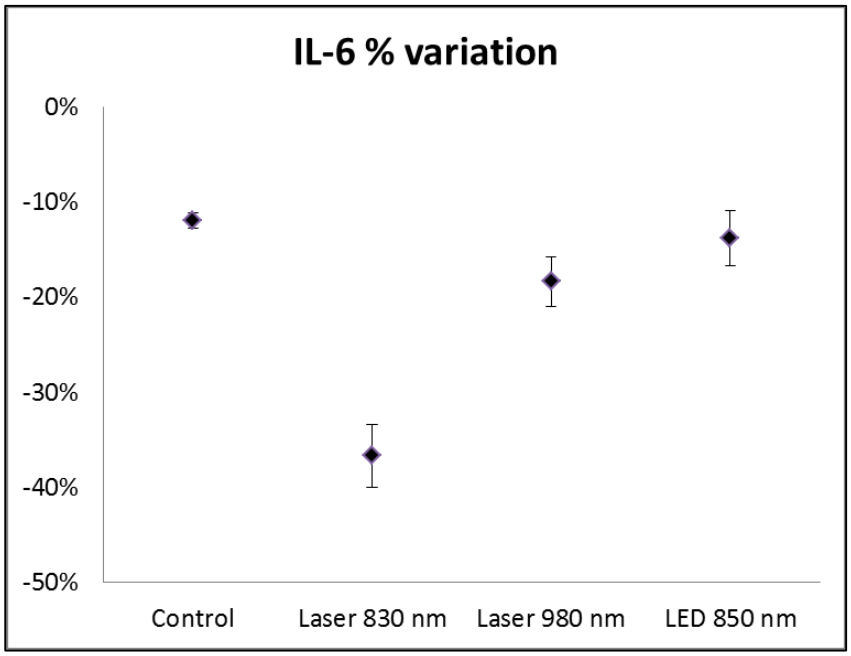

Figure 4.30– Percentage variation of IL-6 concentration from day 0 to day 6 for 40 mW laser (830 nm and 980 nm) and LED irradiation. Error bars indicate standard deviations (SD ±).

4.3.2 Muscle tissue analysis by optical microscopy

Figure 4.31a and Figure 4.31b show images of muscle tissue retrieved from control animals. As in previous experiments, it is possible to observe an infiltration of inflammatory cells. For the animals treated with LED light (Figure 4.31c and Figure 4.31d), we observed infiltration with polymorphonuclear neutrophils and macrophages distributed separately. When we compared the average number of inflammatory cells per image between the experiment groups (see Table 4.16 and Table 4.17) we found significant differences. The treatment effect is clearly higher with laser irradiation than with LED. In fact, we couldn't find differences between the control and the LED groups.

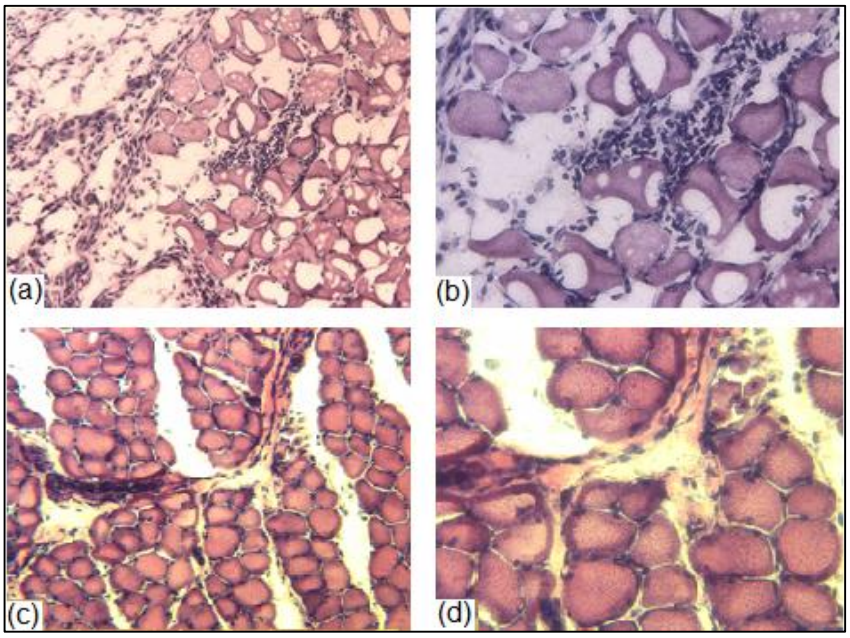

Figure 4.31**–** Muscle microscopy images: Control rat (a) 20X; (b) 40X; Rat from LED 850 nm 40 mW group: (c) 20X; (d) 40X.

Table 4.16– Percentage of inflammatory cells on muscle tissue samples observed by optical microscopy (20X).

Group	Percentage of control of cells ± Std. Dev.
Control	100
830 nm 40 mW	60.76 ± 8.80
980 nm 40 mW	68.83 ± 10.90
LED 850 nm 40 mW	95.52 ± 8.91

Table 4.17–Inflammatory cell counting in images of the gastrocnemius muscle of control and CW treated animals and comparison between groups (ANOVA with Post-hoc Tukey)

	Control	830 nm 40 mW	980 nm 40 mW	LED 850 nm 40 mW
Inflammatory cells ± Std. Dev.	17.84 ± 2.77	10.84 ± 1.57	12.28 ± 1.94	17.04 ± 1.59
Comparison between groups (p values)				
Control		< 0.0001	< 0.0001	0.33
830 nm 40 mW			0.028	< 0.0001
980 nm 40 mW				< 0.0001

4.4 Pulsed wave irradiation effects

For pulsed wave (PW) irradiation, we have chosen a duty cycle of 80%, a peak power of 50 mW, an average power of 40 mW and 5 pulse repetition rates and their proper pulse width and pulse period, as summarized in Table 4.18.

Table 4.18– Experiment laser pulsing parameters.

Duty cycle: 80%, Peak power: 50 mW, Average power: 40 mW		
Frequencies [Hz]	**Pulse width [ms]**	**Pulse period [ms]**
5 Hz	160	200
25 Hz	32	40
50 Hz	16	20
100 Hz	8	10
200 Hz	4	5

In this experiment, following our previous results, we used a laser of 830 nm. The treatment groups were organized in 6 sub-groups of animals. Five groups are irradiated with pulsed light at the five different pulse repetition rates, while the remaining group receives no treatment (control group). Irradiation time was the same for all animals: 3 minutes. The total number of rats used for the experiment was 30 rats, 5 for each group.

4.4.1 Serum cytokines concentration measurements by ELISA

The measurements of serum cytokines concentration are summarized on Table 4.19,

Table 4.20, Table 4.21 and Table 4.22 and on Figure 4.32.

Table 4.19– Serum concentrations of TNF-α measured by ELISA.

Rat Group	**TNF-α concentrations [pg/ml]**			**Rel. Conc. Decrease day 6 [%]**
	day 0	**day 3**	**day 6**	
Control	264.135 ± 8.39	245.353 ± 8.34	224.469 ± 7.66	15.004 ± 1.97
5 Hz	260.879 ± 12.84	236.119 ± 10.04	216.826 ± 7.10	16.793 ± 3.16
25 Hz	268.254 ± 9.15	242.474 ± 10.17	222.262 ± 7.92	17.131 ± 1.82
50 Hz	265.290 ± 8.84	240.330 ± 9.38	211.347 ± 3.55	20.286 ± 2.04
100 Hz	269.084 ± 6.40	233.249 ± 7.50	202.758 ± 5.81	24.637 ± 1.92
200 Hz	262.038 ± 11.55	229.656 ± 7.83	199.541 ± 6.12	23.783 ± 2.65

Results are mean ± SD of 5 rats per group.

Table 4.20– Serum concentrations of IL-1β measured by ELISA.

Rat Groups	IL-1β concentrations [pg/ml]			Rel. Conc. Decrease day 6 [%]
	day 0	day 3	day 6	
Control	917.368 ± 50.94	864.242 ± 51.88	813.644 ± 56.45	11.344 ± 2.58
5 Hz	943.293 ± 42.26	878.239 ± 43.07	821.000 ± 48.03	13.002 ± 1.51
25 Hz	919.142 ± 43.09	857.629 ± 29.59	797.059 ± 28.92	13.237 ± 1.85
50 Hz	928.875 ± 48.01	855.659 ± 50.13	784.720 ± 44.92	15.525 ± 1.73
100 Hz	910.834 ± 48.92	832.923 ± 43.84	746.358 ± 34.37	18.027 ± 1.09
200 Hz	941.692 ± 40.23	860.341 ± 31.10	782.533 ± 22.25	16.847 ± 2.03

Results are mean ± SD of 5 rats per group.

Table 4.21– Serum concentrations of IL-2 measured by ELISA.

Rat Group	IL-2 concentrations [pg/ml]			Rel. Conc. Decrease day 6 [%]
	day 0	day 3	day 6	
Control	156.639 ± 30.04	152.835 ± 29.27	148.760 ± 28.58	5.030 ± 0.47
5 Hz	163.839 ± 33.00	158.704 ± 32.28	153.862 ± 31.11	6.109 ± 0.80
25 Hz	152.221 ± 30.01	147.185 ± 29.26	142.601 ± 28.78	6.364 ± 0.82
50 Hz	167.602 ± 24.81	161.403 ± 23.62	155.577 ± 22.29	7.120 ± 1.35
100 Hz	159.334 ± 22.37	152.636 ± 22.19	146.362 ± 21.65	8.207 ± 1.12
200 Hz	165.353 ± 15.36	158.349 ± 14.61	152.580 ± 13.66	7.695 ± 1.25

Results are mean ± SD of 5 rats per group.

Table 4.22– Serum concentrations of IL-6 measured by ELISA.

Rat Group	IL-6 concentrations [pg/ml]			Rel. Conc. Decrease day 6 [%]
	day 0	day 3	day 6	
Control	2941.939 ± 238.39	2755.240 ± 232.99	2571.136 ± 223.91	12.642 ± 0.86
5 Hz	2842.503 ± 210.81	2639.839 ± 197.66	2436.581 ± 176.49	14.266 ± 1.13
25 Hz	2900.898 ± 204.05	2684.614 ± 175.84	2486.296 ± 169.37	14.276 ± 1.09
50 Hz	2749.020 ± 151.58	2524.737 ± 142.50	2312.448 ± 144.50	15.905 ± 1.10
100 Hz	2756.447 ± 162.69	2507.047 ± 153.30	2252.904 ± 158.64	18.311 ± 1.34
200 Hz	2883.556 ± 221.22	2632.475 ± 212.40	2380.246 ± 206.20	17.499 ± 1.32

Results are mean ± SD of 5 rats per group.

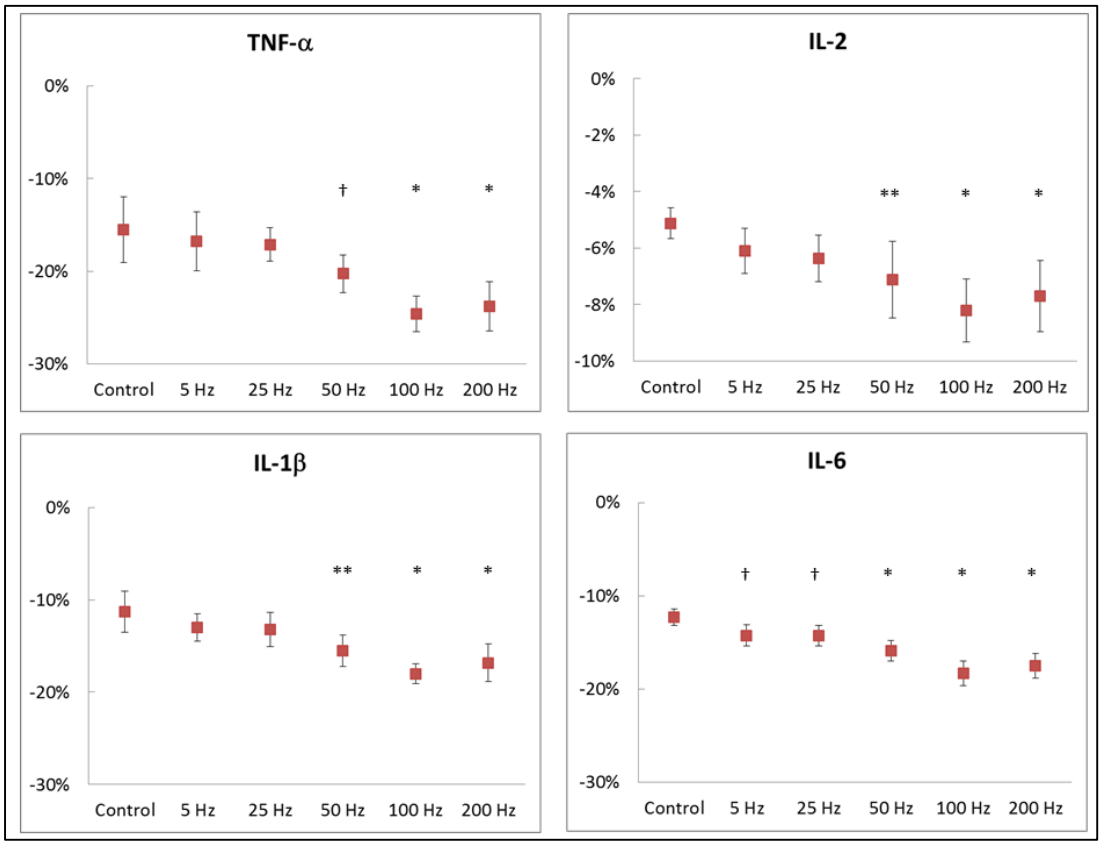

Figure 4.32– Cytokine concentration decrease for PW irradiation at 830 nm, at day 6. Values are expressed as percentage of the concentration at day 0. Error bars indicate standard deviations (SD ±). Significant difference in relative cytokines concentration decrease for comparisons with control group: * $p < 0.001$; ** $p < 0.008$; † $p < 0.05$.

Figure 4.32 shows the decrease in cytokines concentration at day 6, expressed as percentage of the concentration value at day 0, for 830 nm PW irradiation with constant average and peak powers, at different frequencies. Concentration decreases significantly different than those observed for the control group are identified. As Figure 4.32 shows, the treatment effect was higher for irradiation at frequencies higher than 50 Hz. The TNF-α concentration decrease was significantly higher for the 50, 100 and 200 Hz groups. This higher TNF-α decrease could be already observed at day 3, mainly for the 100 Hz group ($p=0.001$) but also for the 200 Hz group ($p=0.010$). The highest variation from day 0 to day 6 was observed in the 100 Hz group. However, it was not statistically different from those observed for the 50 and 200 Hz groups.

The IL-1β and IL-2 measurements show a similar behavior to the TNF-α measurements. Significant differences were found at day 6 for the 50, 100 and 200 Hz groups, when comparing with controls. However, at day 3, differences were only found in IL-2 measurements, for 100 and 200 Hz. The highest variation between day 0 and day 6 was measured for the 100 Hz but again with no statistically differences from the variations observed in the 50 and 200 Hz groups.

The IL-6 cytokine concentration decrease at day 6 is significantly higher for all treatment groups when compared with. This was already true at day 3 for the higher frequencies groups (50, 100 and 200 Hz). The highest variation between day 0 and day 6 occurred again for the 100Hz group. This

time, the concentration decrease observed for 100 Hz is statistically different from the one measured for 50 Hz, but not from the value obtained in the 200 Hz group.

Figure 4.33 compares the decrease in cytokines concentration at day 6, between PW irradiation at 50, 100 and 200 Hz and CW irradiation at 40 mW. All values are for treatment at 830 nm. It is easily seen that the cytokines relative concentration decrease is larger for CW irradiation. The differences are statistically significant, with all but one p value smaller than 0.001 (p=0.005 for IL-2, CW vs. 100 Hz). At day 3, there are already statistically significant differences between the PW group and the CW irradiated animals, for the variation of TNF-α, IL-1β and IL-6 cytokines. For IL-2, no differences were found, at day 3, between the treatment groups.

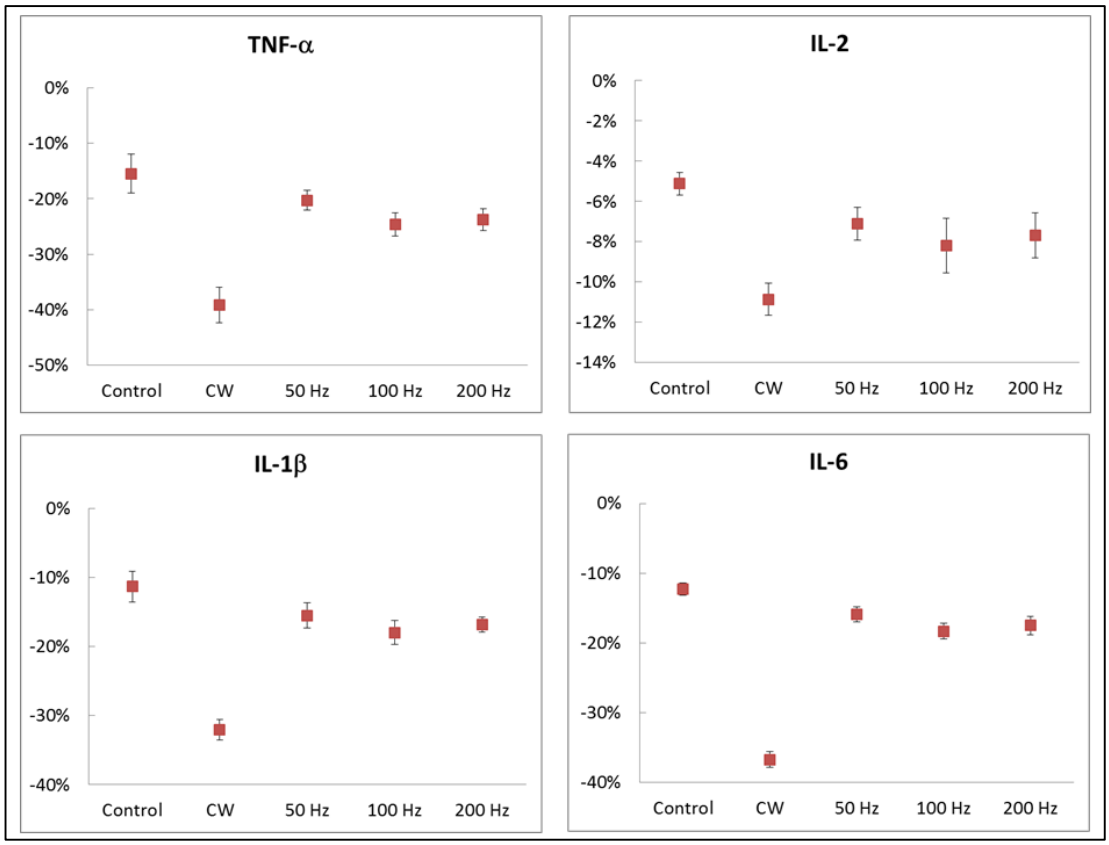

Figure 4.33 – Comparison between cytokine concentration decrease for CW and PW irradiation at 830 nm, at day 6. Values are expressed as percentage of the concentration at day 0. Error bars indicate standard deviations (SD ±).

4.4.2 Muscle tissue analysis by optical microscopy

Figure 4.34 presents images of muscle tissue from a control anima and a rat irradiated with a pulsed laser at 200 Hz. Table 4.23 and Table 4.24 present the inflammatory cell counting for PW irradiation and CW 40 mW at 830 nm. Significant differences were found between the control group and each of the CW, 50, 100 and 200 Hz groups ($p<0.001$). The number of inflammatory cells for the CW is also significantly lower than for every PW irradiation group ($p<0.001$). For PW irradiation, no significant differences can be found between the 50, 100 and 200 Hz groups.

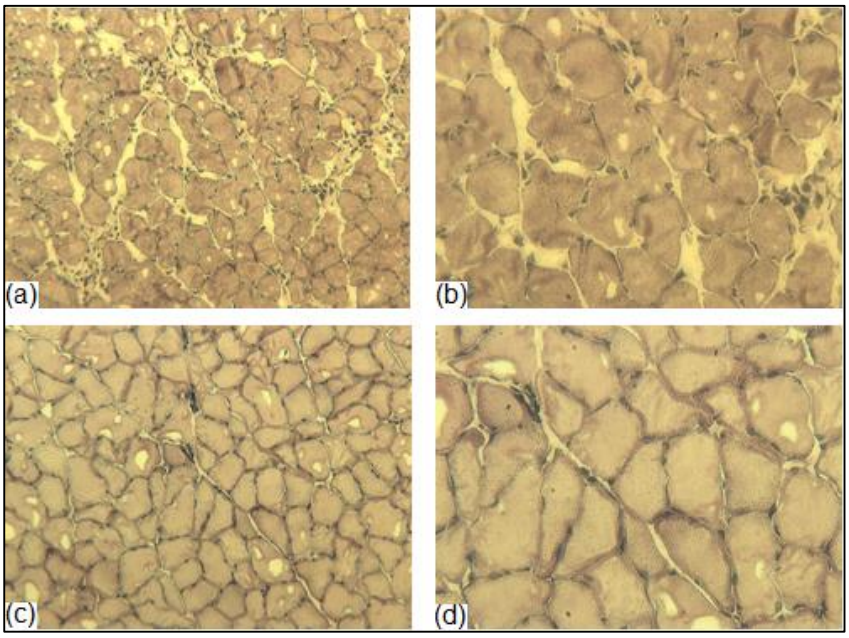

Figure 4.34– Muscle microscopy images: Control rat (a) 20X; (b) 40X; Rat from 100 Hz group: (c) 20X; (d) 40X.

Table 4.23– Percentage of inflammatory cells on muscle tissue samples observed by optical microscopy (20X) for PW irradiation.

Group	Percentage of control of cells ± Std. Dev.
Control	100
5 Hz	94.00 ± 9.09
25 Hz	93.67 ± 10.87
50 Hz	88.46 ± 9.86
100 Hz	82.92 ± 7.08
200 Hz	85.86 ± 6.45

Table 4.24– Inflammatory cell counting in muscle images of control and 40 mW (average power), 830 nm treated animals (CW and PW). Values are average ± SD.

Group	Cell counting
Control	17.76 ± 0.79
CW	10.84 ± 1.57
5 Hz	16.62 ± 1.61
25 Hz	16.56 ± 1.92
50 Hz	15.64 ± 1.74
100 Hz	14.66 ± 1.25
200 Hz	15.18 ± 1.14

4.5 Simulation of light transport in tissue

Figure 4.35 shows the irradiance (W/cm^2/W delivered) distribution in the tissue model, for irradiation at 830 nm and 980 nm, given by the Monte-Carlo simulations. It also includes the normalized irradiance as a function of tissue depth. The results show that there are no differences in the depth irradiation profiles between 830 nm and 980 nm. Therefore, differences on treatment effects between those wavelengths are not due to irradiance differences in the target area.

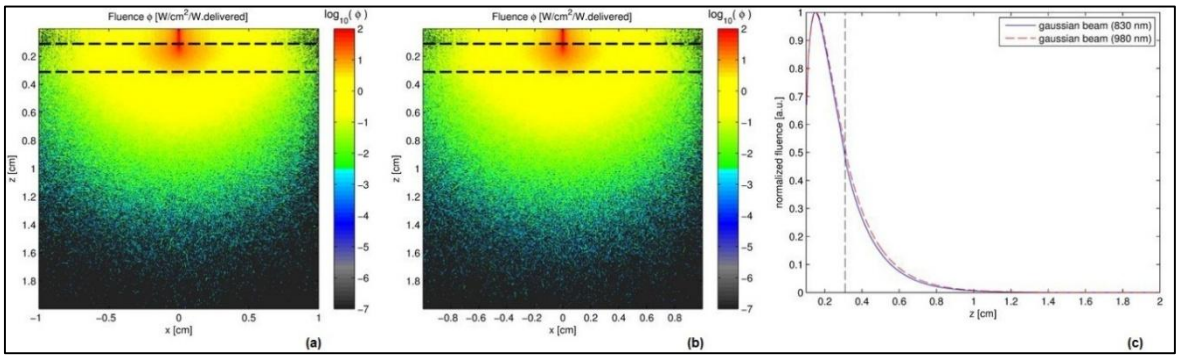

Figure 4.35– Irradiance (W/cm^2/W delivered) distribution in the tissue, for irradiation at 830 nm (a) and 980 nm (b) and normalized irradiance profile as a function of tissue depth (c). In (a) and (b), the dashed top line identifies the air-skin interface. The dashed bottom line corresponds to the skin-muscle interface. In (c) the dashed line corresponds to the skin-muscle interface.

5. Discussion

Our objective was to evaluate the effect of different LLLT irradiation parameters, namely radiant power, wavelength, continuous versus pulsed illumination, and coherent versus non-coherent illumination, on the inflammation phase of skeletal muscle injury. For this purpose, we induced by mechanical trauma, in a controlled, reproducible way, inflammation in the gastrocnemius muscle of Wistar rats. A quantitative evaluation of LLLT effects was achieved by measuring the concentration of inflammatory cytokines (TNF-α, IL-1β, IL-2 and IL-6) in the systemic blood and by histological analysis of muscle tissue.

5.1 Methodology issues

As we said before, our experiments were not designed to validate any of the LLLT action mechanisms currently proposed. However, we intended from the start to evaluate and discuss their results in the framework of the most accepted LLLT cellular-level mechanism, based on CCO as the primary photo-acceptor to red-NIR radiation. This intention was present in the selection of the irradiation wavelengths, as discussed in section 3.1.

The rationale behind the choice for irradiation wavelengths was described in section 3.1. As stated, we selected the 830 nm for being a wavelength located in the band of highest transmission through the combination of skin and muscle (770 – 850 nm) [213], for being one of the two most common wavelengths used in therapeutic light sources and also for being a peak of CCO absorption spectrum, considered to be due to the relatively oxidized Cu_A chromophores [164]. The 980-nm wavelength was selected because it does not correspond to any CCO absorption band. The large water absorption band at 980-nm makes these photons more likely to produce thermal than photochemical effects. Another reason for choosing this irradiation wavelength was mixed reported results for 980-nm-based LLLT. The literature presents conflicting results in wound healing [214,215], positive effects on neuropathic pain relief [216], and no effects on traumatic brain injury [217]. Published data on the effectiveness of 980 nm in the treatment of skeletal muscle inflammation are very scarce.

The criteria for selecting the irradiation powers and energy doses were also presented before, in section 3.2.6. The total energy delivered was selected according to the World Association for Laser Therapy (WALT) recommended treatment doses, for LLLT, which vary between 4 and 16 J. The radiant powers were selected in order to obtain irradiances in the higher half of the common range of values used for stimulation and healing (5 to 50 mW/cm^2) [199] and are similar to those reported for modulation of cytokines expression in skeletal muscle following acute injury [134,136,137]. As there are no reference values available for the treatment of skeletal muscle inflammation, we selected PW repetition rates similar to those reported for pain reduction, since pain relief seems to be obtained by the anti-inflammatory action of LLLT.

We selected four inflammatory cytokines to evaluate LLLT effects: TNF-α, IL-1β, IL-2 and IL-6. Tumor necrosis factor (TNF)-α and interleukin (IL)-1β are two key cytokines, produced in response

to trauma, that promote inflammatory responses, including the recruitment of immune cells to the injured area. IL-6 is also a pro-inflammatory cytokine that is responsible, with TNF-α and IL-1 β, for increasing the liver synthesis of most acute-phase proteins. IL-2 has both pro- and anti-inflammatory roles. It is a potent inducer of T-cell proliferation but also has regulatory roles, namely in the development and function of regulatory T cells. Thus, IL-2 contributes both to the induction and the end of acute inflammatory responses.

Inflammatory cytokines have been used previously to quantify LLLT effects in treating inflammation. Piva et al. [132] reviewed the effect of LLLT on the initial stages of tissue repair, reporting several studies where LLLT decreases the expression of TNF-α, IL-1β and IL-6. In what concerns skeletal muscle injury, one of the reviewed studies shows that TNF-α, IL-1β and IL-6 mRNA expression is decreased when using LLLT to treat inflammation of the subplantar muscle of rat paw [113]. In other studies, LLLT was able to reduce the TNF-α and IL-1β concentration in rat tibialis anterior muscle after cryolesion [134,235]. Although in these studies cytokines concentration is usually measured by ELISA in a muscle sample homogenate, we choose to measure the cytokines concentration in systemic blood serum. This allows obtaining samples during treatment without sacrificing animals. Moreover, this quantification method can be applied to human studies. Zhevago and Samoilova [85] have previously shown, in humans, that transcutaneous irradiation with visible and infrared light modulates cytokines concentration on peripheral systemic blood, namely by decreasing the concentration of TNF-α and IL-6. ELISA measurements of TNF-α in blood samples were also used by Campana et al. [93] to show an anti-inflammatory effect of He-Ne laser irradiation four days after microcrystalline arthropathy induction in rats by DCPP injection.

5.2 Experiments with CW irradiation

Our results show treatment effects, particularly for irradiation with the 830 nm laser. At day 6, the concentration of all measured pro-inflammatory cytokines, in the 30 mW and 40 mW groups, was significantly lower than for the control group. IL-6 concentration was reduced for all treatment groups and TNF-α for all but the 50 mW group. The number of inflammatory cells in muscle tissue samples was also significantly lower in all treatment groups when compared with the control animals.

In normal condition, muscles continually produce cytokines with the purpose of maintaining homeostasis and to regulate their function. Traumas can lead to considerable increase on the expression of pro-inflammatory IL-1β and TNF-α cytokines [231]. The results show that all applied laser infrared radiation doses produced an effect on reducing the number of inflammatory cells and the concentration of TNF-α and IL-1β on the systemic circulation. Reduction of these cytokines, measured locally by mRNA expression, was already reported in irradiated injured muscle tissue, using wavelengths in red spectral region. Albertini et al. [236] observed decreased mRNA expression, for TNF-α and IL-1β, 3 hours after irradiation with wavelengths of 660 and 684 nm at a dose of 7.5 J/cm^2, in inflammation induced by carrageenan injection in subplantar muscle tissue of

rat paws. Using a cryoinjury model of inflammation, Fernandes et al. [137] observed a significant decrease in IL-1β mRNA expression 7 days after injury, in LLLT treated (660 nm, 5 J/cm^2) rats.

As pro-inflammatory cytokines TNF-α and IL-1β upregulate the expression of endothelial-leukocyte adhesion molecules within the endothelium of the adjacent blood vessels [85,137,231,236,237], higher expression of those cytokines can result in the activation of fibroblasts and endothelial cells, leading to the release of more pro-inflammatory cytokines, such as IL-6 [137], which has been shown to attract and regulate neutrophils. The results shown significant differences in IL-6 concentration between day 0 and day 6 for the 40 mW (14.2 J/cm^2) group, for irradiation at 830 nm, and for the 30 mW group, when irradiating at 980 nm. For all the other groups, the concentration differences were not significant. However, the percentage decrease in IL-6 concentration at day 6, in the treatment groups, was always significantly higher than the one observed for the control group ($p<0.01$ for 10 mW; $p<0.001$ for the other groups), for irradiation at 830 nm, proving an IL-6 response to LLLT. Albertini et al. [236] observed decreased mRNA expression for IL-6 cytokines, 3 hours after irradiation with wavelengths of 660 and 684 nm at a dose of 7.5 J/cm^2. In our experiments did not observe any significant concentration difference for a comparable energy dose (7.2 J/cm^2, 20 mW). However, comparison between results is difficult since there are considerable differences between trauma models, cytokine sampling, treatment application and observation time.

We also measured the concentration of IL-2. While IL-1β, IL-6 and TNF-α cytokines are associated to the non-specific (innate) immune system, IL-2 is part of the adaptive immune system. IL-2 is an inducer of T-cell proliferation and Th1 and Th2 effector T-cell differentiation but also has a regulatory function through T cells and by preventing the development of inflammatory Th17 cells. Thus, IL-2 contributes to the induction and the end of inflammatory response [238]. It was shown that LLLT (632.8 nm; 0.2 mW/cm^2) increases IL-2 concentration in healthy mice [239]. Here, we did not observe any statistically significant differences in IL-2 concentration between day 0 and day 6, when considering a confidence level of 5%, both for 830 nm and 980 nm. However, we found differences when comparing relative variations between those days. At day 6, the IL-2 concentration relative decrease was highest for the 40 mW group, for both wavelengths. For 830 nm, the IL-2 decrease observed in the control group was significantly lower from that observed for irradiation with 30 mW ($p=0.008$) and 40 mW ($p<0.001$). For 40 mW, the decrease was already significantly different from the control group at day 3 ($p=0.028$). When irradiating at 980 nm, the control group IL-2 decrease was significantly lower just from the one measured for irradiation with 40 mW ($p<0.02$) and only at day 6. In the literature, we could not find any animal study where the levels of IL-2 were measured after LLLT treatment of muscle inflammation. One study by Novoselova et al. [239], conceived to evaluate the effect of low-level red laser light intensity (0.2 mW/cm^2, wavelength of 632.8 nm) on the immune cell activity, found that, when mice were treated to a single 1 minute exposure (an energy dose of 12 mJ/cm^2), IL-2 production by spleen lymphocytes and its accumulation in the blood plasma significantly increased within 24 h of

radiation exposure. 48 h after the exposure, the secretion of IL-2 did not differ significantly from the control value. However, prolonged irradiation of the thymus zone (1 minute, every two days, during 30 days) induced a significant decrease in IL-2 synthesis and blood concentration, 10 and 20 days after starting laser application. The authors concluded that LLLT can modulate IL-2 production, particularly when irradiation occurs over the thymus. We used energy doses in the range between 2.25 and 13.0 J/cm^2, with the peak effect at 9 − 10 J/cm^2. These doses are much higher than the ones used in the Novoselova et al. study and fall clearly on the dose range that inhibited IL-2 segregation.

Both the cytokines concentration relative variation curves (Figure 4.2, Figure 4.4, Figure 4.6 and Figure 4.8, for irradiation at 830 nm, and Figure 4.11, Figure 4.14, Figure 4.17 and Figure 4.20, for irradiation at 980 nm), and the data on the number of inflammatory cells, show a local minimum. With the exception of TNF-α, the higher cytokines concentrations reductions were always obtained for treatment with 40 mW. The highest reduction in the number of inflammatory cells was also observed for 40 mW. This behavior may suggest a biphasic dose response.

Several authors have demonstrated a biphasic response in LLLT, with the “Arndt-Schulz Law” suggested as a model for dose dependence. These studies were extensively reviewed by Huang et al. [14,199]. The authors state that, in general, doses of red or near infrared laser radiation as low as 3 or 5 J/cm^2 will have a positive effect *in vivo*, while larger doses like 50 or 100 J/cm^2 will not show that effect.

The main mechanism proposed as explanation for biphasic response in LLLT is based on the action of reactive oxygen species (ROS). Evidence suggests that photons are absorbed by the cells mitochondria, stimulating production of ATP and low levels of reactive oxygen species (ROS), leading to the activation of several transcription factors. The most important of these transcription factors is nuclear factor kappa-B (NF-κB), which induces expression of gene products related to cell proliferation and survival [199]. A biphasic dose dependent activation of NF-κB via ROS generation, after laser irradiation, was already demonstrated [240]. However, ROS can have both positive and negative effects as they stimulate cell proliferation at low levels, but inhibit proliferation and present cytotoxic behavior at high levels. There is even the possibility that chemically different ROS result from different laser radiation doses.

Another mechanism proposed for LLLT biphasic response is the Nitric Oxide (NO) photo-release. The amount of released NO should be proportional to the light irradiance. Low amounts of NO may be beneficial, while the release of high levels of NO can result in a less effective or even damaging action. In muscle lesions, IL-1β and TNF-α increase NO levels in the tissue [235,241].

In our experiments, we varied the delivered energy dose (J/cm^2) per application by adjusting the laser power while keeping the irradiation time constant at 3 minutes. For the used radiant powers and the measured beam areas at skin (0.80 cm^2 for 830 nm; 0.69 cm^2 for 980 nm), this amounts to a dose range between 2.25 and 13.0 J/cm^2, with the peak effect at 9-10 J/cm^2. There are some

published studies reporting biphasic responses for comparable energy doses. In one study with macrophage cell lines, irradiated at 820 nm, Bolton et al. [242] observed cell proliferation from 2.4 J/cm^2 to 9.6 J/cm^2, finding a maximum at 7.2 J/cm^2. An animal study [103] on mouse pleurisy induced by carrageenan, treated with a 650 nm laser at three dose values (3, 7.5 and 15 J/cm^2), found the largest inflammatory cell migration reduction at 7.5 J/cm^2. A final conclusion on the biphasic response behavior requires additional measurements, for doses greater than 13.0 J/cm^2, to verify if the LLLT effect still decreases for those doses.

LLLT treatment was less effective at 980 nm. The light transport in a two-layer tissue model was simulated to assess if the lower effect observed with irradiation at 980 nm was due to lower muscle irradiance for that laser wavelength. Our Monte-Carlo simulations showed that the normalized irradiance at the muscle is equal for 830 nm and 980 nm, as Figure 4.35 shows. In fact, although skin absorption is higher for 980 nm scattering in the skin is higher at 830 nm. The combination of the two processes seems to result in very similar profiles for the dependence of irradiance with tissue depth.

The lower treatment effect at 980 nm seems to result from specific absorption properties of the chromophores mediating LLLT effects. The probable photo-acceptor in mammalian cells for visible and near-infrared light is cytochrome c oxidase (CCO), the terminal electron acceptor of the mitochondrial electron transport chain in eukaryotic cells [164]. It is known that the action spectrum of CCO has a peak at 825 nm, thought to be due to the relatively oxidized Cu_A chromophores [164]. Specific extinction spectrum of oxidized and reduced cytochrome c oxidase from bovine heart tissue show larger extinction coefficients at 830 nm, when compared with values measured at 980 nm (1.7 times higher for oxidized CCO and 1.2 times higher for reduced CCO)[243]. This difference may justify the larger treatment effect observed at 830 nm.

The irradiance values on the central region of the irradiated tissue volume, shown in Figure 4.35, raise the issue of whether thermal effects play a role on the experiments. In fact, we planned our experiments considering *a priori* that thermal effects were not significant. This was based on measurements in humans reported by Joensen et al. [244], using a 810 nm laser with an output power of 200 mW, spot size of 0.0314 cm^2 and power density of 6.37W/cm^2, values that produce local irradiances much higher than those we used. The measurements showed small thermal effects in light skin (a condition closer to our experiments with albino rats), with temperature increases ranging from 0.38 °C to 1.58 °C, for 9 J of delivered energy.

The Monte-Carlo simulations of light propagation allow us to do a simple evaluation of possible thermal effects by calculating the average irradiance in skin and muscle and the temperature increase in these tissues. Simulation data show that thermal effects are only relevant in the central region of the beam, taken as the region of the beam profile where intensity is higher than 80% of the peak intensity. From the average fluencies, given by Monte-Carlo simulations, and using the simple thermal model detailed below, we obtained the temperature increases listed in Table 5.1.

Table 5.1– Analysis of temperature increase in skin and muscle for the region of the beam profile where intensity is higher than 80% of the peak intensity.

	830 nm		980 nm	
	skin	**muscle**	**skin**	**muscle**
Average fluence (mW·cm^{-2})	332.08	18.54	306.41	18.66
Heat Source (mW·cm^{-3})	56.45	21.32	107.24	21.45
Heat energy density (J·cm^{-3})	10.16	3.84	19.30	3.86
ΔT (ºC)	2.70	1.03	5.13	1.04

The heat source in the tissue is given by the absorbed power density. This corresponds to the absorbed optical energy per volume per unit of time and is expressed by:

$$H = \mu_a E \quad (5.1)$$

where E is the average irradiance (fluence) in the tissue.

The heat energy density is calculated simply by multiplying the absorbed power density by the exposure time:

$$u = H t_{exp} \quad (5.2)$$

The temperature increase is given by

$$\Delta T = \frac{u}{\rho C_p} \quad (5.3)$$

where ρ is the tissue density and C_p is the tissue specific heat capacity.

Values for skin and muscle density and heat capacity were obtained from a database for thermal and electromagnetic parameters of biological tissues made available by the Foundation for Research on Information Technologies in Society (IT'IS) [245].

Table 5.1 shows that the temperature increase in the muscle is not significant. The calculated value was close to 1 °C and this value does not take in account thermal diffusion or blood convection that would contribute to a lower temperature increase. The temperature increase is larger in the skin, since it absorbs more light, being more pronounced for 980 nm irradiation. This further suggests that thermal effects are not responsible for the observed treatment effects, which are more for pronounced for irradiation at 830 nm.

5.3 Coherent vs. non-coherent irradiation

Following our previous results, in our third experiment we evaluated NIR continuous wave excitation for coherent and non-coherent irradiation at 40 mW. The most relevant result of this study is the large difference in treatment effect between coherent and non-coherent sources

providing equal doses of radiation with similar wavelength. While the 830 nm laser source produced a treatment effect, measured by the statistically significant reduction of pro-inflammatory cytokines, the non-coherent 850 nm LED source failed to produce any significant cytokine concentration decrease when compared with the control group.

As discussed in Section 2.6.2 there is controversy on whether coherent and non-coherent sources with the same wavelength and radiant power produce the same treatment effects It is known that for the range of power densities used in LLLT coherent properties of light do not play a role during light absorption by molecular targets. However, there are several documented clinical cases where the therapeutic effect of coherent light is higher than non-coherent light. This has been attributed to the speckle intensity pattern resulting from coherent radiation established in the irradiated volume. Supposedly this spatially non-homogeneous irradiance distribution could justify the advantages of coherent sources in LLLT: the irradiance spatial fluctuations could provide irradiance values above the treatment effect threshold at greater depths than when using non-coherent radiation.

Hode et al. [201] did speckle simulations to evaluate the importance of coherent radiation when treating bulk tissues. From the modeling of the speckle intensity distribution, they found that intensities of up to five times the mean intensity will occur in the speckle field. This value can be even higher if light polarization is taken in account. It is known that the probability of excitation of a molecule varies with the cosine between the excitation wave electrical field and the absorption dipole of the molecule. The authors concluded that combining the effects of the intensity distribution and polarization patterns in tissue, the photon absorption rate for coherent radiation can be one order of magnitude higher than for non-coherent sources.

In our experiments we used laser diodes as radiation sources. Laser diodes are linearly polarized along the direction parallel to the short axis of the elliptical beam. We did not measure the laser diodes polarization ratio but typical values for the used powers range between 400:1 and 500:1. So, polarization effects are present at our experiments when irradiating with coherent light and certainly contribute to the large difference observed between irradiation with coherent and non-coherent light.

Our experiments were not designed to elucidate the mechanisms responsible for the higher effectiveness of coherent light in the treatment of skeletal muscle inflammation. The goal was just to compare the treatment effects between coherent and non-coherent illumination. The results presented in Section 4.3 were very clear: no treatment effect was observed for LED illumination. These results fit in the currently accepted view that coherent radiation has better results for deep tissues treatment, when compared with non-coherent radiation with equivalent parameters (dose, power, irradiation time).

5.4 Pulsed irradiation

Our fourth experiment concerned the use of pulsed irradiation in LLLT. Our goal was to compare treatment effects with continuous wave illumination and also to obtain information on the better pulsing parameters (frequency, pulse width, duty cycle, peak power and average power).

On the literature it is possible to find several experiments that produced better results using pulsed illumination than with continuous illumination, both *in vitro* [246-248] and *in vivo* [204, 249-252].

In 2011 it was published a review of LLLT pulsing parameters [204], in which the authors discussed the best frequencies for different treatments. None of the discussed cases concerned skeletal muscle inflammation. In studies [253] concerning wound healing, results showed several effective pulse frequencies, like 20, 100, 292 and 500 Hz. In pain treatment, one experiment [254] showed effective treatment at 10, 100 and 8000 Hz. Biological reasons usually proposed for the increased efficiency of PW irradiation, include the modulation of ion channels kinetics in the milliseconds time range or the promotion of multiple nitric oxide photodissociation events from a protein binding site [204].

In our experiments, the animals treated with PW irradiation showed a significant reduction in cytokines concentration only for the higher frequencies (50, 100 and 200 Hz). Even so, the cytokines concentration decrease was much lower than the one obtained for CW irradiation with the same radiant power. The reduction in inflammatory cells was also significantly lower with PW irradiation than the one measured for CW illumination. These results suggest that pulsed irradiation is less effective than CW irradiation with the same average power, in the reduction of the inflammatory phase of skeletal muscle injury.

We used a duty cycle was 80%, resulting in a peak power 20% higher than the CW radiant power. Therefore, during pulse exposure, the irradiance at muscle tissue is 20% higher than during CW irradiation, although the radiant exposure is kept equal. If we examine the existence of irradiance effects on LLLT, which are clearly suggested by observed biphasic dose responses that imply lack of compliance to the Bunsen-Roscoe rule of reciprocity [14], a direct comparison between CW and PW irradiation, with the same average power, may be partially hampered by such effects. The higher irradiance stimulus occurring with PW irradiation may inhibit to some degree the LLLT action, resulting in a treatment effect lower than that observed for CW irradiation at 40 mW. This is supported by the results obtained with CW irradiation at 50 mW.

It is relevant to note that our data yield mixed results when we compare between CW irradiation at 50 mW and PW irradiation at the higher frequencies. PW irradiation was significantly more effective than CW irradiation for reducing TNF-α concentration, as effective as CW irradiation for decreasing IL-2 concentration, and less effective than CW irradiation in what concerns IL-1β and IL-6. CW irradiation at 50 mW also resulted in a lower counting of inflammatory cells than PW irradiation. A new set of PW measurements using a peak power of 40 mW could be useful to address properly the impact of irradiance effects.

None of the published studies comparing CW and PW irradiation deals with skeletal muscle inflammation. Our data suggest that CW irradiation is more effective in the treatment of the inflammation phase of skeletal muscle injury than PW irradiation with the same radiant exposure. However, irradiance effects may hinder this conclusion. Therefore, further investigations are required.

PW irradiation only produced treatment effects for higher frequencies (50, 100 and 200 Hz). Once again, we could not find any study comparing pulse repetition rates in the treatment of muscle inflammation. An *in vitro* study [246], designed to evaluate if pulsed light can overcome the filtering effects of melanin, exposed human HEP-2 cells to 670 nm CW or PW light at several repetition rates (6, 18, 36, 100 and 600 Hz), through melanin filters. The authors found that cell proliferation was increased in the groups treated with PW irradiation, with maximal effects at 100 Hz, suggesting that penetration of PW light, through tissues with high melanin content, depends on pulse frequency. However, this effect does not play a role in our experiments since we used albino Wistar rats. Multiple nitric oxide photodissociation events from a protein binding site is another mechanism proposed for explaining PW effects in LLLT [204]. Although this mechanism may play a significant role for irradiation with pulsed light in red region, near infrared wavelengths are absorbed by a part of CCO not involved in NO binding [255], suggesting that photodissociation is not responsible for the positive effects of PW for NIR irradiation.

The observed larger effects of PW irradiation for 50, 100 and 200 Hz frequencies suggest the existence in this frequency range of some fundamental frequency in involved biological systems or some process with a time scale of milliseconds. The most obvious time constant is the thermal relaxation time of blood vessels, which raises again the question of the involvement of thermal effects.

If we consider the thermal relaxation time of an infinite cylinder, we find that time constants between 5 and 20 ms are associated with thermal relaxation of vessels with diameters between 100 and 200 micrometers, values larger than those found in dermis capillaries [256]. We simulated the thermal behavior of blood vessels, for vessel diameters between 50 and 220 μm and considering the frequencies used in our PW measurements. For that purpose, we used the values of average irradiance for skin and muscle, obtained through our Monte-Carlo simulations, and computed the thermal behavior following a methodology identical to that used by Stuart Nelson et al. [257]. Our simulations showed that for vessels located within the muscle tissue, the temperature increase is always negligible (lower than 0.03 ºC), as shown in Figure 5.1. Significant temperature effects may occur for skin blood vessels with diameters larger than 70 μm. However, these vessel diameters are rarely found in normal dermis. It is also important to note that temperature effects are more significant for low frequencies, which were exactly those that resulted in lower treatment effects. For these reasons, it seems very unlikely that the frequency dependence of our measurements is due to the thermal relaxation of blood vessels.

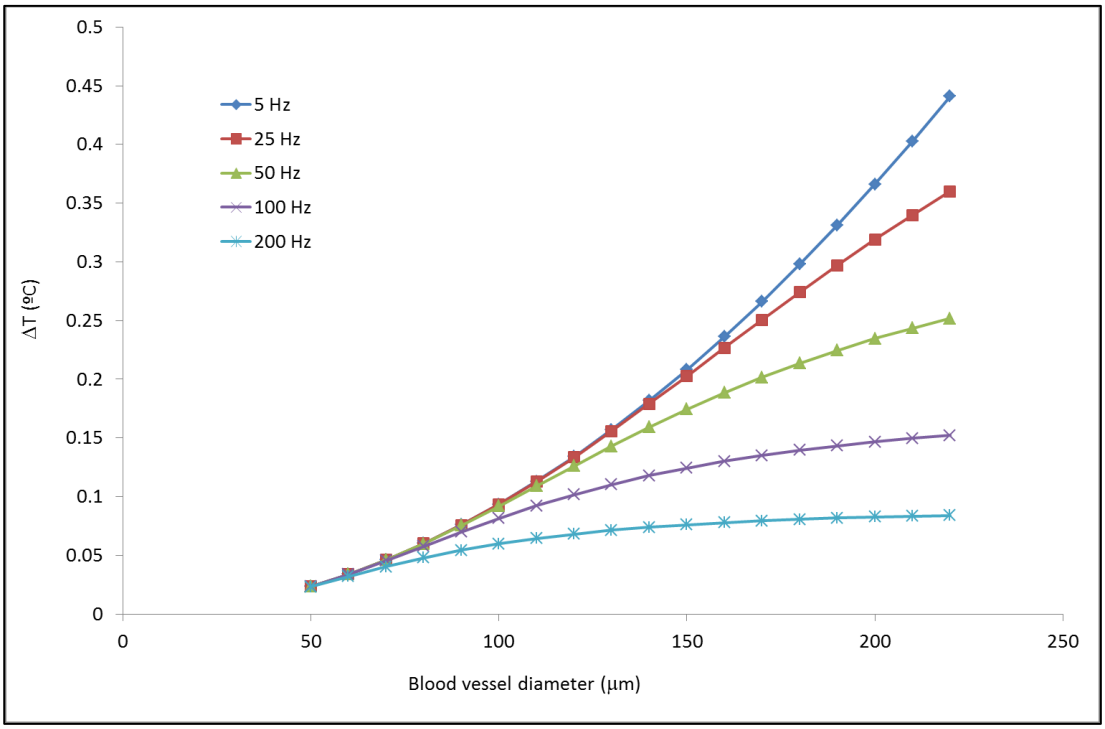

Figure 5.1– Simulation of thermal behavior of blood vessels, for vessel diameters between 50 and 220 µm, considering the frequencies used in PW measurements.

Currently, the more accepted cellular level mechanism for LLLT is the absorption radiation by components of the cellular respiratory chain. Therefore, we looked this chain for processes with time constants in the range of milliseconds. Starting from fully oxidized cytochrome c oxidase, the electronic transfer rate from cytochrome *a* to cytochrome a_3 occurs in the millisecond time range, even with large reductant concentrations [258]. Simulations done by Brunori et al. [258], resulted in forward and reverse rate constants for the electronic transfer from cytochrome *a* to cytochrome a_3 equal to 25 s^{-1} and 125 s^{-1}, respectively. Karu [164] suggests that irradiation intensifies exactly the cytochrome *a* to cytochrome a_3 electron transfer stage, since this is the rate-limiting step in the whole electron transfer within CCO, making more electrons available for the reduction of dioxygen. Taking in account its rate constants, it is possible to suggest that PW irradiation with frequencies comparable to those rates will be more effective in intensifying the cytochrome *a* to cytochrome a_3 electron transfer when compared with irradiation at lower frequencies.

6. Conclusions

Our objective was to evaluate the effect of different LLLT irradiation parameters, namely radiant power, wavelength and continuous versus pulsed illumination, in the inflammation phase of skeletal muscle injury. Quantification of the LLLT effects was obtained by measuring the concentration of inflammatory cytokines (TNF-α, IL-1β, IL-2 and IL-6) in the systemic blood. . The following conclusions can be obtained from our studies:

- We were able to quantify the effect of LLLT on the treatment of inflammation induced in the gastrocnemius muscle of Wistar rats by measuring the concentration of pro-inflammatory cytokines in the systemic blood.
- The used methodology proved to be suitable for measuring LLLT treatment effects on injured muscle. It has the advantage of making possible to follow the treatment effect without sacrificing animals and complies with the three Rs principle (Reduction, Replacement, and Refinement) [211], enabling us to minimize the number of animals used on the experiments while preserving statistical relevance. Its main drawback is to be limited to the treatment of surface muscle traumas.
- The results showed that CW irradiation at 830 nm produced the largest treatment effects, a result in accordance with the action spectrum of cytochrome c oxidase.
- Best results were obtained with an irradiation power of 40 mW, with the data suggesting a biphasic dose response. This suggestion requires further confirmation through experiments using higher radiant powers.
- Irradiation with non-coherent LED light failed to produce a treatment effect. This result is in line with the currently accepted view on the necessity of using coherent radiation to treat bulk tissues.
- PW irradiation at 830 nm, 40 mW average power was less effective that CW irradiation with the same wavelength and power. It remains to verify if this is due to the use of a higher irradiance stimulus with PW irradiation that may inhibit to some degree the LLLT action, according to the probable biphasic dose response.
- PW irradiation at 830 nm, 40 mW average power was only effective for the tested frequencies equal or higher than 50 Hz. This result might be related to the rate constants of the cytochrome c oxidase internal electron transfer stage between cytochrome *a* and cytochrome a_3.

LLLT have been used since 1960s to improve the healing of different soft-tissue pathologies and reduce the perception of both nociceptive and neuropathic pain. Histological studies report increased microvascularization and positive influence on fibroblast proliferation, collagen synthesis and tissue regeneration. In rehabilitation medicine, LLLT was introduced as a non-invasive and

safe treatment, but its efficacy is still controversial because several clinical trials have reported its ineffectiveness to treat pain and inflammation in musculoskeletal disorders. LLLT requires the adequate choice of a large number of dose and irradiation parameters for each treatment. If the choice of parameters is not adequate the treatment may be less effective or even fail. Many of the published papers on LLLT report negative results just because the studies were ill conceived and based on inadequate dose and irradiation parameters.

Researchers and clinicians should consistently report the characteristics of the device, the irradiation parameters and the treatment procedures. If we are able to quantify the effect of LLLT on the relief of pain and inflammation, using a rigorous methodology, best we can choose the therapeutic window, increasing the efficiency and credibility of this physical agent. This work intended to be a contribution toward this goal. Its potential clinical impact results lies on the methodology used to quantify inflammation relief and on the identification of the best irradiation and treatment parameters for achieving that relief.

6.1 Future work

This work left issues without a complete answer. The future work will start by addressing these issues. Measurements will be made using a 830 nm laser diode source with powers greater than 50 mW to confirm the biphasic dose behavior suggested by our results. This will require changes in the instrumentation as the laser diode we used cannot sustain optical powers greater than 50 mW.

The PW measurements will also be repeated using different peak powers in order to clarify if irradiance effects are responsible for decreasing, at least partially, the treatment effect when using pulsed light.

It will be interesting to evaluate if polarization effects contribute as hypothesized to the large difference in treatment effect observed between coherent and non-coherent radiation. Experiments will be performed using the 830 nm laser diode at 40 mW. The laser light will be depolarized before striking the animal leg.

The methodology we used can be applied on other models of inflammation, representative of conditions such as tendinitis or arthritis, in order to obtain the optimal LLLT parameters for each pathology. The assessment of treatment effect can be complemented by other imaging techniques like ultrasound or magnetic resonance imaging. If necessary, cytokines can also be measured in muscle tissue and joints synovial fluid.

Following experiments with animal models, it will be necessary to translate the results to clinical practice. We expect to perform clinical studies in Coimbra University Hospital, at the Physical and Rehabilitation Medicine Department in order to verify the best treatment parameters and to improve the administration technique for decreasing the treatment times, contributing to faster patient recovery.

Today, there are several areas where LLLT can be applied. We can mention orthodontic treatments [259,260], neck pain [261], improvement of fatigue on high-performance athletes [262-265], wound healing [266], acute joint inflammation [267] and hearing treatments [146]. It is possible to extend our studies to these areas. The objective will be the same: to determine the optimal treatment parameters. After that, it is possible to develop low-cost equipment suited for specific therapies, suitable for third world countries, where the access to high-technology is very difficult.

References

1. U. S. National Library of Medicine, National Institutes of Health. http://www.nlm.nih.gov/mesh/newh2002.html. Accessed on September 2014.
2. ThorLaser. http://www.thorlaser.com/photobiomodulation.php. Accessed on September 2014.
3. M. M. Favejee, B. M. A. Huisstede, B. W. Koes, "Frozen shoulder: the effectiveness of conservative and surgical interventions—systematic review" Br J Sports Med 45, 49-56 (2011).
4. L. Bisset, B. Coombes, B. Vicenzino, "Tennis elbow" BMJ Clinical Evidence 2011, 1117 (2011).
5. Myofascial Pain International Association for the Study of Pain (2009).
6. S. Haldeman, L. Carroll, J. D. Cassidy, J. Schubert, Å. Nygren, "The Bone and Joint Decade 2000 –2010 Task Force on Neck Pain and Its Associated Disorders" Lippincott Williams & Wilkins 33, S5–S7 (2008).
7. R. T. Chow, M. I. Johnson, R. A. B. Lopes-Martins, J. M. Bjordal, "Efficacy of low-level laser therapy in the management of neck pain: a systematic review and meta-analysis of randomised placebo or active-treatment controlled trials" The Lancet, 374, 1897-1908 (2009).
8. S. Tumilty, J. Munn, S. McDonough, D. A. Hurley, J. R. Basford, G. D. Baxter, "Low level laser treatment of tendinopathy: a systematic review with meta-analysis" Photomed Laser Surg 28, 3-16 (2010).
9. C. R. Carcia, R. L. Martin, J. Houck, D. K. Wukich, "Achilles Pain, Stiffness, and Muscle Power Deficits: Achilles Tendinitis" Clinical Practice Guidelines Linked to the International Classification of Functioning, Disability, and Health from the Orthopaedic Section of the American Physical Therapy Association, J Orthop Sports Phys Ther. 40, A1-A26 (2010).
10. J. M. Bjordal, R. J. Bensadoun, J. Tuner, L. Frigo, K. Gjerde, R. A. Lopes-Martins, "A systematic review with meta-analysis of the effect of low-level laser therapy (LLLT) in cancer therapy-induced oral mucositis" Supportive Care in Cancer 19, 1069-1077 (2011).
11. J. M. Bjordal, C. Couppe, R. T. Chow, J. Tuner, E. A. Ljunggren, " A systematic review of low level laser therapy with location-specific joint disorders" Australian Journal of Physiotherapy 49, 107-116 (2003).
12. J. C. Rojas, F. Gonzalez-Lima, "Low-level light therapy of the eye and brain" Dove Medical Press Ltd. Eye and Brain 3, 49–67 (2011).
13. F. Aimbire, R. Albertini, M. T. Pacheco, H. C. Castro-Faria-Neto, P. S. Leonardo, V. V. Iversen, R. A. Lopes-Martins, J. M. Bjordal, "Low-level laser therapy induces dose-dependent reduction of TNFalpha levels in acute inflammation" Photomed. Laser Surg. 24, 33-37 (2006).
14. Y. Huang, A. C. H. Chen, Carrol, M. R. Hamblin, "Biphasic dose response in low level light therapy" Dose-Response 7, 358-383 (2009).
15. P. A. Jenkins, J. D. Carroll, "How to report low-level laser therapy (LLLT)/photomedicine dose and beam parameters in clinical and laboratory studies" Photomed Laser Surg. 29, 785-7 (2011).
16. U. S. Food and Drug Administration. http://www.fda.gov/radiation-emittingproducts/resourcesforyou radiationemittingproducts/ucm252761.htm. Accessed on September 2014.
17. J. D. Carroll, "Photomedicine and LLLT literature watch" Photomed. Laser Surg. 27, 829 (2009).
18. R. Steiner, "Laser-Tissue Interactions" Laser and IPL Technology in Dermatology and Aesthetic Medicine, 23-36 (2011).
19. M. A. Ansari, E. Mohajerani, "Mechanisms of Laser-Tissue Interaction: I. Optical Properties of Tissue" Journal of Lasers in Medical Sciences 2 Num. 3 (2011).
20. J. Mobley, T. Vo-Dinh, V. V. Tuchin, "Biomedical Photonics Handbook, Second Edition: Fundamentals, Devices, and Techniques" CRC Press, 23-35 (2014).
21. E. I. Altinoglu, J. H. Adair, "Near infrared imaging with nanoparticles" John Wiley & Sons, Inc. Vol. 2 (2010).
22. S. L. Jacques, "Skin Optics" Oregon Medical Laser Center News (1998)

23. S. L. Jacques, D. J. McAuliffe, "The melanosome: threshold temperature for explosive vaporization and internal absorption coefficient during pulsed laser irradiation" Photochem. Photobiol. 53, 769-775 (1991).
24. I. S. Saidi, "Transcutaneous Optical Measurement of Hyperbilirubinemia in Neonates" PhD thesis, Rice University (1992).
25. R. Huang, S. Jacques, unpublished data, mentioned in Skin Optics Summary, http://omlc.org/news/jan98/skinoptics.html. Accessed on September 2014..
26. S. L. Jacques, "Origins of tissue optical properties in the UVA, Visible, and NIR regions" OSA TOPS on Advances in Optical Imaging and Photon Migration 2, 364-369 (1996).
27. C. F. Bohren, D. R. Huffman, "Absorption and scattering of light by small particles" John Wiley & Sons (1983).
28. A. A. Bashkatov, E. A. Genina, V. I. Kochubey, V. V. Tuchin, "Optical properties of human skin, subcutaneous and mucous tissues in the wavelength range from 400 to 2000 nm" J Phys D: Appl Phys 38, 2543-55 (2005).
29. L. Oliveira, M. Carvalho E. Nogueira, V. Tuchin, “The optical properties of rat abdominal wall muscle” Workshop on Internet Biophotonics VI, Saratov Fall Meeting (2013).
30. C. R. Simpson, M. Kohl, M. Essenpreis, M. Cope, "Near infrared optical properties of ex-vivo human skin and subcutaneous tissues measured using the Monte Carlo inversion technique" Phys Med Biol 43, 2465-2478 (1998).
31. R. Simpson, J. Laufer, M. Kohl, M. Essenpreis, M. Cope, "Skin Optical Properties" http://www.ucl.ac.uk/medphys/research/borl/intro/skin. Accessed on September 2014.
32. A. N. Bashkatov, E. A. Genina, V. V. Tuchin, “Optical properties of skin, subcutaneous, and muscle tissues: a review” Journal of Innovative Optical Health Sciences 4, 9 – 38 (2011).
33. M. H. Niemz, "Laser-Tissue Interactions, Fundamentals and Applications" Springer, Third Enlarged Edition, Chap. 3 (1996).
34. B. Cox, "Introduction to Laser-Tissue Interactions" MPHY3886, MPHYM886, MPHYG886 Optics in Medicine (2013).
35. A. J. Welch, M. J. C. van Gemert, "Optical-Thermal Response of Laser-Irradiated Tissue" Springer, 2nd ed. XIII (2011).
36. D. Gazdaru, C. Chilom, M. A. Calin, C. Geanta, A. Popescu, "Laser radiation propagation and heat transfer into cells and tissues" Romanian J. Biophys., Vol. 18, No. 1, 73–85 (2008).
37. P. A. Quinto-Su, V. Venugopalan, "Mechanisms of Laser Cellular Microsurgery" Methods in Cell Biology 82 (2007).
38. A. Vogel, J. Noack, G. Huttman, G. Paltauf, "Mechanisms of femtosecond laser nanosurgery of cells and tissues" Appl. Phys. B 81, 1015–1047 (2005).
39. F. H. Loesel, M. H. Niemz, J. F. Bille, T. Juhasz, "Laser-induced optical breakdown on hard and soft tissues and its dependence on the pulse duration: Experiments and model" IEEE J. Quantum Electron. 32, 1717–1722 (1996).
40. K. R. Rau, A. G. Guerra III, A. Vogel, V. Venugopalan, "Investigation of laser-induced cell lysis using time-resolved imaging" Appl. Phys. Lett. 84, 2940–2942 (2004).
41. A. Vogel, S. Busch, U. Parlitz, "Shockwave emission and cavitation bubble generation by picosecond and nanosecond optical breakdown in water" J. Acoust. Soc. Am. 100, 148–165 (1996).
42. A. Vogel, J. Noack, K. Nahen, D. Theisen, S. Busch, U. Parlitz, D. X. Hammer, G. D. Noojin, B. A. Rockwell, R. Birngruber, "Energy balance of optical breakdown in water at nanosecond to femtosecond time scales" Appl. Phys. B 68(2), 271–280 (1999).
43. A. Vogel, M. R. C. Capon, M. N. Asiyo-Vogel, R. Birngruber, "Intraocular photo disruption with picosecond and nanosecond laser pulses: Tissue effects in cornea, lens, and retina" Investig. Ophthalmol. Vis. Sci. 35, 3032–3044 (1994).
44. L. Pauling, "Die Natur der chemischen Bindung" Verlag Chemie GmbH (1962).
45. J. L. Boulnois, "Photophysical Processes in Recent Medical Laser: Developments: a Review" Lasers in Medical Science 1, 47-66 (1986).
46. T. Karu, "Laser biostimulation: a photobiological phenomenon" J Photochem Photobiol B 3, 638-640 (1989).
47. T. I. Karu, "Photobiological Fundamentals of Low-Power Laser Therapy" IEEE Journal of Quantum Electronics, vol. 23, no. 10, 1703-1717 (1987).
48. T. I. Karu, "Low power laser therapy" Biomedical Photonics Handbook CRC Press 48, 1–25 (2003).

49. H. Chung, T. Dai, S. K. Sharma, Y. Huang, J. D. Carroll, M. R. Hamblin, "The Nuts and Bolts of Low-level Laser (Light) Therapy" Ann Biomed Eng. 40, 516–533 (2012).
50. P. Volpi, G. Melegati, D. Tornese, "Muscle strains in soccer: a five-year survey of an Italian major league team" Knee Surg Sports Traumatol Arthrosc 12, 482-485 (2004).
51. P. Volpi, "Football Traumatology Current Concepts: from Prevention to Treatment" Springer ed, 153-163 (2006).
52. W. E. Jr. Garrett, "Muscle strain injuries" Am J Sports Med. 24, S2-8 (1996).
53. M. J. Järvinen, M. U. K. Lehto, "The Effects of Early Mobilisation and Immobilisation on the Healing Process Following Muscle Injuries" Sports Medicine 15, 78-89 (1993).
54. T. A. Järvinen, T. L. Järvinen, M. Kääriäinen, H. Kalimo, M. Järvinen, "Muscle injuries: biology and treatment" Am J Sports Med. 33, 745-764 (2005).
55. J. G. Tidball, "Inflammatory processes in muscle injury and repair" J Physiol Regul Integr Comp Physiol Pharmacol 76, 345-353 (2005).
56. J. G. Tidball, "Inflammatory cell response to acute muscle injury" Med Sci Sports Exerc 27, 1022-1032 (1995).
57. Y. Li, J. Cummins, J. Huard, "Muscle injury and repair" Curr Opin Orthop 12, 409-415 (2001).
58. C. Smith, M. J. Kruger, R. M. Smith, K. H. Myburgh, "The Inflammatory Response to Skeletal Muscle Injury" Sports Medicine 38, 947-969 (2008).
59. P. García Barreno, "Inflamación" Rev. R. Acad. Cienc. Exact. Fis. Nat. 102, 91-159 (2008)
60. V. Cuacuas Cano, M. Escobar Martínez, J. L. Torres Méndez, E. Hernández Aureoles, "Trauma de alta energía y su respuesta inflamatoria sistémica" Medigraphic Artemisa en linea 4, 39-50 (2008)
61. D. W. Cain, G. Kelsoe, "Inflammation: Acute" John Wiley & Sons Ltd. Garnett (2010).
62. J. L. Gallin, "Inflammation" in Fundamental Immunology, W. E. Paul, ed. pp. 721-733 (1989).
63. D. K. Male, B. Champion, A. Cooke, M. Owen, "Advanced Immunology" J.B. Lippincoll Company, Gower Medical Publishing, (1991).
64. R. A. de Bie, H. C. de Vet, T. F. Lenssen, F. A. van den Wildenberg, G. Kootstra, P. G. Knipschild, "Low-level laser therapy in ankle sprains: a randomized clinical trial" Arch. Phys. Med. Rehabil. 79, 1415-1420 (1998).
65. A. Mauro, "Satellite cell of skeletal muscle fibers"J Biophys Biochem Cytol. 9, 493-5 (1961).
66. R. Bischoff, "Interaction between satellite cells and skeletal muscle fibers" Development 109, 943-952 (1990).
67. H. Ishikawa, "Electron microscopic observations of satellite cells with special reference to the development of mammalian skeletal muscles" Z. Anat. Entwicklungsgesch 125, 43-63 (1966).
68. P. Seale, A. Polesskaya, M. A. Rudnicki, "Adult stem cell specification by Wnt signaling in muscle regeneration" Cell Cycle 2, 418–9 (2003).
69. M. H. Parker, P. Seale, M. A. Rudnicki, "Looking back to the embryo: defining transcriptional networks in adult myogenesis" Nat. Rev. Genet. 4, 497–507 (2003).
70. M. Yamaura, M. Yao, I. Yaroslavsky, R. Cohen, M. Smotrich, I. E. Kochevar, "Low level light effects on inflammatory cytokine production by rheumatoid arthritis synoviocytes" Lasers Surg Med. 41; 4:282-90 (2009).
71. A. M. B. Bilate, "Inflamação, citocinas, proteínas de fase aguda e implicações terapêuticas" Temas de Reumatologia Clínica 8, 47-51 (2011).
72. C. A. Feghali, T. M. Wright, "Cytokines in acute and chronic inflammation" Frontiers in Bioscience 2, d12-26 (1997).
73. R. Devi Ramnath, S. Weing, M. He, J. Sun, H. Zhang, M. S. Bawa, M. Bhatia, "Inflammatory mediators in sepsis: Cytokines, chemokines, adhesion molecules and gases" Journal of Organ Dysfunction, vol 2: 80-92 (2006).
74. T. Kishimoto, "The Biology of Interleukin-6" The Journal of The American Society of Hematology 74, 1 (1989).
75. P. M. Tiidus "Radical species in inflammation and overtraining" Canadian Journal of Physiology and Pharmacology 76, 533-538 (1998).
76. B. Klarlund Pedersen "Exercise and cytokines" Immunology and Cell Biology 78, 532–535 (2000).
77. J. A. Woods, V. J. Vieira, K. T. Keylock, "Exercise, Inflammation, and Innate Immunity" Immunology and Allergy Clinics of North America 29, 381–393 (2009).
78. K. Ostrowski, T. Rohde, S. Asp, P. Schjerling, B. K. Pedersen, "Pro- and anti-inflammatory

cytokine balance in strenuous exercise in humans" J Physiol. 515.1 287-291 (1999).
79. F. Zaldivar, J. Wang-Rodriguez, D. Nemet, C. Schwindt, P. Galassetti, P. J. Mills, L. D. Wilson, D. M. Cooper, "Constitutive pro- and anti-inflammatory cytokine and growth factor response to exercise in leukocytes" J Appl Physiol 100, 1124-1133 (2006).
80. P. E. Whiteley, S. A. Dalrymple, "Models of Inflammation: Carrageenan-Induced Paw Edema in the Rat" UNIT 5.4 Current Protocols in Pharmacology - Wiley Online Library (2001).
81. R. Radhakrishnan, S. A. Moore SA, K. A. Sluka, "Unilateral carrageenan injection into muscle or joint induces chronic bilateral hyperalgesia in rats" Pain 104, 567-577 (2003).
82. J. R. Bunn, J. Canning, G. Burke, M. Mushipe, D. R. Marsh, G. Li, "Production of consistent crush lesions in murine quadriceps muscle-A biomechanical, histomorphological and immunohistochemical study" Journal of Orthopaedic Research 22, 1336-1344 (2004).
83. F. A. Facio, V. B. Minamoto, "Análise morfológica a curto e longo prazo do músculo tibial anterior após contusão" Fisioterapia em movimento 19 (2006).
84. K. A. Samoilova, K. D. Obolenskaya, A. V. Vologdina, S. A. Snopov, E. V. Shevchenko, "Single skin exposure to visible polarized light induces rapid modification of entire circulating blood: I. Improvement of rheologic and immune parameters" Proc. SPIE 3569, Effects of Low-Power Light on Biological Systems IV, 90 (1998).
85. N. A. Zhevago, K. A. Samoilova, "Pro- and anti-inflammatory cytokine content in human peripheral blood after its transcutaneous (in vivo) and direct (in vitro) irradiation with polychromatic visible and infrared light" Photomed. Laser Surg. 24, 129-139 (2006).
86. T. De Marchi, E. C. Leal Junior, C. Bortoli, S. S. Tomazoni, R. A. Lopes-Martins, M. Salvador, "Low-level laser therapy (LLLT) in human progressive-intensity running: effects on exercise performance, skeletal muscle status, and oxidative stress" Lasers Med Sci. 27, 231-6 (2012).
87. V. S. Hentschke, R. B. Jaenisch, L. A. Schmeing, P. R. Cavinato, L. L. Xavier, P. Dal Lago, "Low-level laser therapy improves the inflammatory profile of rats with heart failure" Lasers Med Sci. 28, 1007-16 (2013).
88. M. S. Moreira , I. T. Velasco, L. S. Ferreira, S. K. Ariga, D. F. Barbeiro, D. T. Meneguzzo, F. Abatepaulo, M. M. Marques, "Effect of phototherapy with low intensity laser on local and systemic immunomodulation following focal brain damage in rat" J Photochem Photobiol B. 97, 145-51 (2009).
89. G. B. Lauria Silva, N. Tomoko Sacono, A. Ferreira Othon-Leite, E. Francisco Mendonça, A. Moraes Arantes, C. Bariani, L. Garcia Lobo Duarte, M. H. Nogueira Abreu, C. Martins Queiroz-Júnior, T. A. Silva, A. Carvalho Batista, "Effect of low-level laser therapy on inflammatory mediator release during chemotherapy-induced oral mucositis: a randomized preliminary study" Lasers in Medical Science 30, 117-126 (2015).
90. International Association for the Study of Pain (IASP), "Global Year against Musculoskeletal Pain" Myofascial Pain IASP (2009).
91. D. Rodrigues dos Santos, R. E. Liebano, C. Schiavinato Baldan, I. Bordello Masson, R. Paranhos Soares, I. Esteves Junior, "The low-level laser therapy on muscle injury recovery: literature review" J. Health Sci Inst. 28, 286-8 (2010).
92. R. A. B. Lopes-Martins, S. C. Penna, J. Joensen, V. V. Iversen, J. M. Bjordal, "Low level laser therapy [LLLT] in inflammatory and rheumatic diseases: a review of therapeutic mechanisms" Current Rheumatological Reviews 3, 147-154 (2007).
93. V. Campana, M. Moya, A. Gavotto, J. C. Simes, L. Spitale, F. Soriano, and J. A. Palma, "He-Ne laser on microcrystalline arthropathies" J. Clin. Laser Med. Surg. 21, 99-103 (2003).
94. F. Aimbire, R. Albertine, R. G. de Magalhaes, R. A. Lopes-Martins, H. C. Castro-Faria-Neto, R. A. Zangaro, M. C. Chavantes, M. T. Pacheco, "Effect of LLLT Ga-Al-As (685 nm) on LPS-induced inflammation of the airway and lung in the rat" Lasers Med. Sci. 20, 11-20 (2005).
95. M. G. Bouma, W. A. Buurman, F. A. J. M. vandenWildenberg, "Low energy laser irradiation fails to modulate the inflammatory function of human monocytes and endothelial cells" Lasers in Surgery and Medicine 19, 207-215 (1996).
96. K. Nomura, M. Yamaguchi, Y. Abiko, "Inhibition of interleukin-1 beta production and gene expression in human gingival fibroblasts by low-energy laser irradiation" Lasers in Medical Science 16, 218-223 (2001).
97. T. Qadri, L. Miranda, J. Tuner, A. Gustafsson, "The short-term effects of low-level lasers as adjunct therapy in the treatment of periodontal inflammation" J. Clin. Periodontol. 32, 714-719 (2005).
98. K. Mizutani, Y. Musya, K. Wakae, T. Kobayashi, M. Tobe, K. Taira, T. Harada, "A clinical study

on serum prostaglandin E2 with low-level laser therapy" Photomed. Laser Surg. 22, 537-539 (2004).
99. Y. Sakurai, M. Yamaguchi, Y. Abiko, "Inhibitory effect of low-level laser irradiation on LPS-stimulated prostaglandin E-2 production and cyclooxygenase-2 in human gingival fibroblasts" European Journal of Oral Sciences 108, 29-34 (2000).
100. A. Pourzarandian, H. Watanabe, S. M. P. M. Ruwanpura, A. Aoki, K. Noguchi, I. Ishikawa, "Er : YAG laser irradiation increases prostaglandin E-2 production via the induction of cyclooxygenase-2 mRNA in human gingival fibroblasts" Journal of Periodontal Research 40, 182-186 (2005).
101. Y. Ozawa, N. Shimizu, Y. Abiko, "Low-energy diode laser irradiation reduced plasminogen activator activity in human periodontal ligament cells" Lasers in Surgery and Medicine 21, 456-463 (1997).
102. E. S. Pessoa, R. M. Melhado, L. H. Theodoro, V. G. Garcia, "A histologic assessment of the influence of low-intensity laser therapy on wound healing in steroid-treated animals" Photomed. Laser Surg. 22, 199-204 (2004).
103. R. A. Lopes-Martins, R. Albertini, P. S. Martins, J. M. Bjordal, H. C. Faria Neto, "Spontaneous effects of low-level laser therapy (650 nm) in acute inflammatory mouse pleurisy induced by carrageenan" Photomed. Laser Surg. 23, 377-381 (2005).
104. L. Schindl, M. Schindl, L. Polo, G. Jori, S. Perl, A. Schindl, "Effects of low power laser-irradiation on differential blood count and body temperature in endotoxin-preimmunized rabbits" Life Sciences 60, 1669-1677 (1997).
105. R. A. B. Lopes-Martins, R. Albertini, P. S. L. Lopes-Martins, F. A. S. De Carvalho, H. C. C. F. Neto, V. V. Iversen, J. M. Bjordal, "Steroid receptor antagonist mifepristone inhibits the anti-inflammatory effects of photoradiation" Photomedicine and Laser Surgery 24, 197-201 (2006).
106. A. Amano, K. Miyagi, T. Azuma, Y. Ishihara, S. Katsube, I. Aoyama, I. Saito, "Histological studies on the rheumatoid synovial membrane irradiated with a low energy laser" Lasers Surg. Med. 15, 290-294 (1994).
107. A. Stergioulas, "Low-level laser treatment can reduce edema in second degree ankle sprains" J. Clin. Laser Med. Surg. 22, 125-128 (2004).
108. N. Ozkan, L. Altan, U. Bingol, S. Akln, M. Yurtkuran, "Investigation of the supplementary effect of GaAs laser therapy on the rehabilitation of human digital flexor tendons" J. Clin. Laser Med. Surg. 22, 105-110 (2004).
109. R. Albertini, F. S. Aimbire, F. I. Correa, W. Ribeiro, J. C. Cogo, E. Antunes, S. A. Teixeira, N. G. De, H. C. Castro-Faria-Neto, R. A. Zangaro, R. A. Lopes-Martins, "Effects of different protocol doses of low power gallium-aluminum-arsenate (Ga-Al-As) laser radiation (650 nm) on carrageenan induced rat paw ooedema" J. Photochem. Photobiol. B 74, 101-107 (2004).
110. A. Honmura, A. Ishii, M. Yanase, J. Obata, E. Haruki, "Analgesic effect of Ga-Al-As diode laser irradiation on hyperalgesia in carrageenin-induced inflammation" Lasers Surg. Med. 13, 463-469 (1993).
111. V. Campana, M. Moya, A. Gavotto, H. Juri, "The relative effects of He-Ne laser and meloxicam on experimentally induced inflammation" Laser Therapy 11, 36-41 (1999).
112. M. V. M. Pinto, D. M. da Costa, L. L. V. Rocha, H. R. dos Santos, A. L. S. Silva, L. G. Barbosa, J. B. A. dos Reis, M. Bernardo-Filho, "Comparative Study of the Effects of the Ga-As (904 nm, 150mW) Laser and the Pulsed Ultrasound of 1 MHz in Inflammation of Tibialis Muscle of Wistar Rats" Brazilian Archives of Biology and Technology 51, 225-230 (2008).
113. R. Albertini, A. B. Villaverde, F. Aimbire, M. A. Salgado, J. M. Bjordal, L. P. Alves, E. Munin, M. S. Costa, "Anti-inflammatory effects of low-level laser therapy (LLLT) with two different red wavelengths (660 nm and 684 nm) in carrageenan-induced rat paw edema" J. Photochem. Photobiol. B 89, 50-55 (2007).
114. J. M. Bjordal, V. Iversen, R. A. B. Martins-Lopes, "Low level laser therapy reduces inflammation in activated achilles tendinitis" M. R. Hamblin, R. W. Waynant, and J. Anders, eds. pp. 61400G-1-61400G-8 (2006).
115. C. Antipa, I. I. Bruckner, N. Crangulescu, C. I. Moldovan, A. G. Podoleanu, V. Stanciulescu, E. Ionescu, "Our clinical experience in low-energy laser medical treatments" Optical Engineering 35, 1367-1371 (1996).
116. M. M. Atihé, "Redução de processo inflamatório com aplicação de laser de arseneto de gálio alumínio (l = 830nm) em pós-operatório de exodontias de terceiros molares inferiores

inclusos ou semi-inclusos" Faculdade de Odontologia, Universidade de São Paulo (2002).
117. A. N. Alves, K. P. S. Fernandes, A. M. Deana, S. K. Bussadori, "Effects of Low-Level Laser Therapy on Skeletal Muscle Repair: A Systematic Review" American Journal of Physical Medicine & Rehabilitation 93, 1073-1085 (2014).
118. W. H. B. Vieira, R. Goes, F. C. Costa, N. A. Parizotto, S. E. A. Perez, V. Baldissera, F. S. Munin, M. L. B. Schwantes, "Adaptation of LDH enzyme in rats undergoing aerobic treadmill training and low intensity laser therapy" Rev Bras Fisioter 10, 205-211 (2006).
119. X. G. Liu, Y. J. Zhou, T. C. Liu, J. Q. Yuan, "Effects of low-level laser irradiation on rat skeletal muscle injury after eccentric exercise" Photomed Laser Surg. 27, 863-9 (2009).
120. D. A. Sussai, P. de T. Carvalho, D. M. Dourado, A. C. Belchior, F. A. dos Reis, D. M. Pereira, "Low-level laser therapy attenuates creatine kinase levels and apoptosis during forced swimming in rats" Lasers Med Sci. 25, 115-20 (2010)
121. R. A. Lopes-Martins, R. L. Marcos, P. S. Leonardo, A. C. Jr. Prianti, M. N. Muscará, F. Aimbire, L. Frigo, V. V. Iversen, J. M. Bjordal, "Effect of low-level laser (Ga-Al-As 655 nm) on skeletal muscle fatigue induced by electrical stimulation in rats" J Appl Physiol 101, 283-8 (2006).
122. E. C. Jr. Leal, R. A. Lopes-Martins, P. de Almeida, L. Ramos, V. V. Iversen, J. M. Bjordal, "Effect of low-level laser therapy (GaAs 904 nm) in skeletal muscle fatigue and biochemical markers of muscle damage in rats" Eur J Appl Physiol. 108, 1083–8 (2010).
123. P. de Almeida, R. A. Lopes-Martins, S. S. Tomazoni, J. A. Jr. Silva, P. T. de Carvalho , J. M. Bjordal, E. C. Jr. Leal, "Low-level laser therapy improves skeletal muscle performance, decreases skeletal muscle damage and modulates mRNA expression of COX-1 and COX-2 in a dose-dependent manner" Photochem Photobiol. 87, 1159–63 (2011).
124. A. S. Gorgey, A. N. Wadee, N. N. Sobhi, "The effect of low-level laser therapy on electrically induced muscle fatigue: a pilot study" Photomed Laser Surg. 26, 501–6 (2008).
125. P. de Almeida, R. A. Lopes-Martins, T. De Marchi, S. S. Tomazoni, R. Albertini, J. C. Corrêa, R. P. Rossi, G. P. Machado, D. P. da Silva, J. M. Bjordal, E. C. Jr. Leal, "Red (660 nm) and infrared (830 nm) low-level laser therapy in skeletal muscle fatigue in humans: what is better?" Lasers Med Sci. 27,453–8 (2012).
126. E. C. Jr. Leal, R. A. Lopes-Martins, F. Dalan, M. Ferrari, F. M. Sbabo, R. A. Generosi, B. M. Baroni, S. C. Penna, V. V. Iversen, J. M. Bjordal, "Effect of 655-nm low-level laser therapy on exercise-induced skeletal muscle fatigue in humans" Photomed Laser Surg. 26, 419–24 (2008).
127. E. C. Jr. Leal, R. A. Lopes-Martins, A. A. Vanin, B. M. Baroni, D. Grosselli, T. De Marchi, V. V. Iversen, J. M. Bjordal, "Effect of 830 nm low-level laser therapy in exercise-induced skeletal muscle fatigue in humans" Lasers Med Sci. 24, 425–31 (2009).
128. E. C. Jr. Leal, R. A. Lopes-Martins, L. Frigo, T. De Marchi, R. P. Rossi, V. de Godoi, S. S. Tomazoni, D. P. Silva, M. Basso, P. L. Filho, F. de Valls Corsetti, V. V. Iversen, J. M. Bjordal, "Effects of low-level laser therapy (LLLT) in the development of exercise-induced skeletal muscle fatigue and changes in biochemical markers related to postexercise recovery" J Orthop Sports Phys Ther. 40, 524–32 (2010).
129. B. M. Baroni, E. C. Jr. Leal, T. De Marchi, A. L. Lopes, M. Salvador, M. A. Vaz, "Low level laser therapy before eccentric exercise reduces muscle damage markers in humans" Eur J Appl Physiol. 110, 789–96 (2010).
130. C. Ferraresi, R. Panepucci, R. Reiff, R. Júnior, V. Bagnato, N. Parizotto, "Molecular effects of low-level laser therapy (808 nm) on human muscle performance". Phys Ther Sport. 13 (2012).
131. R. L. Toma , H. T. Tucci, H. K. Antunes, C. R. Pedroni, A. S. de Oliveira, I. Buck, P. D. Ferreira, P. G. Vassão, A. C. Renno, "Effect of 808 nm low-level laser therapy in exercise-induced skeletal muscle fatigue in elderly women" Lasers Med Sci. 28, 1375-82 (2013).
132. J. A. Piva, V. Santos Silva, E. M. Carvalho Abreu, R. A. Nicolau, "Effect of low-level laser therapy on the initial stages of tissue repair: basic principles" An Bras Dermatology. 86, 947-954 (2011).
133. L. Ramos, L. Junior, E. C. Pinto, R. Capp Pallotta, L. Frigo, R. Labat Marcos, M. H. Catelli de Carvalho, J. M. Bjordal, R. Á. B. Lopes-Martins, "Infrared (810 nm) Low-Level Laser Therapy in Experimental Model of Strain-Induced Skeletal Muscle Injury in Rats: Effects on Functional Outcomes" Photochem. Photobiol. 88, 154–160 (2012).
134. C. F. Rizzi, J. L. Mauriz, D. S. Freitas Corrêa, A. J. Moreira, C. G. Zettler, L. I. Filippin, N. P.

Marroni, J. González-Gallego, "Effects of low-level laser therapy (LLLT) on the nuclear factor (NF)-κB signaling pathway in traumatized muscle" Lasers Surg. Med. 38, 704–713 (2006).
135. G. R. F. Bertolini, T. S. Silva, A. P. Ciena, D. L. Trindade, "Efeitos do laser de baixa potência sobre a dor e edema no trauma tendíneo de ratos" Rev Bras Med Esporte. 14, 362-6 (2008).
136. R. A. Mesquita-Ferrari, M. D. Martins, J. A. Jr. Silva, T. D. da Silva, R. F. Piovesan, V. C. Pavesi, S. K. Bussadori, K. P. Fernandes, "Effects of low-level laser therapy on expression of TNF-α and TGF-β in skeletal muscle during the repair process" Lasers Med Sci. 26, 335-340 (2011).
137. K. P. S. Fernandes, A. N. Alves, F. D. Nunes, N. H. C. Souza, J. A. Silva Jr., S. K. Bussadori, R. A. Ferrari, "Effect of photobiomodulation on expression of IL-1β in skeletal muscle following acute injury" Lasers Med Sci 28, 1043-1046 (2013).
138. L. Assis, A. I. S. Moretti, T. B. Abrahão, V. Cury, H. P. Souza, M. R. Hamblin, N. A. Parizotto, "Low-level laser therapy (808 nm) reduces inflammatory response and oxidative stress in rat tibialis anterior muscle after cryolesion" Lasers Surg. Med. 44, 726–735 (2012).
139. L. Assis, A. I. S. Moretti, T. B. Abrahão, H. P. de Souza, M. R. Hamblin, N. A. Parizotto, "Low-level laser therapy (808 nm) contributes to muscle regeneration and prevents fibrosis in rat tibialis anterior muscle after cryolesion" Lasers in medical science 28, 947-955 (2013).
140. N. C. Rodrigues, L. Assis, K. R. Fernandes, A. Magri, D. A. Ribeiro, R. Brunelli, D. C. Abreu, A. C. Renno, "Effects of 660 nm low-level laser therapy on muscle healing process after cryolesion" J Rehabil Res Dev. 50, 985–96 (2013).
141. T. Y. Fukuda, M. M. Tanji, S. R. Silva, M. N. Sato, H. Plapler, "Infrared low-level diode laser on inflammatory process modulation in mice: pro- and anti-inflammatory cytokines" Lasers in Medical Science 28, 1305-1313 (2013).
142. G. Shefer, T. A. Partridge, L. Heslop, J. G. Gross, U. Oron, O. Halevy, "Low-energy laser irradiation promotes the survival and cell cycle entry of skeletal muscle satellite cells" J. Cell Sci. 115(7):1461-9 (2002).
143. J. Nakano, H. Kataoka, J. Sakamoto, T. Origuchi, M. Okita, T. Yoshimura, "Low level laser irradiation promotes the recovery of atrophied gastrocnemius skeletal muscle in rats" Exp. Physiol. 94, 1005-15 (2009).
144. J. T. Hashmi, Y. Huang, B. Z. Osmani, S. K. Sharma, M. A. Naeser, M. R. Hamblin, "Role of Low-Level Laser Therapy in Neurorehabilitation" American Academy of Physical Medicine and Rehabilitation (2010).
145. C. Rhee, C. W. Bahk, J. Y. Jung, J. Ahn, M. Suh, "Cochlea Hair Cell Rescue after a Noise-Induced Hearing Loss using a Low Level Laser Therapy (LLLT)" Photonic Therapeutics and Diagnostics VII, Proc. of SPIE Vol. 7883 (2011).
146. S. S. Goodman, R. A. Bentler, A. Dittberner, I. B. Mertes "The Effect of Low-Level Laser Therapy on Hearing" ISRN Otolaryngology, Volume 2013 (2013).
147. L. J. Walsh "The current status of low level laser therapy in dentistry. Part 2. Hard tissue applications" Australian Dental Journal 42; 4:247-54 (1997).
148. M. A. Calin, T. Coman "The laser in veterinary medicine" Turk. J. Vet. Anim. Sci. 35;5: 351-357 (2011).
149. Thor Laser Veterinarian Treatments, http://blog.thorlaser.com/are-you-a-veterinarian-free-webinar-by-dr-ron/. Accessed on September 2014.
150. Biocare Systems Inc. http://www.biocaresystems.com. Accessed on September 2014.
151. K-Laser. http://www.klaser.es. Accessed on September 2014.
152. Kondortech Equipamentos Odontológicos Ltda. http://www.kondortech.com.br. Accessed on September 2014.
153. LaserLight. http://www.laserlight.biz/products_Compact_CombiLaser.html. Accessed on September 2014.
154. Laserex Technologies. http://www.laserex.net/shop/laser-therapy/lasertens-2000-ir. Accessed on September 2014.
155. Medicom a.s. http://www.medicom.cz. Accessed on September 2014.
156. MedX Health. http://www.medxhealth.com. Accessed on September 2014.
157. Meridian Medical. http://www.lapexbcs.com. Accessed on September 2014.
158. MicroLight Co. http://www.microlightcorp.com. Accessed on September 2014.
159. MKW Lasersystem. http://www.mkw-laser.de. Accessed on September 2014.
160. Sunny Optoelectronic Technology Co., Ltd. http://sunny01.en.alibaba.com. Accessed on September 2014.

161. TerraQuant Medical Devices. http://www.terraquant.org. Accessed on September 2014.
162. THOR Photomedicine Ltd. http://www.thorlaser.com/products. Accessed on September 2014.
163. R. Martin, "Laser-accelarated inflammation/pain reduction and healing" Pratical Pain Management 3, 20-25 (2003).
164. T. I. Karu, "Multiple roles of cytochrome c oxidase in mammalian cells under action of red and IR-A radiation" IUBMB Life 62, 607-10 (2010).
165. T. I. Karu, L. V. Pyatibrat, S. F. Kolyakov, N. I. Afanasyeva, "Absorption measurements of a cell monolayer relevant to phototherapy: Reduction of cytochrome c oxidase under near IR radiation" Journal of Photochemistry and Photobiology B-Biology 81, 98-106 (2005).
166. D. Pastore, M. Greco, S. Passarella, "Specific helium–neon laser sensitivity of the purified cytochrome c oxidase" Int. J. Radiat. Biol. 6, 863–870 (2000).
167. V. G. Artyukhov, O. V. Basharina, A. A. Pantak, L. S. Sveklo, "Effect of helium-neon laser on activity and optical properties of catalase" Bull Exp Biol Med 129, 537-40 (2000).
168. A. Mandel, R. Dumoulin-White, L. Lilge, "Understanding the mechanisms of Low Level Laser Therapy" White Paper (2011).
169. T. I. Karu, N. I. Afanasyeva, S. F. Kolyakov, L. V. Pyatibrat, L. Welser, "Changes in absorbance of monolayer of living cells induced by laser radiation at 633, 670, and 820 nm" IEEE Journal of Selected Topics in Quantum Electronics 7, 982-988 (2001).
170. Y. Huang, A. C. -H. Chen, M. Hamblin, "Low-level laser therapy: an emerging clinical paradigm" SPIE Newsroom (2009).
171. T. I. Karu, L. V. Pyatibrat, N. I. Afanasyeva, "Cellular effects of low power laser therapy can be mediated by nitric oxide" Lasers Surg Med 36, 307-14 (2005).
172. Y. Moriyama, E. H. Moriyama, K. Blackmore, M. K. Akens, L. Lilge, "In Vivo Study of the Inflammatory Modulating Effects of Low-level Laser Therapy on iNOS Expression Using Bioluminescence Imaging" Photochem Photobiol 81, 1351-5 (2005).
173. R. Duan, T. C. Liu, Y. Li, H. Guo, Y. B. Yao, "Signal transduction pathways involved in low intensity He-Ne laser-induced respiratory burst in bovine neutrophils: a potential mechanism of low intensity laser biostimulation" Lasers Surg Med.29, 174-8 (2001).
174. M. R. Hamblin, T. N. Demidova, "Mechanisms of Low Level Light Therapy – an Introduction" Proc SPIE 6140, 1-12 (2006).
175. Y. Zhang, S. Song, C. C. Fong, C. H. Tsang, Z. Yang, M. Yang, "cDNA microarray analysis of gene expression profiles in human fibroblast cells irradiated with red light" J Invest Dermatol. 120:849-57 (2003).
176. J. de Castro e Silva, S. Zucoloto, L. A. Menegazzo, R. G. Granato, L. G. Marcassa, V. S. Bagnato, "Laser enhancement in hepatic regeneration for partially hepatectomized rats" Lasers Surg. Med. 29, 73-77 (2001).
177. R. Lubart, H. Friedman, R. Lavie, "Photobiostimulation as a function of different wavelengths" Journal of Laser Therapy 12, 38-41 (2000).
178. T. I. Karu, "Mitochondrial signaling in mammalian cells activated by red and near IR radiation" Photochem Photobiol 84: 1091–1099 (2008).
179. H. Friedmann, R. Lubart, I. Laulicht, S. Rochkind, "A possible explanation of laser-induced stimulation and damage of cell cultures" J Photochem Photobiol B 11, 87-91 (1991).
180. M. Eichler, R. Lavi, A. Shainberg, R. Lubart, "Flavins are source of visible-light-induced free radical formation in cells" Lasers Surg Med 37, 314-9 (2005).
181. L. B. Silveira, M. S. Ribeiro, A. A. Garrocho, M. D. Novelli, H. A. Marigo, E. B. Groth, "In vivo study on mast cells behavior following low-intensity visible and near infrared laser radiation" Lasers in Surgery and Medicine 82 (2002).
182. M. A. Trelles, M. Vélez, J. Rigau, E. Mayayo, "LLLT in vivo effects on mast cells" in Abstract from the 7th International Congress of European Medical Laser Association (2000).
183. G. Tam, "Action of 904 nm diode laser in orthopedics and traumatology" in Abstract from the 7th International Congress of European Medical Laser Association (2000).
184. R. Lubart, Y. Wollman, H. Friedmann, S. Rochkind, I. Laulicht, "Effects of visible and near-infrared lasers on cell cultures" J. Photochem. Photobiol. B 12, 305-310 (1992).
185. N. Grossman, N. Schneid, H. Reuveni, S. Halevy, R. Lubart, "780 nm low power diode laser irradiation stimulates proliferation of keratinocyte cultures: Involvement of reactive oxygen species" Lasers in Surgery and Medicine 22, 212-218 (1998).
186. P. Moore, T. D. Ridgway, R. G. Higbee, E. W. Howard, M. D. Lucroy, "Effect of wavelength on

low-intensity laser irradiation-stimulated cell proliferation in vitro" Lasers Surg. Med. 36, 8-12 (2005).
187. I. Stadler, R. Evans, B. Kolb, J. O. Naim, V. Narayan, N. Buehner, R. J. Lanzafame, "In vitro effects of low-level laser irradiation at 660 nm on peripheral blood lymphocytes" Lasers in Surgery and Medicine 27, 255-261 (2000).
188. J. M. Bjordal, C. Couppe, "What is optimal dose, power density and timing for low level laser therapy in tendon injuries? A review of in vitro and in vivo trials" in Abstract from the 7th International Congress of European Medical Laser Association (2000).
189. J. Kubota, "Laser and sports medicine in plastic and reconstructive surgery" in Abstract from II Congress of the Internat. Assn for Laser and Sports Medicine (2000).
190. P. Lievens, P. H. Van de Veen, "Wound healing process: influence of LLLT on the proliferation of fibroblasts and on the lymphatic regeneration" in Abstract from the 7th International Congress of European Medical Laser Association (2000).
191. T. I. Karu, "Mechanisms of low-power laser light action on cellular level" in Lasers in Medicine and Dentistry, Z. Simunovic, ed., 97-125 (2000).
192. A. P. Castano, T. Dai, I. Yaroslavsky, R. Cohen, W. A. Apruzzese, M. H. Smotrich, M. R. Hamblin MR, "Low level laser therapy for zymosan-induced arthritis in rats: importance of illumination time" Lasers Surg Med. 39, 543–550 (2007).
193. V. Haxsen, D. Schikora, U. Sommer, A. Remppis, J. Greten, C. Kasperk, "Relevance of laser irradiance threshold in the induction of alkaline phosphatase in human osteoblast cultures" Lasers Med Sci. 23, 381–384 (2008).
194. R. J. Lanzafame, I. Stadler, A. F. Kurtz, R. Connelly, T. A. Peter, P. Brondon, D. Olson, "Reciprocity of exposure time and irradiance on energy density during photoradiation on wound healing in a murine pressure ulcer model" Lasers Surg Med. 39, 534–542 (2007).
195. E. Mester, A. F. Mester, A. Mester, "The biomedical effects of laser application" Lasers Surg Med. 5, 31–39 (1985).
196. A. P. Sommer, A. L. Pinheiro, A. R. Mester, R. P. Franke, H. T. Whelan, "Biostimulatory windows in low intensity laser activation: lasers, scanners, and NASA's light-emitting diode array system" J Clin Laser Med Surg. 19, 29–33 (2001).
197. C. Webb, M. Dyson, W. H. Lewis, "Stimulatory effect of 660 nm low level laser energy on hypertrophic scar--derived fibroblasts: possible mechanisms for increase in cell counts" Lasers Surg Med. 22, 294–301 (1998).
198. F. Martius, "Das Amdt-Schulz Grandgesetz" Munch Med Wschr. 70, 1005–1006 (1923).
199. Y. Huang, S. K. Sharma, J. Carrol, M. R. Hamblin, "Biphasic dose response in low level light therapy - an update" Dose-Response 9, 602-618 (2011).
200. T. I. Karu, L. Kalichman, V. S. Letokhov, V. V. Lobko, "Biostimulation of HeLa cells by low intensity visible light" Nuov. Cim. D, 1, 828 (1982).
201. T. Hode, D. Duncan, S. Kirkpatrick, P. Jenkins, L. Hode, "The importance of coherence in phototherapy" SPIE BiOS: Biomedical Optics 716507-716507 (2009).
202. J. Tuner, L. Hode, "Low Level Laser Therapy. Clinical Practice and Scientific Background" Prima Books, Grängesberg-Sweden (1999).
203. T. I. Karu, "Cellular mechanism of low power laser therapy: new questions" Lasers in Medicine and Dentistry 3, 79-100 (2003).
204. J. T. Hashmi, Y. Huang, S. K. Sharma, D. Balachandran Kurup, L. De Taboada, J. D. Carroll, M. R. Hamblin, "Effect of Pulsing in Low-Level Light Therapy" Lasers Surg Med. 42, 450–466 (2010).
205. M. S. Ribeiro, D. D. F. T. Da Silva, C. E. N. De Araújo, S. F. De Oliveira, C. M. R. Pelegrini, T. M. T. Zorn, D. M. Zezell, "Effects of low-intensity polarized visible laser radiation on skin burns: a light microscopy study" Journal of clinical laser medicine & surgery 22, 59-66 (2004).
206. A. L. Pinheiro, D. H. Pozza, M. G. de Oliveira, "Polarized light (400–2000 nm) and non-ablative laser (685 nm), A description of the wound healing process using immunohistochemical analysis" J. Photomed. Laser Surg. 23, 485–492 (2005).
207. T. Kubasova, M. Fenyo, "Effect of visible light on some cellular and immune parameters" Immunol. Cell Biol. 73, 239–244 (1995).
208. L. Hode, J. Tuner, "Low level laser therapy (LLLT) contra light-emitting diode therapy (LEDT) – what is the difference?" Laser Florence 99: Proceedings of SPIE 4166, 90–97 (2000).
209. M. Mantineo, J. P. Pinheiro, A. M. Morgado, "Methodology for assessment of low level laser

therapy (LLLT) irradiation parameters in muscle inflammation treatment" Proc. SPIE 9032, Biophotonics—Riga 2013, 90320P (2013).
210. M. Mantineo, A. M. Morgado, J.P. Pinheiro, "Effects of Low Level Laser Therapy (LLLT) on Injured Muscle: A pilot study" Libro de Actas XXX CASEIB 2012 - 19 a 21 de noviembre - San Sebastián ISBN – 10: 84-616-2147-6, ISBN – 13: 978-84-616-2147-7 (2012).
211. W. Russell, R. Burch, "The principles of humane experimental technique" Publisher Methuen (1959).
212. C. Kilkenny, W.J. Browne, I.C. Cuthill, M.Emerson, D.G. Altman, "Improving Bioscience Research Reporting: The ARRIVE Guidelines for Reporting Animal Research" PLoS Biology, 8 (2010).
213. K. R. Byrnes, R. W. Waynant, I. K. Ilev, X. Wu, L. Barna, K. Smith, R. Heckert, H. Gerst, J. J. Anders, “Light promotes regeneration and functional recovery and alters the immune response after spinal cord injury” Lasers Surg Med 36,171-185 (2005).
214. A. Gupta, T. Dai, M. R. Hamblin, “Effect of red and near-infrared wavelengths on low-level laser (light) therapy-induced healing of partial-thickness dermal abrasion in mice” Lasers Med. Sci, 29, 257-265 (2014).
215. F. A. H. Al-Watban, X. Y. Zhang, B. L. Andres, “Low-Level Laser Therapy Enhances Wound Healing in Diabetic Rats: A Comparison of Different Lasers,” Photomedicine and Laser Surgery, 25, 72-77 (2007).
216. M. Masoumipoor, S. B. Jameie, A. Janzadeh, F. Nasirinezhad, M. Soleimani, M. Kerdary, “Effects of 660- and 980-nm low-level laser therapy on neuropathic pain relief following chronic constriction injury in rats ciatic nerve” Lasers Med.Sci. (2014).
217. Q. Wu, Y. Huang, S. Dhital, S. K. Sharma, A. C.-H. Chen, M. Whalen, M. R. Hamblin, “Low level laser therapy for traumatic brain injury” Proc SPIE 7552, Mechanisms for Low-Light Therapy V, 755206. (2010).
218. The European Parliament and the Council, "Directive 2010/63/EU of on the protection of animals used for scientific purposes" Official Journal of the European Union (2010).
219. W. Heine, "Environmental Management in Laboratory Animal Units" PABST Science Publishers (1998).
220. Canadian Council on Animal Care, "Guidelines on Laboratory animal facilities - characteristics, design and development" (2003).
221. M. F. W. Festing, P. Overend, R. Gaines Das, M. Cortina Borja, M. Berdoy, "The Design of Animal Experiments: Reducing the use of animals in research through better experimental design" Laboratory Animals Ltd., 79-81 (2011).
222. M. Mantineo, A. M. Morgado, J.P. Pinheiro, "Low Level Laser Therapy on Injured Rat Muscle" 2013 IEEE 3rd Portuguese Meeting in Bioengineering (ENBENG), 978-1-4673-4859-1 (2013).
223. M. Mantineo, J. P. Pinheiro, A. M. Morgado, "Low level laser therapy on injured rat muscle" Proc. SPIE 8803, Medical Laser Applications and Laser-Tissue Interactions VI, 88030E (2013).
224. J. J. Crisco, P. Jokl, G. T. Heinen, M. D. Connell, M. M. Panjabi, "A muscle contusion injury model. Biomechanics, physiology, and histology" J Sports Med. 22, 702-710 (1994).
225. M. J. Kruger, C. Smith, "Postcontusion Polyphenol Treatment Alters Inflammation and Muscle Regeneration" Medicine & Science in Sports & Exercise 44, 872–880 (2012).
226. P. Hedenqvist, "Anaesthesia and analgesia for surgery in rabbits and rats: A comparison of the effects of different compounds" PhD Thesis Karolinska Institutet (2008).
227. M. F. Toft, M. H. Petersen, N. Dragsted, A. K. Hansen, "The impact of different blood sampling methods on laboratory rats under different types of anaesthesia" Laboratory Animals 40, 261-274 (2006).
228. Peprotech, "Rat TNF-alpha, Rat IL-1beta, Rat IL-2, Rat IL-6 ELISA Protocol" (2012).
229. B. Close, K. Banister, V. Baumans, E. M. Bernoth, N. Bromage, J. Bunyan, W. Erhardt, P. Flecknell, N. Gregory, H. Hackbarth, D. Morton, C. Warwick, "Recommendations for euthanasia of experimental animals: Part 1. DGXI of the European Commission" Lab Anim 30, 293-316 (1996).
230. H. J. G. Gundersen, T. F. Bendtsen, L. Korbo, N. Marcussen, A. Moller, K. Nielsen, J. R. Nyengaard, B. Pakkenberg, F. B. Sorensen, A. Vesterby, M. J. West, "Some New, Simple and Efficient Stereological Methods and Their Use in Pathological Research and Diagnosis - Review Article" APMIS 96, 379-394 (1988).

231. T. A. Butterfield, T. M. Best, M. A. Merrick, "The dual roles of neutrophils and macrophages in inflammation: a critical balance between tissue damage and repair" J. Athl. Train. 41, 457-465 (2006).
232. J. H. Zar, "Biostatistical Analysis" Prentice-Hall International Inc. (1984).
233. S. Jacques, T. Li, S. Prahl, “mcxyz.c, a 3D Monte Carlo simulation of heterogeneous tissues” http://omlc.ogi.edu/software/mc/mcxyz/index.html. Accessed on September 2014.
234. W. F. Cheong, S. A. Prahl, A. J. Welch, “A review of the optical properties of biological issues” IEEE J. Quantum Electron. 26, 2166–2185 (1990).
235. L. Assis, A. I. S. Moretti, T. B. Abrahao, V. Cury, H. P. Souza, M. R. Hamblin, N. A. Parizotto, "Low-level laser therapy (808 nm) reduces inflammatory response and oxidative stress in rat tibialis anterior muscle after cryolesion" Lasers in Surgery and Medicine 44, 726-735 (2012).
236. R. Albertini, A. B. Villaverde, F. Aimbire, J. Bjordal, A. Brugnera, J. Mittmann, J. A. Silva, M. Costa, "Cytokine mRNA expression is decreased in the subplantar muscle of rat paw subjected to carrageenaninduced inflammation after low-level laser therapy" Photomed. Laser Surg. 26, 19-24 (2008).
237. J. G. Cannon, B. A. St Pierre, "Cytokines in exertion-induced skeletal muscle injury" Mol. Cell Biochem. 179, 159-167 (1998).
238. K. K. Hoyer, H. Dooms, L. Barron, A. K. Abbas, "Interleukin-2 in the development and control of inflammatory disease" Immunol. Rev. 226, 19-28 (2008).
239. E. G. Novoselova, O. V. Glushkova, D. A. Cherenkov, V. M. Chudnovsky, E. E. Fesenko, "Effects of low-power laser radiation on mice immunity" Photodermatol. Photoimmunol. Photomed. 22, 33-38 (2006).
240. A. C. H. Chen, P. R. Arany, Y. Huang, E. M. Tomkinson, S. K. Sharma, G. B. Kharkwal, T. Saleem, D. Mooney, F. E. Yull, T. S. Blackwell, M. R. Hamblin, "Low-Level Laser Therapy Activates NF-kB via Generation of Reactive Oxygen Species in Mouse Embryonic Fibroblasts" Plos One 6, (2011).
241. L. I. Filippin, A. J. Moreira, N. P. Marroni, R. M. Xavier, "Nitric oxide and repair of skeletal muscle injury" Nitric Oxide-Biology and Chemistry 21, 157-163 (2009).
242. S. Young, P. Bolton, M. Dyson, W. Harvey, C. Diamantopoulos, "Macrophage Responsiveness to Light Therapy" Lasers in Surgery and Medicine 9, 497-505 (1989).
243. P. R. Rich, A. J. Moody, W. J. Ingledew, “Detection of a near infrared absorption band of ferrohaem a3 in cytochrome c oxidase” FEBS Lett. 305, 171–173 (1992).
244. J. Joensen, J. H. Demmink, M. I. Johnson, V. V. Iversen, R. A. Lopes-Martins, J. M. Bjordal, “The thermal effects of therapeutic lasers with 810 and 904 nm wavelengths on human skin” Photomed. Laser Surg. 29, 145–153 (2011).
245. P. A. Hasgall, F. Di Gennaro, C. Baumgartner, E. Neufeld, M. C. Gosselin, D. Payne, A. Klingenböck, N. Kuster, “IT’IS Database for thermal and electromagnetic parameters of biological tissues,” Version 2.6, www.itis.ethz.ch/database. Accessed on September 2014.
246. P. Brondon, I. Stadler, R. J. Lanzafame, "Pulsing Influences Photoradiation Outcomes in Cell Culture" Lasers in Surgery and Medicine 41, 222–226 (2009).
247. T. I. Karu, T. P. Ryabykh, S. N. Antonov, "Different Sensitivity of Cells from Tumor-Bearing Organisms to Continuous-Wave and Pulsed Laser Radiation (=632.8 nm) Evaluated by Chemiluminescence Test" Laser in the Life Sciences 7, 99-105 (1996).
248. S. El Sayed, M. Dyson, "Effect of Laser Pulse Repetition Rate and Pulse Duration on Mast Cell Number and Degranulation" Lasers in Surgery and Medicine 19, 433- 437 (1996).
249. Y. Ueda, N. Shimizu, "Effects of Pulse Frequency of Low-Level Laser Therapy (LLLT) on Bone Nodule Formation in Rat Calvarial Cells" Journal of Clinical Laser Medicine & Surgery 21, Num 5 (2003).
250. L. Longo, S. Evangelista, G. Tinacci, A. G. Sesti, "Effect of diodes-laser silver arsenide-aluminium (Ga-Al-As) 904nm on healing of experimental wounds" Lasers Surg Med 7, 444–447 (1987).
251. P. A. Lapchak, K. F. Salgado, C. H. Chao, J. A. Zivin, "Transcranial near-infrared light therapy improves motor function following embolic strokes in rabbits: An extended therapeutic window study using continuous and pulse frequency delivery modes" Neuroscience 148, 907–914 (2007).
252. F. A. H. Al-Watban, X. Y. Zhang, "The Comparison of Effects between Pulsed and CW Lasers on Wound Healing" Journal of Clinical Laser Medicine & Surgery 22, 15-18 (2004).
253. F. Ceccherelli, L. Altafini, G. Lo Castro, A. Avila, F. Ambrosio, G.P. Giron, "Diode laser in

cervical myofascial pain: A double-blind study versus placebo" Clin J Pain 5, 301–304 (1989).
254. B. S. Sushko, P. Lymans'kyi Iu, S. O. Huliar, "Action of the red and infrared electromagnetic waves of light-emitting diodes on the behavioral manifestation of somatic pain" Fiziol Zh 53, 51–60 (2007).
255. N. Lane, "Cell biology: power games" Nature 443, 901–903 (2006).
256. R. Archid, A. Patzelt, B. Lange-Asschenfeldt, S. S. Ahmad, M. Ulrich, E. Stockfleth, S. Philipp, W. Sterry, J. Lademann, "Confocal laser-scanning microscopy of capillaries in normal and psoriatic skin" J. Biomed. Opt. 17, 101511. (2012).
257. J. S. Nelson, T. E. Milner, L. O. Svaasand, S. Kimel, "Laser pulse duration must match the estimated thermal relaxation time for successful photothermolysis of blood vessels" Lasers Med. Sci. 10, 9–12 (1995).
258. M. Brunori, A. Giuffrè, E. D'Itri, P. Sarti, "Internal electron transfer in Cu-heme oxidases: thermodynamic or kinetic control?" J. Biol. Chem. 272, 19870–19874 (1997).
259. H. Long, Y. Zhou, J. Xue, L. Liao, N. Ye, F. Jian , Y. Wang, W. Lai, "The effectiveness of low-level laser therapy in accelerating orthodontic tooth movement: a meta-analysis" Lasers Med Sci, Springer-Verlag (2013).
260. G. Nimeri, C. H. Kau, N. S. Abou-Kheir, R. Corona, "Acceleration of tooth movement during orthodontic treatment - a frontier in Orthodontics" Progress in Orthodontics 14, 42 (2013).
261. A. R. Gross, S. Dziengo, O. Boers, C. H. Goldsmith, N. Graham, L. Lilge, S. Burnie, R. White, "Low Level Laser Therapy (LLLT) for Neck Pain: A Systematic Review and Meta-Regression" The Open Orthopaedics Journal 7:4, 396-419 (2013).
262. Y. Morimoto, A. Saito, Y. Tokuhashi, "Low level laser therapy for sports injuries" JMLL Laser Therapy 22.1, 17-20 (2013).
263. C. Ferraresi, T. de Brito Oliveira, L. de Oliveira Zafalon, R. B. de Menezes Reiff, V. Baldissera, S. E. de Andrade Perez, E. Matheucci Júnior, N. A. Parizotto NA. "Effects of low level laser therapy (808 nm) on physical strength training in humans" Lasers Med Sci 26, 349–58 (2011).
264. T. dos Santos Maciel, I. S. Sepúlveda Muñoz, R. A. Nicolau, D. Vilela Nogueira, L. A. Hauck, R. A. Lazo Osório, A. Rodrigues de Paula Júnior, "Phototherapy effect on the muscular activity of regular physical activity practitioners" Lasers Med Sci (2013).
265. W. H. Vieira, C. Ferraresi, S. E. Perez, V. Baldissera, N. A. Parizotto, "Effects of low-level laser therapy (808 nm) on isokinetic muscle performance of young women submitted to endurance training: a randomized controlled clinical trial" Lasers Med Sci 27, 497–504 (2012).
266. P. Kee Min, B. Leo Goo, "830 nm light-emitting diode low level light therapy (LED-LLLT) enhances wound healing: a preliminary study" JMLL Laser Therapy 22.1, 43-49 (2013).
267. S. Almeida dos Santos, A. C. Araruna Alves, E. C. Pinto Leal-Junior, R. Albertini, R. de Paula Vieira, A. P. Ligeiro, J. A. Silva Junior, P. de Tarso Camillo de Carvalho, "Comparative analysis of two low-level laser doses on the expression of inflammatory mediators and on neutrophils and macrophages in acute joint inflammation" Lasers Med Sci (2013).

Appendices

Appendix 1: Recommended doses tables for LLLT

Recommended treatment doses for Low Level Laser Therapy

Laser class 3 B, 780 - 860nm GaAlAs Lasers. Continuous or pulsed, mean output: 5 - 500mW

Irradiation times should range between 20 and 300 seconds

Diagnoses

Tendinopathies	**Points or cm2**	**Joules 780 - 820nm**	**Notes**
Carpal-tunnel	2-3	8	Minimum 4 Joules per point
Lateral epicondylitis	1-2	4	Maximum 100mW/cm2
Biceps humeri c.l.	1-2	6	
Supraspinatus	2-3	8	Minimum 4 Joules per point
Infraspinatus	2-3	8	Minimum 4 Joules per point
Trochanter major	2-4	8	
Patellartendon	2-3	8	
Tract. Iliotibialis	1-2	4	Maximum 100mW/cm2
Achilles tendon	2-3	8	Maximum 100mW/cm2
Plantar fasciitis	2-3	8	Minimum 4 Joules per point
Arthritis	**Points or cm2**	**Joules**	
Finger PIP or MCP	1-2	4	
Wrist	2-4	8	
Humeroradial joint	1-2	4	
Elbow	2.4	8	
Glenohumeral joint	2-4	8	Minimum 4 Joules per point
Acromioclavicular	1-2	4	
Temporomandibular	1-2	4	
Cervical spine	4-12	16	Minimum 4 Joules per point
Lumbar spine	4-8	16	Minimum 4 Joules per point
Hip	2-4	12	Minimum 6 Joules per point
Knee medial	3-6	12	Minimum 4 Joules per point
Ankle	2-4	8	

Daily treatment for 2 weeks or treatment every other day for 3-4 weeks is recommended
Irradiation should cover most of the pathological tissue in the tendon/synovia.
Start with energy dose in table, then reduce by 30% when inflammation is under control
Therapeutic dose windows typically range from +/- 50% of given values, and doses outside these windows are inappropriate and should not be considered as Low Level Laser Therapy.
Recommended doses are for white/caucasian skin types based on results from clinical trials or extrapolation of study results with similar pathology and ultrasonographic tissue measurements.

Disclaimer

The list may be subject to change at any time when more research trials are being published.
World Association of Laser Therapy is not responsible for the application of laser therapy in patients, which should be performed at the sole discretion and responsibility of the therapist.

Revised April 2010

Recommended treatment doses for Low Level Laser Therapy

Laser class 3B, 904 nm GaAs Lasers
(Peak pulse output >1 Watt, mean output >5 mW and power density > 5mW/cm2)
Irradiation times should range between 30 and 600 seconds

Diagnoses	**Min. area/points**	**Min. total dose**	
Carpal-tunnel	2-3	4	Minimum 2 Joules per point
Lateral epicondylitis	2-3	2	Maximum 100mW/cm2
Biceps humeri cap.long.	2-3	2	
Supraspinatus	2-3	4	Minimum 2 Joules per point
Infraspinatus	2-3	4	Minimum 2 Joules per point
Trochanter major	2-3	2	
Patellartendon	2-3	2	
Tract. Iliotibialis	2-3	2	Maximum 100mW/cm2
Achilles tendon	2-3	2	Maximum 100mW/cm2
Plantar fasciitis	2-3	4	Minimum 2 Joules per point
Arthritis	**Points or cm2**	**Joules 904nm**	
Finger PIP or MCP	1-2	1	
Wrist	2-3	2	
Humeroradial joint	2-3	2	
Elbow	2-3	2	
Glenohumeral joint	2-3	2	Minimum 1 Joules per point
Acromioclavicular	2-3	2	
Temporomandibular	2-3	2	
Cervical spine	4	4	Minimum 1 Joules per point
Lumbar spine	4	4	Minimum 1 Joules per point
Hip	2	4	Minimum 2 Joules per point
Knee anteromedial	4-6	4	Minmum 1 Joules per point
Ankle	2-4	2	

Daily treatment for 2 weeks or treatment every other day for 3-4 weeks is recommended
Irradiation should cover most of the pathological tissue in the tendon/synovia.

Start with energy dose in table, then reduce by 30% when inflammation is under control
Therapeutic dose windows typically range from +/- 50% of given values, and doses outside these windows are inappropriate and should not be considered as Low Level Laser Therapy.
Recommended doses are for white/caucasian skin types based on results from clinical trials or extrapolation of study results with similar pathology and ultrasonographic tissue measurements.

Disclaimer
The list may be subject to change at any time when more research trials are being published.
World Association of Laser Therapy is not responsible for the application of laser therapy in patients, which should be performed at the sole discretion and responsibility of the therapist.

Revised April 2010

Appendix 2: HL8338MG GaAlAs Laser Diode Specifications

Features

- Infrared light output: λp = 830 nm Typ
- Optical output power: 50 mW (CW)
- Low operating current: 75 mA Typ
- Low operating voltage: 1.9 V Typ
- Built-in monitor photodiode
- Single longitudinal mode

Package Type
• HL8338MG: MG

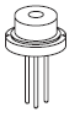

Internal Circuit

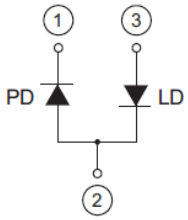

Absolute Maximum Ratings

(T_C = 25°C)

Item	Symbol	Ratings	Unit
Optical output power	P_O	50	mW
LD reverse voltage	$V_{R(LD)}$	2	V
PD reverse voltage	$V_{R(PD)}$	30	V
Operating temperature	Topr	–10 to +60	°C
Storage temperature	Tstg	–40 to +85	°C

Appendix 3: L9805E2P5 GAAlAs Laser Diode Specifications

TECHNICAL DATA

Structure: Index guided, single transverse mode
Lasing wavelength: 980nm typ.
Output power: 50 mW cw
Package: 5.6mm, TO-18

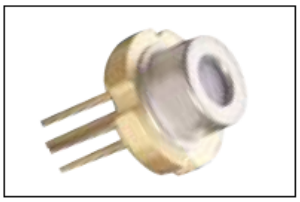

PIN CONNECTION

1) Laser diode cathode
2) Laser diode anode and photodiode cathode
3) Photodiode anode

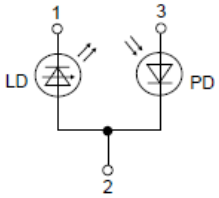

5,6mm package

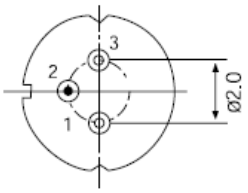

NOTE!
LASERDIODE
MUST BE COOLED!

Maximum Ratings (Tc = 25°)

CHARACTERISTIC	SYMBOL	RATING	UNIT
Optical Output Power	P_o	50	mW
LD Reverse Voltage	$V_{R(LD)}$	2	V
PD Reverse Voltage	$V_{R(PD)}$	30	V
Operation Case Temperature	T_C	-10 .. +60	°C
Storage Temperature	T_{STG}	-40 .. +85	°C

Appendix 4: LED M850L3 Specifications

Thorlabs' Mounted High-Power LED M850L3 has a dominant wavelength of 850 nm, outputs more than 900 mW of power, and is mounted to the end of a heat sink equipped with internal SM1 (1.035"-40) threads. This LED needs to be supplied with a constant current that must not exceed 1000 mA. The current source must be able to deliver this current at a Forward Voltage of 2.9 V.

Specifications

Specification	Value
Color	IR
Nominal Wavelength	850 nm
Power LED Output (Min)	900 mW
Power LED Output (Typical)	1100 mW
Test Current for Typical LED Power	1000 mA
Maximum Current (CW)	1000 mA
Forward Voltage	2.9 V
Bandwidth (FWHM)	30 nm
Viewing Angle	90°
Typical Lifetime	100,000 h